The
GEOLOGIAL BULLETIN
of the
PUNJAB UNIVERSITY

Number 27 *December, 1992*

CONTENTS

Geol. Bull. Punjab Univ. 1992, 27, 1—13

SOME ENGINEERING GEOLOGICAL PROPERTIES OF SOILS AT A BRIDGE SITE OVER THE GAMBILA RIVER ON BANNU—D. I. KHAN ROAD

By
MUHAMMAD HUSSAIN MALIK AND SAEED FAROOQ
Institute of Geology, Punjab University, Lahore 54590, Pakistan
AND
SYED NAJAM TAMEEM
Geoconsult Associates, Model Town, Lahore, Pakistan

Abstract : *A large number of soil samples were obtained from boreholes drilled for investigation purposes for construction of bridge. Both disturbed and undisturbed samples were tested for gradations, density. Atterberg, limits, unconfined and triaxial compression. The soil strata consist of clay with variable percentage of silt and sand. Unconfined compression tests show a slight increase in strength with depth. Similarly, triaxial tests show an increase in C and I values with increase in depth, although the grain size analysis do not show a pronounced variation.*

INTRODUCTION

The Bannu—D.I. Khan Road is an important highway which connects the two district headquarters in the N.W.F.P. It crosses the Gambila River at Mile 25 on Bannu-D. I. Khan Road (Fig.1) by an existing narrow bridge, which also serves as railway bridge for the narrow gauge railway line connecting Kalabagh and Bannu. This narrow bridge was constructed during late 19th century. The bridge has not only out lived its useful life but has also become bottleneck for the present day heavy and fast moving traffic, resulting in one way operation which causes considerable delays in traffic movements over the bridge.

The National Highway Board, Government of Pakistan rightfully decided to provide a new 8.5 meters wide bridge with 0.80 meter curbs on entire side to be designed for the severest of Class A or Class AA loading to cater for the present and future requirements projected over 25 years. The confirmatory soil investigations were carried out alongwith laboratory and field testing. (ASCE 1974; Brierly et al; 1979; Casagrande 1948), which are discussed in this paper.

GEOLOGY

The Bannu Quadrangle covers an area of more than 4,300 square miles in north central Pakistan between latitudes 32° and 33° N and longitudes 70° and 71° E. This area contains two main physiographic units — the alluvial low lands, which include the structurally undisturbed Indus and Bannu Plains, and the folded belt, which include the khisor, Marwat, Bhittani and Sulaiman Ranges as well as the highlands of Waziristan.

Surficial deposits of Quaternary age, in the Bannu Quadrangle include alluvium and sand dunes of the Indus and Bannu Plains, alluvial fans along the hill fronts and unconsolidated detritus along the slopes and in the valleys of the mountain ranges and foothills. These deposits are of Holocene age.

Total stratigraphic thickness exceeds 38,000 feet in the Sulaiman Range-Waziristan area. Sedimentary rocks of Jurassic, Cretaceous, Tertiary and Quaternary age are present. Rocks-

of Paleocene and Eocene age are particularly well developed in this region, at places, exceeding 13,000 feet in thickness.

The project lies in the Bannu Trough in the tectonic zone of Himalayan Fold Belt. The Himalayan Fold Belt is part of folded foredeep shelf of Indo Pakistan Plate, (Tectonic map of Pakistan, Published by the Geological Survey of Pakistan, 1982).

Preliminary investigations were carried out in 1984, for the design of foundations of the proposed bridge. Six boreholes were drilled upto 65 feet depth from NSL and borehole logs were prepared. The pile foundations of 30 inches diameter of each pile were designed on the basis of the data provided in the preliminary investigations.

PRESENT INVESTIGATIONS

The present confirmatory site investigations were carried out to obtain additional detailed information on the nature of the strata and groundwater in area prior to the construction of the bridge. For this reason three 12" diameter boreholes were advanced, one in the centre of the proposed bridge and one each under the abutments. Borehole logs were prepared, in-situ tests performed and disturbed and undisturbed samples were collected. Table 1 gives ground elevation and depth of each borehole. The Geotechnical Profile along the proposed bridge is shown in Fig. 2.

TABLE—1

B.H. No.	Location	G. Elevation (m)	Botton Elevation (m)	Total Depth (m)
1.	Right Abutment	271.475	232.000	39.55
2.	Centre of Gambila River	265.350	232.000	33.55
3.	Left	271.385	232.000	39.36

Drilling boreholes by Percussion Method upto required depth, performing in-situ tests, collecting samples and preparing field borehole logs and testing samples in the laboratory collectively covers the scope of the geotechnical investigation (B.S. 1377, 1975).

Three boreholes were drilled upto a bottom selevation of 232.000 meters. The sampling and in-sit testing were carried out from an elevation of 254.00 meters downward which is assumed as the scouring depth. The boreholes were drilled using 12" diameter steel casing. A single drum winch machine with 45 H.P. diesel engine was used for advancing the holes. The subsurface material recovered during drilling was carefully inspected and the visual classification was made and recorded on the borehole logs.

STANDARD PENETRATION TESTS (SPT)

Standard Penetration Tests were performed in the boreholes on undisturbed soil below the bottom of casing at appropriate depth intervals. The tests were carried out by driving a standard 2" outer dia split tube sampler with the help of a 140 pound hammer dropping freely under gravity. For every six inches penetration (as required) the number of blows were counted and a total length of 1.5 feet was penetrated. The number of blows for last 12 inches penetration were recorded as SPT blow counts and were denoted as 'N' value.

The soil samples recovered by SPT sampler were carefully preserved in the plastic bags with sampling sheet showing site no., date of sampling, sample depth etc., before transportation and testing.

DISTURBED SAMPLES

The disturbed samples were collected from split tube sampler during Standard Penetration Tests. Large disturbed samples were also aken during drilling. These samples were properly preserved in double plastic bags to carry out moisture tests, particle size anaysis and Atterberg's Limits Tests in the laboratory (Littleton and Farmilo, 1977; B. S. 1337, 1975).

UNDISTURBED SAMPLES

Undisturbed samples were taken by Shelby tubes which were pushed by hammering with the 140 pounds. hammer of SPT apparatus. The borehole bottom was cleanded, prior to the process of sampling upto the level from which the sample was to be taken.

After the extraction of the shelby tube, the sample was waxed from ends by pouring melted parafine wax in the field immediately to prevent any moisture loss. These sample were carried to Soil Testing Laboratory. Triaxial and unconfined compression tests were performed on these undisturbed samples.

LABORATORY TESTING

The samples collected from the site from all the three boreholes were transported to Soil Testing Laboratory at Lahore. From the bulk of samples collected in the field, selection of samples were made after a careful study. Following laboratory tests were performed in the laboratory on the chosen samples. The summary of these tests is given in Table 1.

(a) Natural moisture content test

(b) Gradation analysis

(c) Bulk denstiy test

(d) Atterberg's Limits

(e) Unconfined compression tests

(f) Triaxial compression test

The method of sieving was used for coarse grained sandy soils, whereas method of sedimentation was used for fine grained (clayey) soils. The results of gradation analysis as particle size distribution curves are presented

in Fig. 7.

The unconfined compressive strength (UCS) is the compressive strength at failure of a soil specimen subjected to unconfined compressive load. It provides a direct quantitative measure of consistancy of cohsive soils. The UCS tests were carried out on undisturbed soil samples from different horizons. The results of these are presented as strain curves in Fig.4.

The tests performed on the undisturbed soii samples were undrained Q-tests. In these tests no drainage and, hence, no dissipation of pore pressure is permitted during the application of the all round stress. No. drainage is allowed during the application of the deviator stress. The results are preseted in Figs 5 — 6.

CONCLUSION

The subsurface soil strata at site mainly consist of clay with variable percentages of silt and sand at different horizons. The clay is dense to very dense in compactness and plastic in nature. These alluvial deposits carried by River Gambila were deposited in shallow environments in the area. The variation of grain size does dot seem to be the only factor in the increase of unconfined and triaxial compression strength. It appears that the compactness rendered to soil with depth, is responsible for gain in strength.

ACKNOWLEDGEMENTS

The authors are deeply indebted to M/s Geoconsult Associates Lahore for providing the drilling data and extending laboratory facilities. They are also thankful to Mr. Zahoor Ahmed Qadri for typing the script.

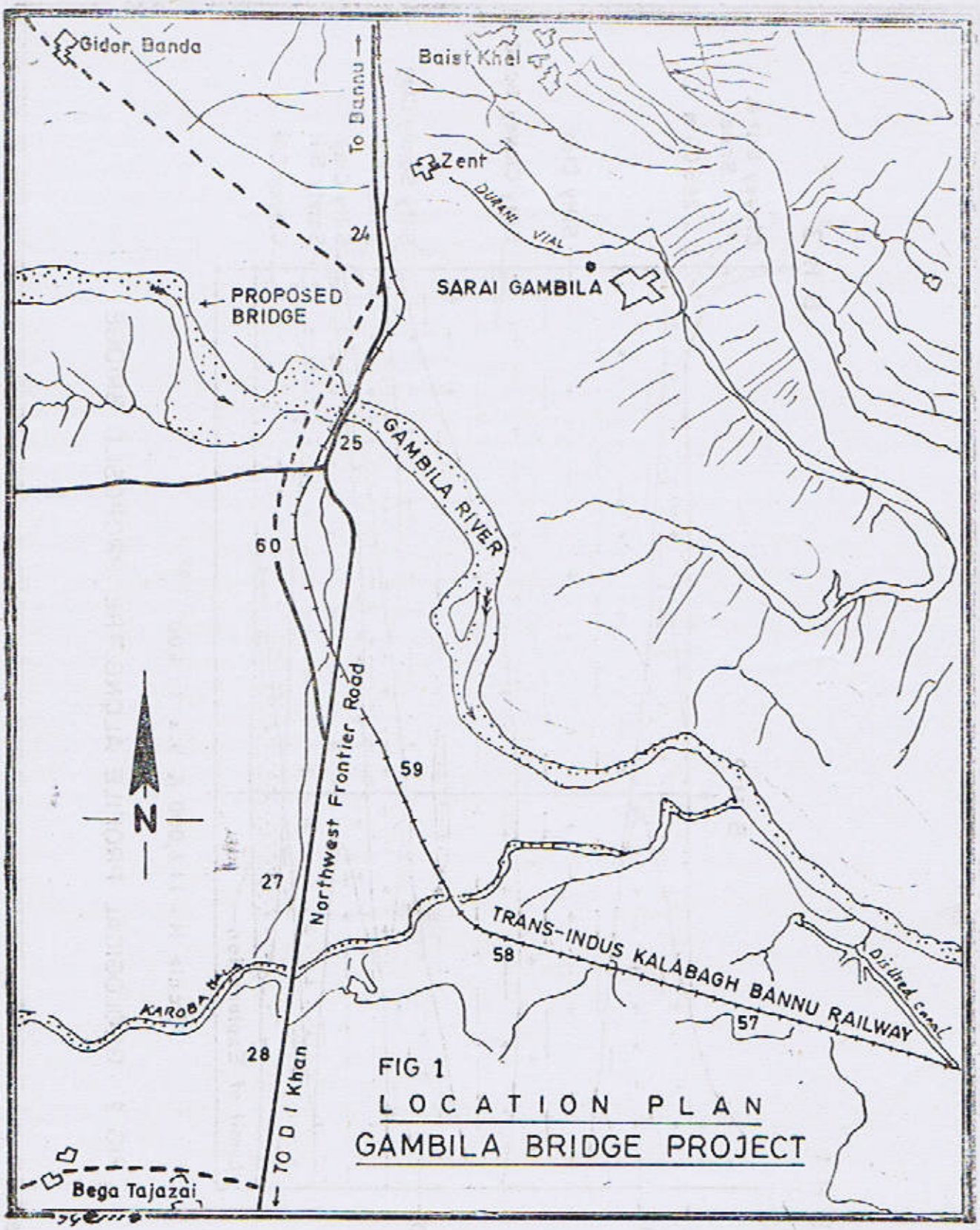

FIG 1

LOCATION PLAN

GAMBILA BRIDGE PROJECT

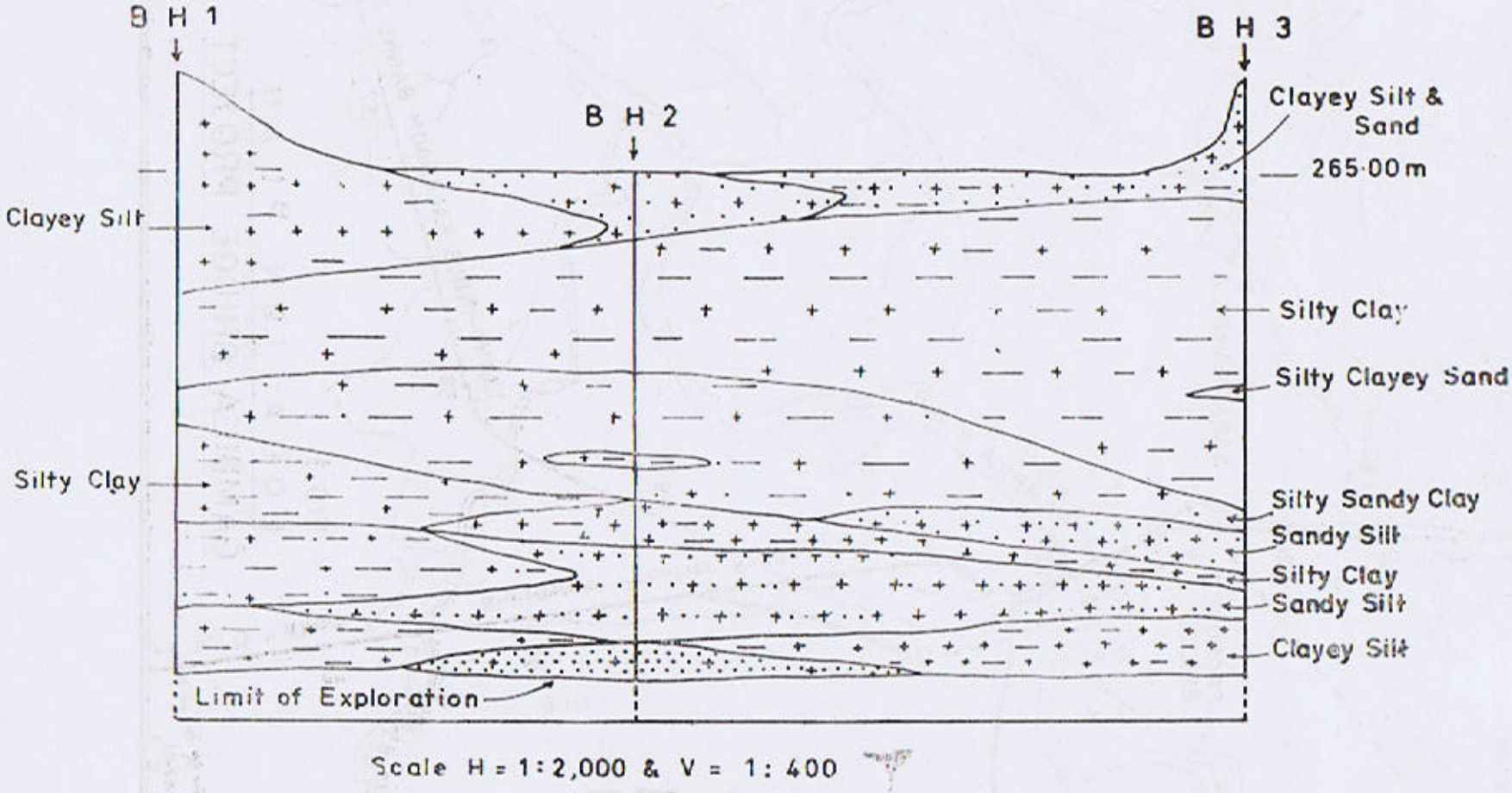

FIG 2 GEOLOGICAL PROFILE ALONG THE PROPOSED BRIDGE

FIG. 3. PARTICLE SIZE DISTRIBUTION CURVES

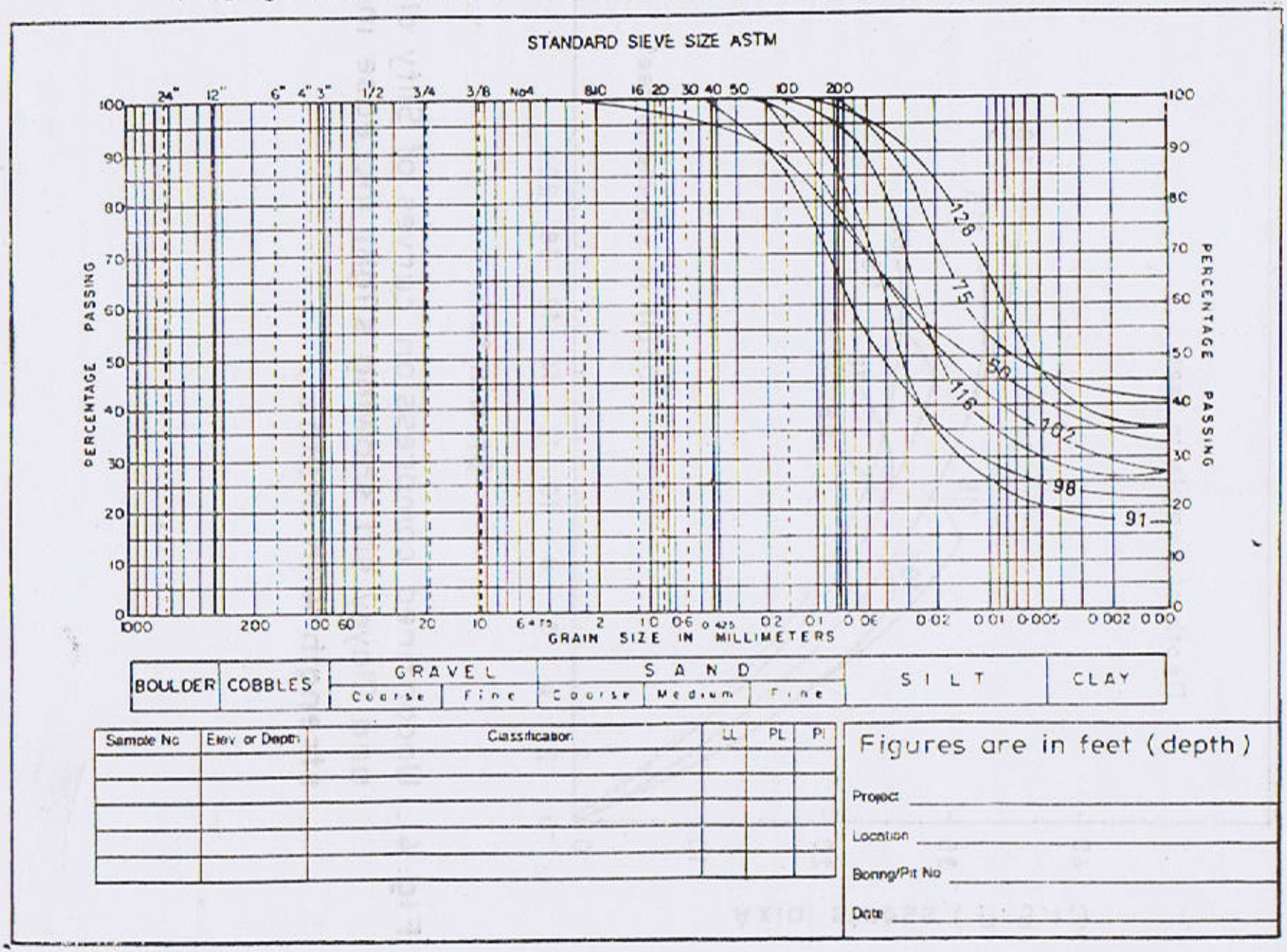

Sample No	Elev or Depth	Classification	LL	PL	PI

Figures are in feet (depth)

Project _____

Location _____

Boring/Pit No _____

Date _____

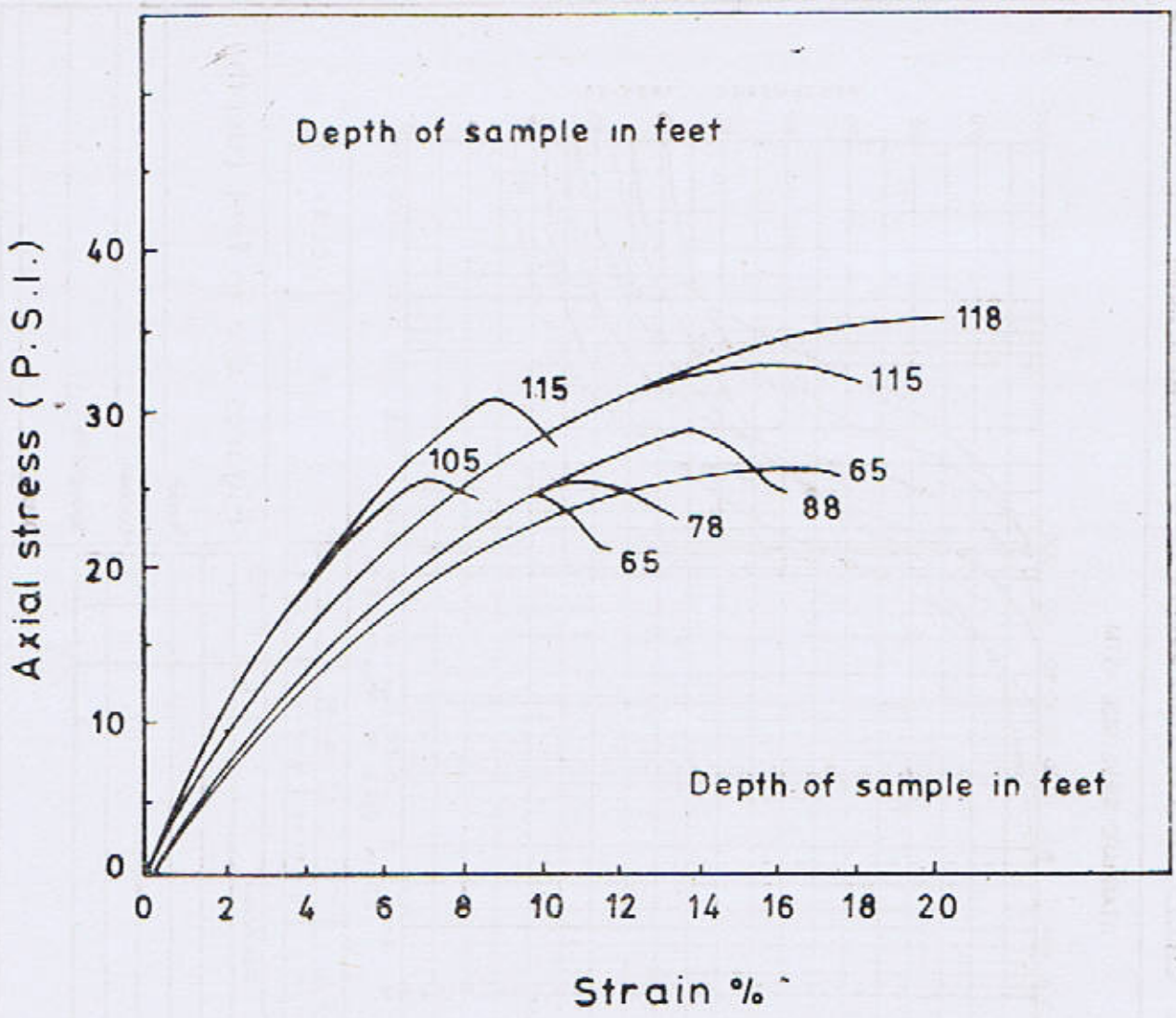

Fig. 4 - Unconfined compression curves of Silty clay and Clayey silt showing slight increase in strength with depth.

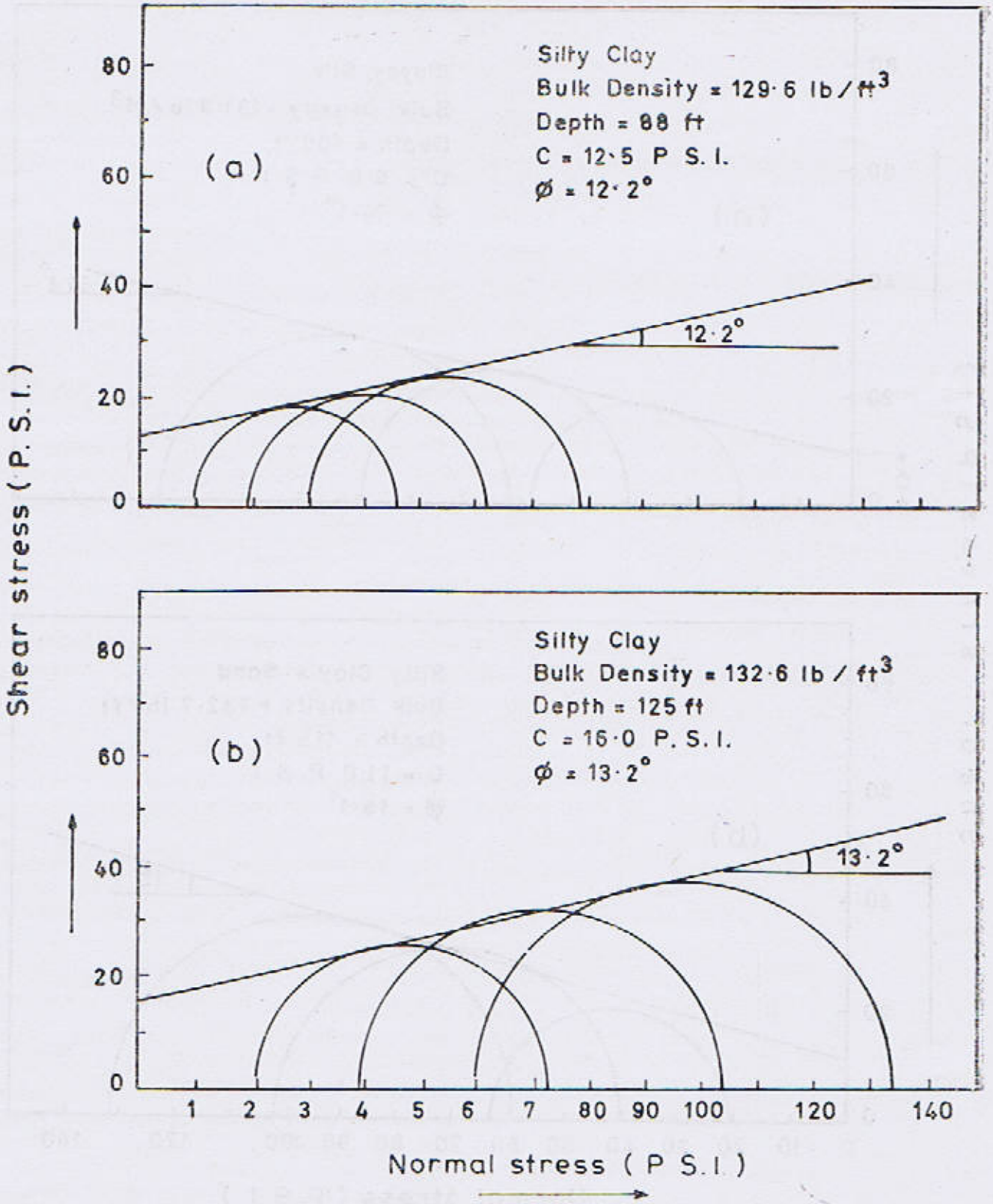

Fig. 5. a & b _ Triaxial compression tests on Silty clay showing higher values of C & ø with depth

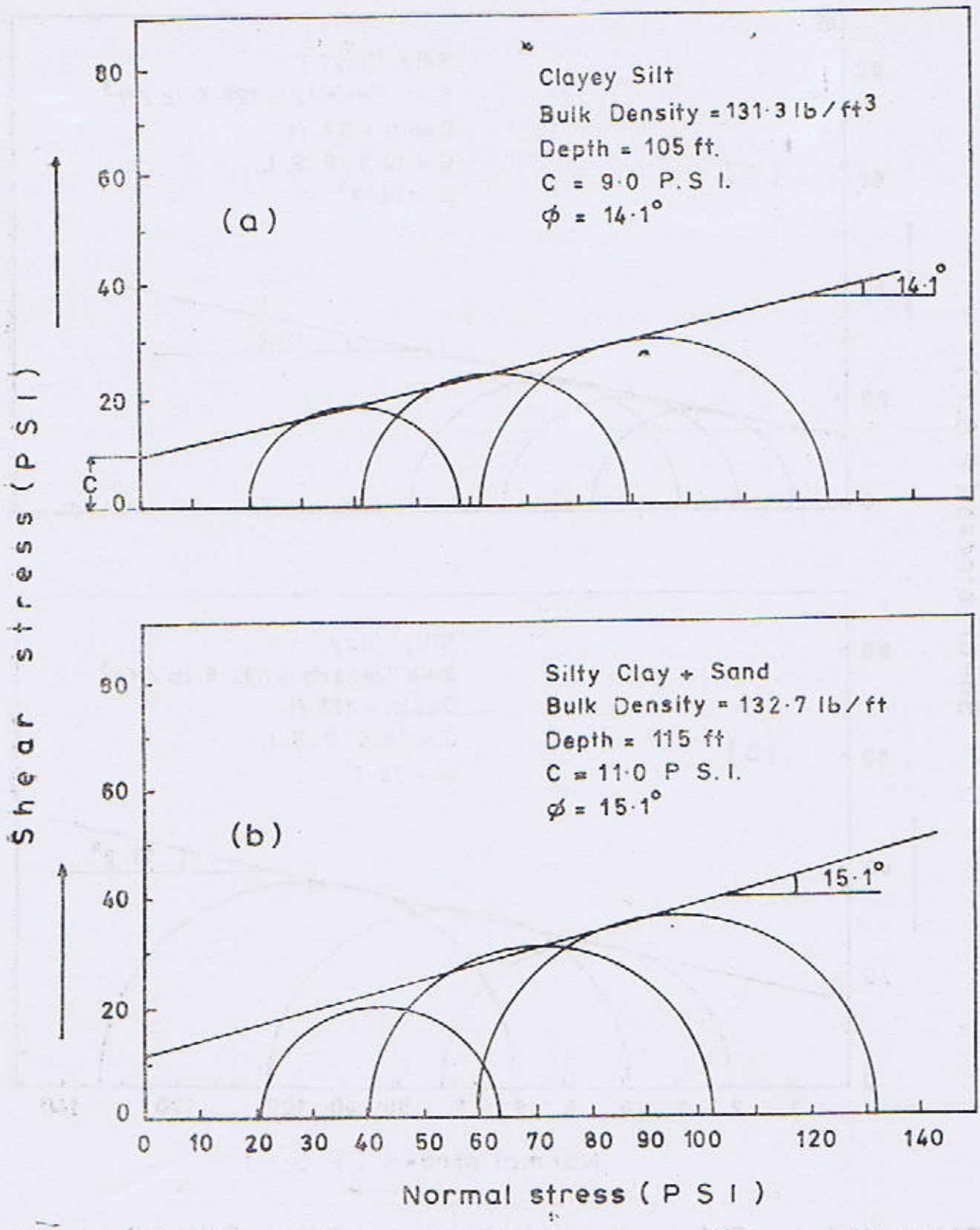

Fig. 6a & b_ Triaxial compression tests on Clayey silt and Silty clay with sand showing slight increase in friction

SUMMARY OF TEST RESULTS

BH/ DH/ Pit No	Sample No.	Location	Depth	No. of S.P.T. Blows	M/C %	Particle Size Distribution					Atterberg Limits %			Compaction Test %			Triaxial Compression Test			Shear Box Test		Consolidation Test			S.P. Gr	Unconfined Compression		Remarks
						0.005 mm Clay	0.074 mm Silt	4.76 mm Sand	76.0 mm Gravel	300.00 mm Cobbles	LL	PL	PI	Type	Max Dry Density Mg/m³	Optm m/c %	Density lb/ft³	C Psi	∅ Deg	C Psi	∅ Deg	Cv ft²/yr	Mv ft²/yr	K ft/sec		Cu Tons Sq./ft.	C p.s.i.	
1	-	Right	20.0	-	18.71	-	-	-	-	-	-	-	-	-	-	-	123.1	-	-	-	-	-	-	-	-	1.59		
		Abut-	23.5	22.0	22.16	41	58	1	-	-	42	28	14	-	-	-	122.3	-	-	-	-	-	-	-	-	-		
		ment	25.0	-	19.13	-	-	-	-	-	-	-	-	-	-	-	127.7	-	-	-	-	-	-	-	-	1.62		
			25.0	28	21.97	38	61	1	-	-	41	29	12	-	-	-	121.9	-	-	-	-	-	-	-	-	-		
			27.5	-	19.72	-	-	-	-	-	-	-	-	-	-	-	129.6	12.5	12.2	-	-	-	-	-	-	1.81		
			30.0	-	14.61	20	41	39	-	-	26	20	6	-	-	-	129.2	-	-	-	-	-	-	-	-	-		
			32.0	-	18.32	17.5	61.5	21	-	-	-	-	-	-	-	-	131.3	9.0	14.1	-	-	-	-	-	-	1.66		
			32.5	58	19.56	17	62	21	-	-	27	21	6	-	-	-	131.4	-	-	-	-	-	-	-	-	-		
			35.0	-	21.23	-	-	-	-	-	-	-	-	-	-	-	132.7	11.0	15.1	-	-	-	-	-	-	1.97		
			35.0	72	23.04	44	55	1	-	-	46	29	17	-	-	-	134.1	-	-	-	--	-	-	-	-	-		
			36.5	-	21.31	-	-	-	-	-	-	-	-	-	-	-	132.6	16.0	13.2	-	-	-	-	-	-	2.1		
			38.1	-	22.03	42	55	3	-	-	44	28	16	-	-	-	133.3	-	-	-	-	-	-	-	-	-		

SUMMARY OF TEST RESULTS

BH/ DH/ Pit No	Sample No.	Location	Depth	No. of S.P.T. Blows	M/C %	Particle Size Distribution					Atterberg Limits %			Compaction Test %			Triaxial Compression Test			Shear Box Test		Consolidation Test			S.G.	Unconfined Compression		Remarks
						0.006 mm Clay	0.074 mm Silt	4.76 mm Sand	76.0 mm Gravel	300.00 mm Cobbles	LL	PL	PI	Type	Max Dry Density Mg/m³	Optm m/c %	Density lb/ft³	C Psi	∅ Deg	C Psi	∅ Deg	Cv ft²/yr	Mv ft²/yr	K ft/sec		Qu Tons/sq.ft.	C p.s.i.	
2		Centre	15.5	10	26.7%	32	45	23	-	-	38	29	9	-	-	-	138.2	-	-	-	-	-	-	-	-	-	-	
		of	17.0	-	18.5	-	-	-	-	-	-	-	-	-	-	-	138.3	9.5	14.3	-	-	-	-	-	-	1.63		
		River	19.0	18	26.48	48	52	-	-	-	45	31	14	-	-	-	137.4	-	-	-	-	-	-	-	-	-	-	
		Gambia	21.0	23	24.12	45	43	12	-	-	43	30	13	-	-	-	132.2	-	-	-	-	-	-	-	-	-	-	
			23.5	>50	19.7	47	32	21	-	-	39	29	10	-	-	-	133.9	-	-	-	-	-	-	-	-	-	-	
			24.7	-	21.35	-	-	-	-	-	-	-	-	-	-	-	131.6	-	-	-	-	-	-	-	-	1.72		
			26.6	-	18.41	-	-	-	-	-	-	-	-	-	-	-	128.7	8.2	15.4	-	-	-	-	-	-	1.61		
			29.5	32	18.4	-	-	-	-	-	-	-	-	-	-	-	133.7	-	-	-	-	-	-	-	-	-		
			31.17	38	15.20	35	35	30	-	-	31	24	7	-	-	-	-	-	-	-	-	-	-	-	-	-		
			32.0	-	22.76	-	-	-	-	-	-	-	-	-	-	-	129.6	-	-	-	-	-	-	-	-	1.52		
			33.2	39	16.9	-	-	-	-	-	-	-	-	-	-	-	129.1	-	-	-	-	-	-	-	-	-		

SUMMARY OF TEST RESULTS

BH/ DH/ Pit No	Sample No.	Location	Depth	No. of S.P.T. Blows	M/C %	Particle Size Distribution					Atterberg Limits %			Compaction Test %			Triaxial Compression Test			Shear Box Test		Consolidation Test			S.P.	Unconfined Compression		Remarks
						0.005 mm Clay	0.074 mm Silt	4.76 mm Sand	76.0 mm Gravel	300.00 mm Cobbles	LL	PL	PI	Type	Max Dry Density Mg/m³	Optm m/c %	Density lb/ft³	C Psi	∅ Deg	C Psi	∅ Deg	Cv ft²/yr	Mv ft²/yr	K ft/sec	Gr	qu Tons/ Sq./Ft.	C p.s.i.	
3		Left	18.0	8	23.7	39	59	2	-	-	41	28	13	-	-	-	121.3	-	-	-	-	-	-	-	-	-	
		abut-	20.0	-	23.17	-	-	-	-	-	-	-	-	-	-	-	132.3	11.5	13.0	-	-	-	-	-	-	1.73	
		ment	21.0	32	19.43	-	-	-	-	-	-	-	-	-	-	-	132.2	-	--	-	-	-	-	-	-	-	
			24.0	29	22.80	41	57	2	-	-	44	30	14	-	-	-	130.1	-	-	-	-	-	-	-	-	-	
			27.0	59	22.12	-	-	--	-	-	-	-	-	-	-	--	-	-	-	-	-	-	-	-	-	-	
			27.5	-	17.81	-	-	-	-	-	-	-	-	-	-	-	132.3	14.5	13.3	-	-	-	-	-	-	2.13	
			28.5	67	-	13	69	18	-	-	34	26	8	-	-	-	134.6	-	-	-	-	-	-	-	-	-	
			30.25	-	18.03	-	-	-	-	-	-	-	-	-	-	-	129.7	-	-	-	-	-	-	-	-	-	
			31.0	-	21.65	-	-	-	-	-	-	-	-	-	-	-	132.4	-	-	-	-	-	-	-	-	1.63	
			33.0	48	17.76	-	-	-	-	-	-	-	-	-	-	-	-	-	-	-	-	-	-	-	-	-	
			33.5	-	23.12	-	-	-	-	-	-	-	-	-	-	-	133.7	10.5	15.3	-	-	-	-	-	-	1.91	
			34.5	37	-	13	63	24	-	-	33	25	8	-	-	-	-	-	-	-	-	-	-	-	-	-	
			36.0	63	24.87	25	70	5	-	-	39	28	11	-	-	-	135.3	-	-	-	-	-	-	-	-	-	
			36.5	-	19.61	-	-	-	-	-	-	-	-	-	-	-	131.3	-	-	-	-	-	-	-	-	2.20	
			37.5	52	-	31	66	3			39	27	12	-	-	-	131.2	-	-	-	-	-	-	-	-	-	
			38.5	67	22.17	-	-	-	-	-	-	-	-	-	-	-	132.5	-	-	-	-	-	-	-	-	2.15	
			39.0	58	22.56	-	-	-	-	-	-	-	-	-	-	-	132.1	-	-	-	-	-	-	-	-	-	

REFERENCES

ASCE, 1946. Pile Foundations and Pile Structure. Manual of Practical **37**, 72.

Bowles, J.E., 1987. Elastic Foundation Settlements on Sand Deposits, JGED, ASCE, **113**, (8) 846-860.

Brierley G.S. et al., 1979. Interpreting End Bearing Pile Load Test Results, ASTM, STP **670**, 181-198.

B.S., 1377 ; 1975. Methods of test for Civil Engineering Purposes. British Standard Institution, London.

Casagrande, A., 1948. Classification and Identification of Soils, Trans, ASCE, 113, 901-991.

Littleton, I. and Farmilo, M., 1970. Some observations on liquid limit values with reference to penetiation and Casagrande tests. Ground Engineering, **10**, (4).

Geol. Bull. Punjab Univ. 1992, 27, 14-27

GEOTECHNICAL INVESTIGATION OF BRIDGE SITES NEAR SEHWAN DISTRICT DADU INDUS HIGHWAY N-55 PROJECT

BY

MUHAMMAD HUSSAIN MALIK AND SAEED FAROOQ

Institute of Geology, Punjab University, Lahore 54590, Pakistan

AND

SYED NAJAM TAMEEM

Geoconsult Associates, Model Town, Lahore, Pakistan.

Abstract : *Undisturbed soil samples were collected using Pitcher and Denison samplers while rock cores were obtained using double tube core barrel. Based on the analysis of field and laboratory data the load carrying capacity of single pile were computed for the foundation design. Pile load tests are suggested to supplement the results.*

INTRODUCTION

The improvement and design of existing Indus Highway (N-55) is one of the major projects of National Highway Board. National Engineering Services Pakistan (Pvt.) Ltd. were appointed as consultants for the design of Dadu-Kotri section of N-55 project from Sann to Bhan Saiyidabad (Fig. 1). The geotechnical investigation for the proposed two new bridges at RD 34+348 km and 58+345 km near Sehwan were carried out. The site investigations comprised of drilling two boreholes (by rotary method) at each site in addition to insitu testing and sampling. Undisturbed soil samples were collected by using Denison and Pitcher samplers while SPT samples were collected as disturbed samples. Rock core samples through NX size double tube core barrel were also taken from three boreholes.

The field investigations were followed by the laboratory testing (B.S. 1377 : 1977 ; B.S. 410 : 1969 ; Head, 1976) of selected soil, rock and water samples.

This study covers details of subsurface investigations carried out at the proposed bridge sites near Sehwan Sharif, District Dadu and gives an evaluation of subscrface condition alongwith analysis of field and laboratory data. Recommendations for design of foundation of the project alongwith relevant geotechnical parameters are suggested.

The proposed bridge sites are located on Indus Highway N-55 Kotri-Dadu Section One at km 54-348, will be constructed over channel Aral Wah and the other at Km 58-345 will be constructed over channel Aral Tail. The existing bridges at these sites are very old and narrow and cannot cope with the enhanced traffic loads and are creating traffic problems.

METHODOLOGY

The subsoil investigations at the proposed sites were aimed at obtaining informations regarding geo-engineering character of subsoil at the location of each bridge. This was accomplished in the following manner :—

— Drilling of boreholes using straight Rotary Method upto a maximum depth of 30 meters below natural surface level.

- Performance of Standard Penetration Tests (SPTs) in the boreholes wherever required at a depth interval of 1.5 meter together with collection of SPT samples.
- Collection of undisturbed soil samples from boreholes using Pitcher and Denison Samplers.
- Collection of rock core samples from boreholes using double tube core barrel.
- Collection of water samples from boreholes.

Two boreholes were drilled at each site (Figs. 2 - 3). At Aral Wah bridge site, one borehole of 30 meters and other upto 21 meters was drilled. At Aral Tail site, the depth of boreholes were 10.6 meters and 14.6 meters.

Standard Penetration Tests were conducted in all the boreholes at a depth interval of 1.5 meters except where undisturbed sampling was attempted. These tests were performed in accordance with ASTM D1586. The SPT samples collected from Split Spoon Sampler were preserved for laboratory testing. The SPT blow count for last 30 cm penetration of the Split Spoon Sampler along the depth of boreholes was recorded in the logs of all the boreholes.

SAMPLING

From boreholes disturbed soil samples were collected at every 1.5 meter depth interval through SPT Split Spoon and undisturbed soil samples were collected through Pitcher and Denison Samplers and were properly preserved and labelled for laboratory testing. A double tube core barrel was used to extract undisturbed rock cores from the borehole to confirm bed rock. Rock coring was done in three boreholes.

Water samples from boreholes were collected to carry out chemical analysis. The results of these tests are presented in Table 1.

LABORATORY TESTING

Selected disturbed and undisturbed soil samples collected during subsurface investigations were tested in the laboratory for determination of physical, strength, consolidation and chemical characteristics (B.S. 1377 : 1975 ; Lamb, 1951).

All the testing was done as per ASTM Standards or the equivalent British Standards. The following laboratory tests were performed on the soil samples and are presented in the form of summary of test results in Table 2.

- Grain size analysis
- Natural moisture content
- Bulk density
- Atteberg's Limits
- Specific gravity
- Consolidation
- Unconfined compression (Table 3)
- Sulphate content (Table 4)
- Organic matter content
- pH value

Tables 1 to 4 present the results of laboratory tests which are discussed hereunder :

Sixteen respresentative samples from various substrata encountered at the sites were analysed for particle size distribution by carrying out sieve and hydrometer method (where relevant) analysis. The corresponding curves are shown in Figs. 5 and 6.

Eleven cohesive samples were tested for determination of natural moisture content. The results vary from 26.2% to 33.7%.

Bulk density of the five tested samples varied from 124.1 to 129.6 lb/cft.

Seven samples tested for determination of

Atterberg Limits yielded liquid limit (LL) from 28 to 39 with Plasticity Index ranging between 7 to 14. The samples tested can, therefore, be rated as possessing low to medium compressibility and plasticity characteristics.

Two rock core samples were put to specific gravity tests. The results range from 2.61 to 2.63.

One soil sample taken from the borehole No. AW-3 was subjected to consolidation test to study the settlement potential and the time versus settlement behaviour of the fine grained soil. From the analyses of test data, Compression Index was estimated as 0.106 with initial void ratio (e) of 0.520.

Three undisturbed samples were put to unconfined compression test. The results show failure strength ranging from 0.62 to 1.3 T/sq. ft. Fig. 4 shows higher strength of silty clay than clayey silt.

Four soil samples were tested for estimation of percent soluble sulphate content. The extent of sulphate content in the soil varies from 0.25 to 0.46%. This percentage warrants use of specific type of cement in foundation (Table 4).

The four samples were tested for the presence of organic matter content. The test results ranging from 0.85 to 1.93% are within the tolerable limits (Table 4).

SUBSURFACE CONDITIONS

Careful logging of all the boreholes was done to describe the lithology and stratigraphy of subsurface materials. Other relevant informations like boring details, SPT data and GWL were also noted on these logs.

SITE-1 (ARAL WAH) RD 54 + 348 KM

The stratigraphy reveals that the top layer of soil about 1.5 to 2.5 meter thick in both the boreholes is fill material, (comprising of silt, clay and sand mixture alongwith brick pieces), which is underlain by a layer of cohesive soil.

The cohesive soil layer is directly in contact with bed rock (siltstone) in AW-2 whereas a sand layer of about 4 meter was found in between cohesive layer and bed rock in AW-1. The bed rock in both the boreholes is siltstone (clayey) which is weak and slightly weathered to greyish and yellowish brown in colour.

DIYR-2 (ARAL TAIL) RD 58 + 345 KM

At this site, the overburden has a thickness of 5 meters in borehole AT-1 and about 9 meters in borehole AT-2.

The top soil in AT-1 is 2.8 meter thick, consisting of a mixture of sand, gravel and silt with some brick pieces. It is followed by a silty clay layer of 1.2 meter thickness, which is underlain by 1 meter of thick clayey silt deposit having some percentage of sand. The bed rock was found in contact with this layer at 5 meters depth which is silty sandstone.

In borehole AT-2, the top soil is sandy silt with little clay and is underlain by silty sand deposit of 5.1 meters thickness which is followed by a 1.6 meter thick clayey silt (with some sand) layer. The bed rock is encountered at 8.9 meters below NSL. It is sandstone, yellowish brown in colour, weak, fine grained and slightly weathered. Ferruginous material is also observed in core samples of this rock.

FOUNDATION DESIGN CONSIDERATION

Keeping in view the geotechnical character of subsoil at site and the type of structure, possibility of provision of pile foundation at the top or within the bed rock appears an appropriate consideration for the project.

Based upon the analysis of field and laboratory data, the load carrying capacity of single pile has been computed and is outlined below :—

LOAD CARRYING CAPACITY OF SINGLE RCC BORED AND CAST IN SITU PILE

The load carrying capacity of single pile has been estimated using the following formula by Tarzaghi and Peck (1967)

$$Qd = Qf + Qp$$

where Qd = Ultimate bearing capacity

Qf = Skin friction component

Qp = Point resistance

$Qp = \Lambda R^2 \times CNc$

and $Qf = 2 \Lambda Rhfs$

h = Length of pile embedded in supporting soil

R = Radius of pile

C = Cohesion which is taken as 0.5 times unconfined strength at the top of pile.

Nc = Bearing capacity factor which is taken as 9

fs = Unit skin friction, which is based on unconfined strength of cohesive soil

For the estimation of point resistance, the unconfined strength of rock has been used, whereas skin friction component has been calculated on the basis of data of the over lying soil deposits. The bearing capacity of piles of three different diameters has been calculated for both the sites which is given below :—

SITE-1 (RD 54+348) BOREHOLE AT-1

The calculation is based on unconfined strength of rock at 14.5 meters depth.

$$Qd = Qf + Qp$$

$$= 2 \Lambda Rhfs + \Lambda R^2 CNc$$

(A) for 22" dia pile

R = 0.92 feet

h = 38 feet (after excluding tops oil of 2.8 meters thickness)

fs = 800 (assumed for cohesive soil)

C = 0.5 × qu = 6.59 Ton/sq. ft.

Nc = 9

Qd = 78.45 + 157.7

= 236.15 Tons

Applying FOS = 3, we get allowable load

Qall = 78.7 Tons

(B) for 26" dia pile

R = 1.08 feet

Qd = 92.09 + 218.0

= 310.36 Tons

Qall = 103.36 Tons

(C) for 30" dia pile

R = 1.25 feet, Rs = 1.56 sq. feet

Qd = 106.59 + 290.67

= 397.26 Tons

Qall = 132.42 Tons

SITE-2 (RD 58+345 KM BOREHOLE AW-2

The calculations are based on unconfined strength of rock at 21 meters depth below NSL. The top soil of 2.3 m. has been ignored.

qu of rock at 21 meters = 15.91 Tons/sq. feet

C = 0.5 × 15.91 = 7.95 Tons/sq.

h = 61 feet

fs = 786 based on average unconfined strength of cohesive soil in borehole AW-2

(A) for 22" dia pile

$Qd = 2 \Lambda Rhf \times \Lambda R^2CNc$

$= 120.89 + 190.25$

$Qall = 103.7$ Tons for FOS of 3.

where $Qall$ = Allowable load.

(B) for 26" dia pile

$R = 1.08$ feet

$R2 = 1.17$ feet

$Qd = 141.91 + 262.99$

$= 404.91$

$Qall = 134.97$ Tons

(C) for 30" dia pile

$R = 1.25$ feet

$R2 = 156$ sq. feet

$Qd = 141.92 + 262.99$

$= 404.91$

$Qall = 134.97$ Tons

SITE	PILE DEPTH (M)	*ALLOWABLE LOAD ON SINGLE PILE* 22"	26"	30"
1	14.5	78.7 Tons	103.36 Tons	132.42 Tons
2	21.0	103.7 Tons	134.97 Tons	171.64 Tons

CONCLUSIONS

1. The allowable load carrying capacities given above are for single pile only. Due allowance must be made for group action of piles for proper foundation design.
2. The load on single pile is calculated using static formula. Therefore, these values must be confirmed through full scale pile loading test for better foundation design.

ACKNOWLEDGEMENTS

The authors are deeply indebted to M/s Geoconsult Associates, Lahore for providing the drilling data and extending laboratory facilities. They are also thankful to Mr. Zahoor Ahmed Qadri for typing the script.

REFERENCES

B. S. 410 : 1969 Test Sieves British Standard Institution, London.

B. S. 1377 : 1975 Methods of test for Soils for Civil Engineering Purposes British Standard Institution, London.

Head, K. H. (1976) : Particle Size Analysis forfine Grained soils Ground Engineering, 9, (7).

Lamb, T. M. (1951) : Soil Testing for Engineers, John Wiley, New York.

Terzaghi, K., Peck, R. B. (1967) : Soil Mechanics in Engineering Prectice, 2nd Ed. John Wiley, New York.

Wilson. S. D. (1970) : Suggested method of test for moisture-density relations of soils using Harvard compaction apparatus special procedures for soil and rock for Engineering purposes. ASTM STP 479.

TABLE—1

Chemical Test Restults of Water Samples.

B. H. No.	Sulphate Content	Organic Matter PH-value
AW-2	70 mg/litre	8
AT-1	478 mg/litre	7.8

TABLE—3

Unconfined Compression Test Results of Rock Samples

B. H. No.	Depth in Meters	M. C. %	Deviator stress lbs/sq. In.	Type of material	Remarks.
AW-2	20.8 to 21.0 m.	10.8	247.54	siltstone	Brittle failure
AT-1	14.40 to 14.50 m.	5.6	205.08	sandstone calcarueos	intermediate failure

TABLE—4

Chemical Test Restults of Soil Samples

B.H. No.	Depth in Metters	Sulphate Content %	Organic Matter %
AW-1	1.5	0.25	1.93
AW-2	1.5	0.28	1.56
AT-1	1.5	0.46	0.96
AT-2	1.5	0.38	0.85

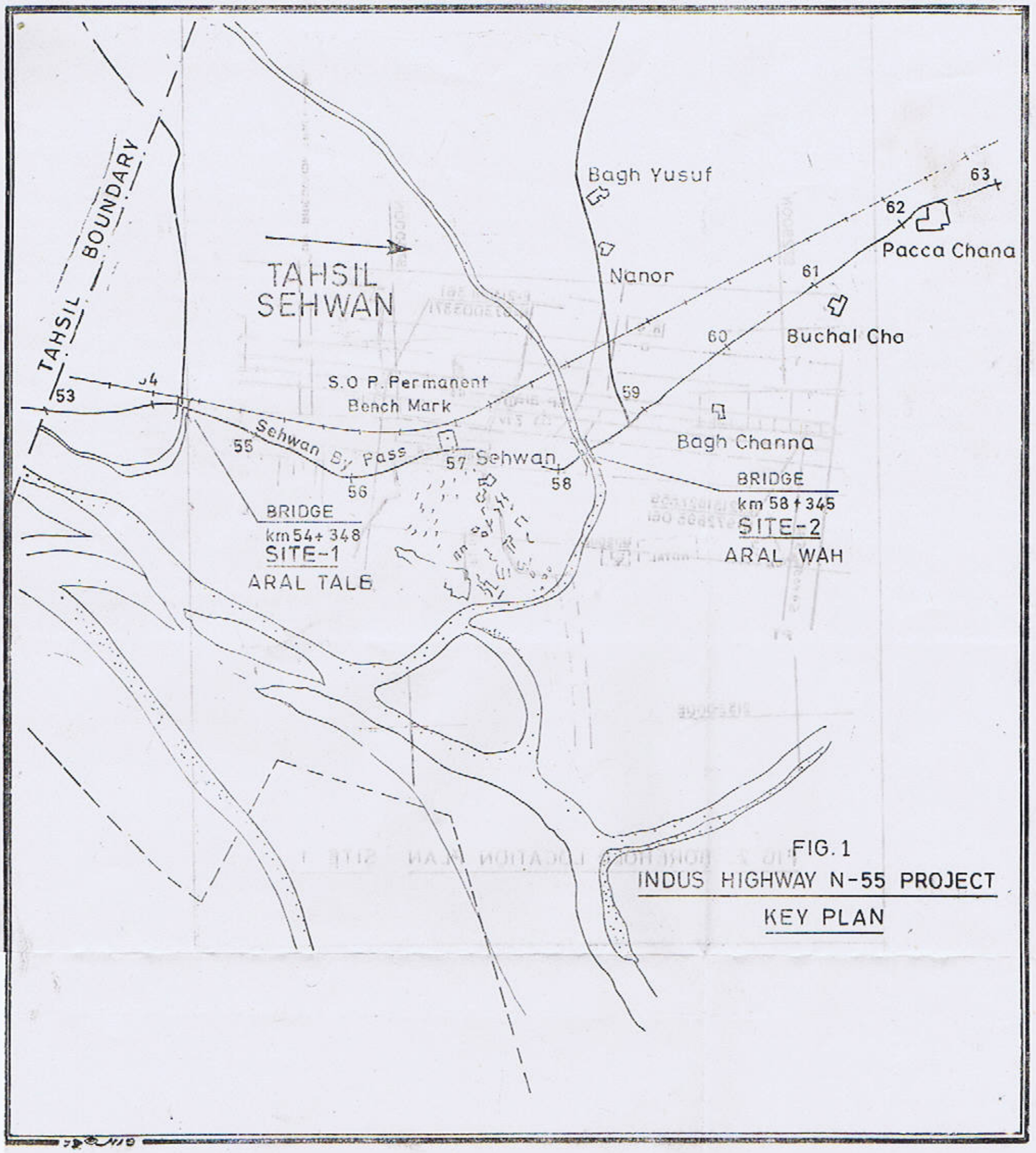

FIG. 1
INDUS HIGHWAY N-55 PROJECT
KEY PLAN

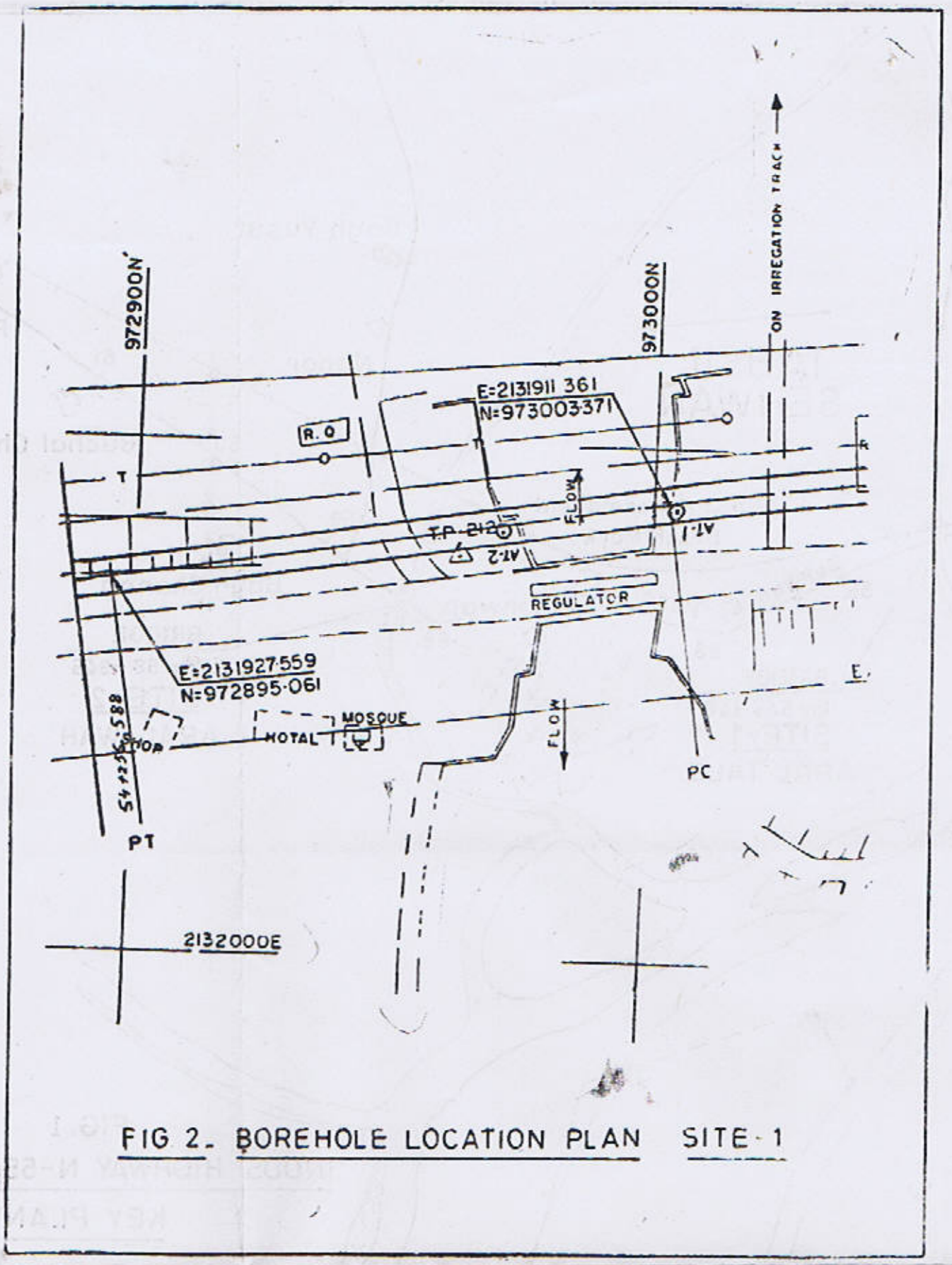

FIG 2. BOREHOLE LOCATION PLAN SITE-1

FIG.3 INDUS HIGHWAY N-55 PROJECT

BOREHOLE LOCATION PLAN

SITE - 2

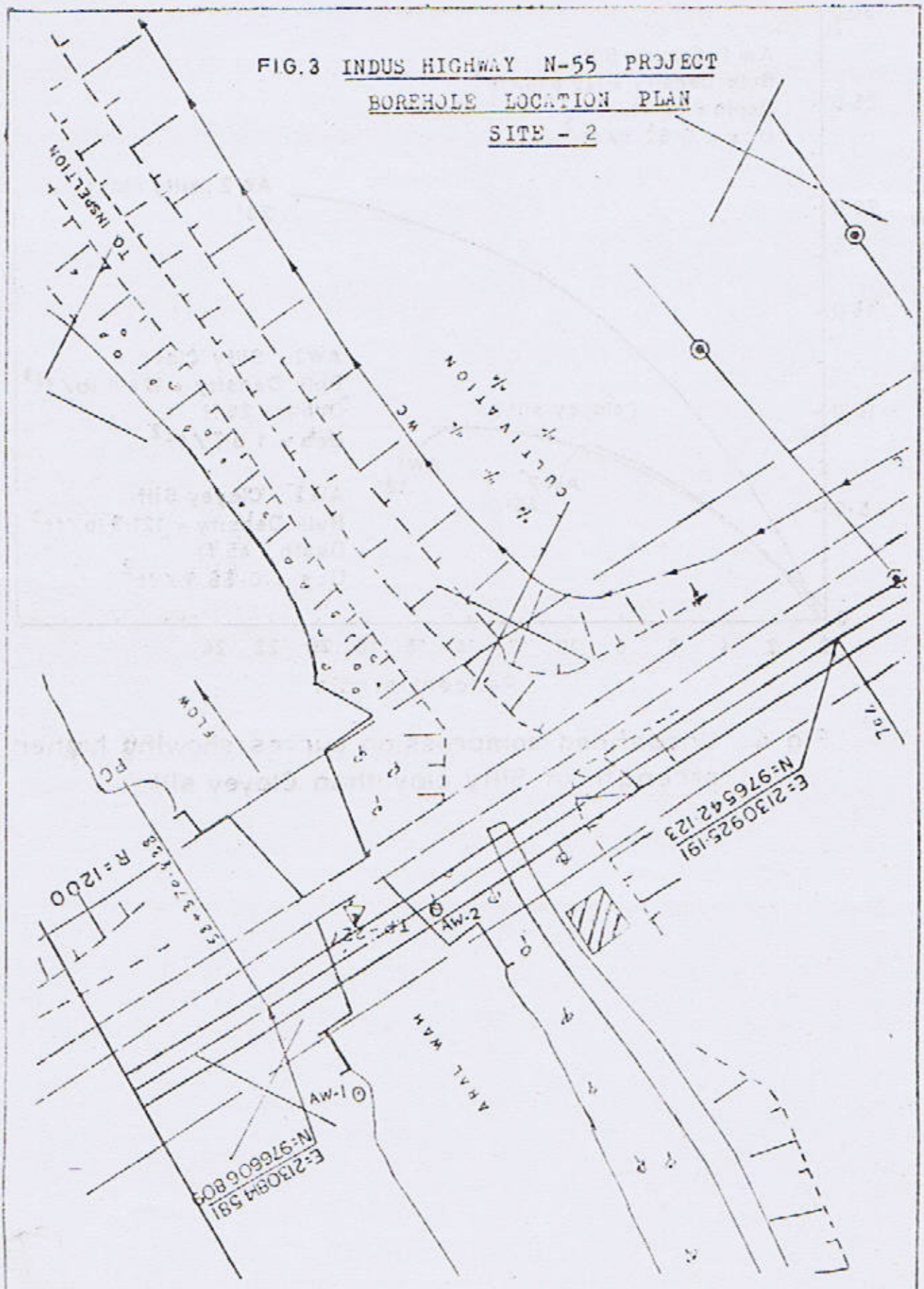

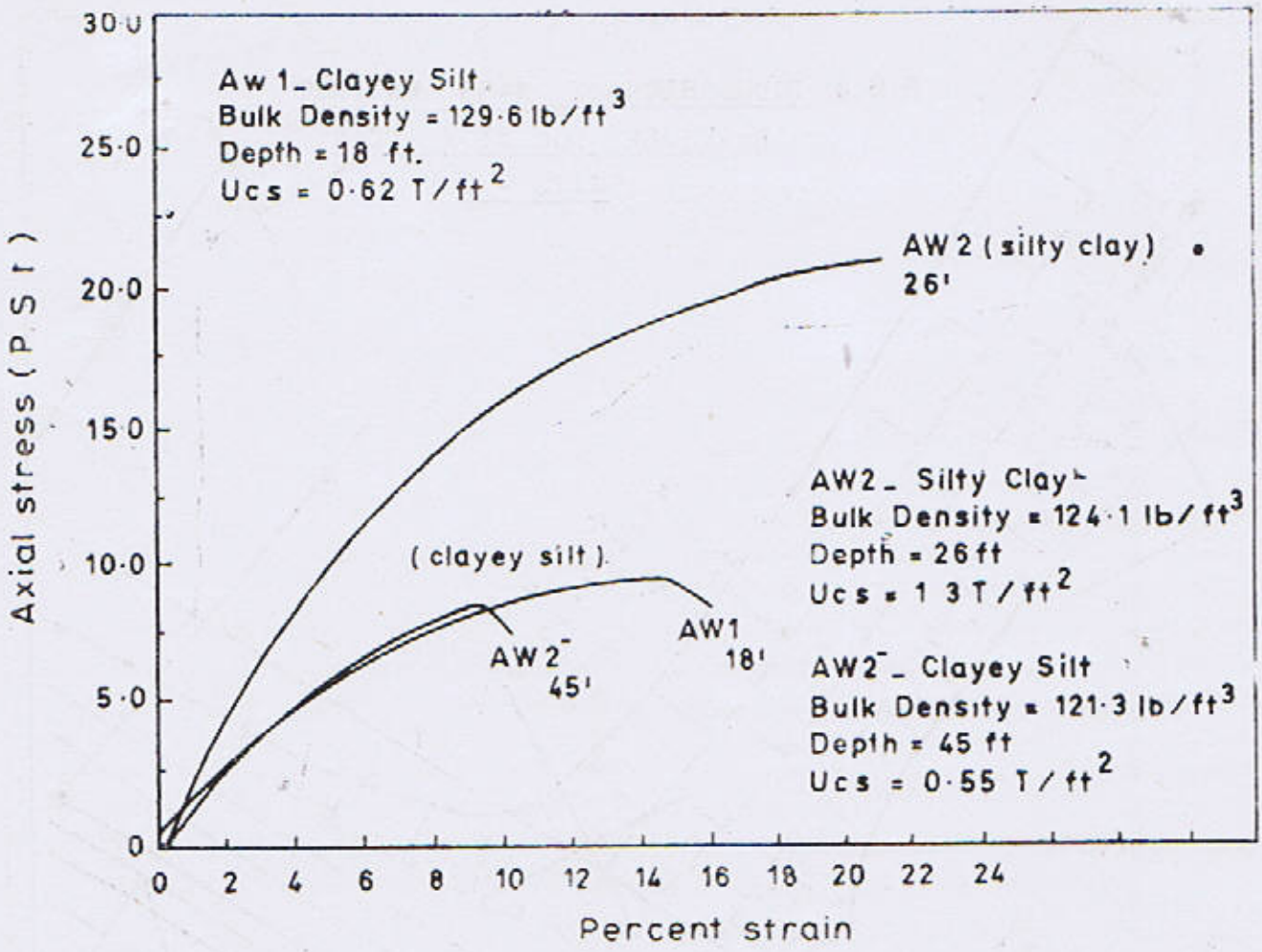

Fig. 4. Unconfined compression curves showing higher strength of Silty clay than Clayey silt.

FIG. 5. PARTICLE SIZE DISTRIBUTION CURVES

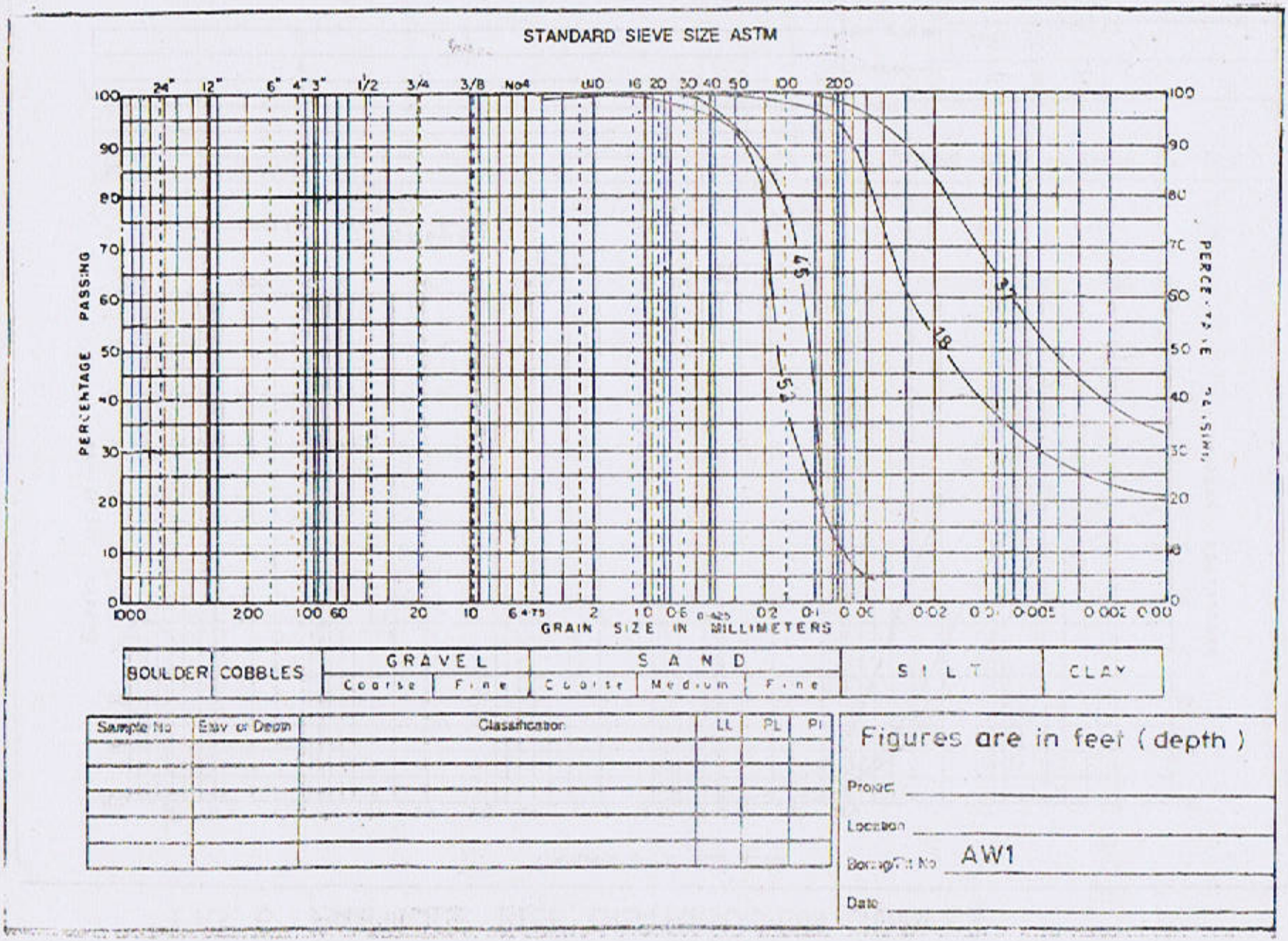

FIG. 6 PARTICLE SIZE DISTRIBUTION CURVES

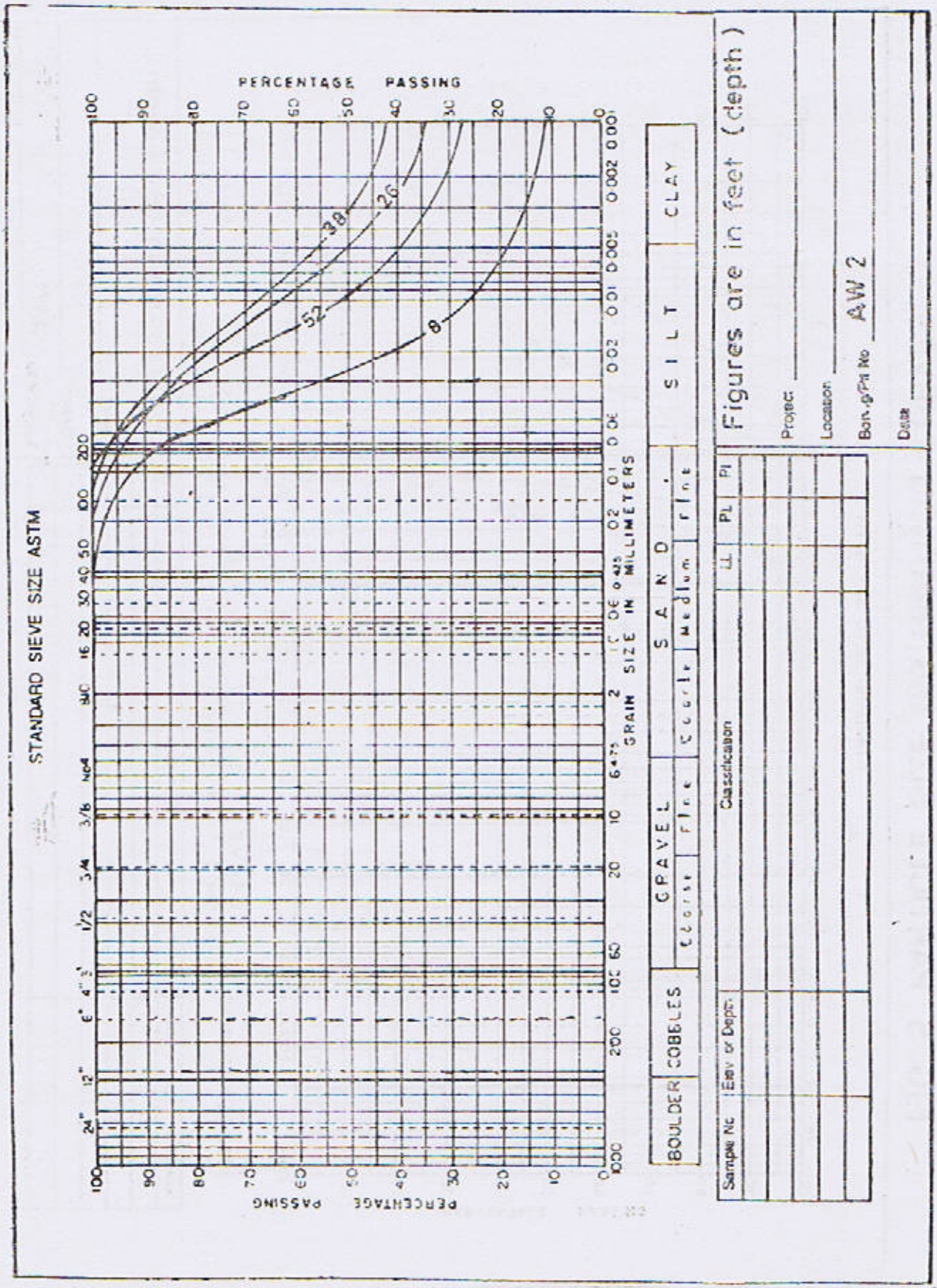

SUMMARY OF TEST RESULTS

BH/ DP/ Pit No	Sample No	Location	Depth	No. of S.P.T. Blows	M/C %	Particle Size Distribution					Atterberg Limits %			Compaction Test %			Triaxial Compression Test			Shear Box Test		Consolidation Test			S.P. Gr	Unconfined Compression		Remarks
						0.005 mm Clay	0.074 mm Silt	4.76 mm Sand	76.0 mm Gravel	300.00 mm Cobbles	LL	PL	PI	Type	Max Dry Density Mg/m³	Optm m/c %	Density lb/ft³	C Psi	∅ Deg	C Psi	∅ Deg	Cv ft²/yr	Mv ft²/yr	K ft/sec		qu Tons/Sq./Ft.	C p.s.i.	
AT-1	spt-2	ARAL TAIL RD 14+318KM	3.0	61		46	42	12	-	-	33	20	13															
	SPT-3		4.5	55		30	50	20	-	-	37	27	10															
	SAND STONE		14																					2.63				
AT-2	SPT-2		3.0	9		14	30	56	-	-																		
	SPT-3	ARAL TAIL RD 14+318KM	4.5	9		17	33	50	-	-																		
	SPT-4		6.0	5		15	33	52	-	-																		
	SPT-5		7.5	22		28	45	27	-	-																		

SUMMARY OF TEST RESULTS

BH/ DH/ Pit No	Sample No.	Location	Depth	No. of S.P.T. Blows	M/C %	Particle Size Distribution					Atterberg Limits %			Compaction Test %			Triaxial Compression Test			Shear Box Test		Consolidation Test			S.G.	Unconfined Compression		Remarks
						0.005 mm Clay	0.074 mm Silt	4.76 mm Sand	76.0 mm Gravel	300.00 mm Cobbles	LL	PL	PI	Type	Max Dry Density Mg/m³	Optm m/c %	Density lb/ft³	C Psi	∅ Deg	C Psi	∅ Deg	Cv ft²/yr	Mv ft³/yr	K ft/sec		cu Tons/ S.q.Ft.	C p.s.i.	
AW-1	UD-1		5.6	-	32.2	26	68	6	-	-	29	22	7				129.6									0.62		
	SPT-7	ASHL WAY RD 58,345 KM.	11.4	4		50	48	2	-	-																	
	UDS-8		13.8	-	33.7	-	5	95	-	-	Non plastic																	
	SPT-9		16	31		-	7	93	-	-																		
AW-2	UDS-1		2.6	-	26.2	14	74	12	-	-	Non	Plastic					125.9											
	UDS-2		8.0	-	29.7	47	47	6	-	-	39	25	14				124.1									1.3		
	SPT-7	ASHL WAY RD 58,345 KM	11.5	5		55	43	2	-	-																		
	UDS-3		14	-	29.9	26	66	8	-	-	28	20	8													0.55		
	SPT-9		14.7	5		25	69	6	-	-																		
	SPT-X		16.2	4		35	63	2																				
	SILTSTONE (COAL)		20.8																						2.61			

Geol. Bull. Punjab Univ., 1992, 27, 29-44

STRATIGRAPHY, STRUCTURE AND SEDIMENT-HOSTED MINERALIZATION OF THE DUDDAR DEPOSITS : CONTRASTS AND SIMILARITIES

By

ARSHAD MAHMOOD BHUTTA

Geological Survey of Pakistan, 68-D, Model Town, Lahore, Pakistan

AND

IRSHADUL HAQ QURAISHI

Geological Survey of Pakistan, Street 17,Block 2, KDA Scheme 36, Karachi, Pakistan

Abstract : *Zinc, lead and barite deposits, located in the southern part of the Lasbela-Khuzdar Belt in the Balochistan Province, form Duddar and Kharrari ore bodies within the Shirinab Formation along the northwestern edge of the Indo-Pakistan Plate. The Shirinab Formation, distinctly divisible into three members, and predominantly composed of limestone, shale and sandstone of lower to middle Jurassic age, hosts sulfide mineralization.*

All the ore bodies, located near each other, occur at different stratigraphic horizons of the Shirinab Formation. The Duddar are bodies ore hosted by the upper Anjira Member, whereas the Kharrari ore bodies lie in the lower Spingwar and middle Loralai Members. The mineralization, though similar qualitatively, differs in occurrence and attitude. At Duddar, the sulfide zones and the barite bodies are exposed mostly concordant to the enclosing lithologic units. The mineralization is distributed in an irregular pattern and occurs mostly along the structural sites in the Kharrari ore bodies.

INTRODUCTION

A number of lead-zinc-barite occurrences are found in a narrow, northerly trending Bela-Khuzdar Metallogenic Zone. The most significant deposits discovered to date are Gunga, Surmai, Malkhore and Shekhran in the Khuzdar area and Duddar—the area under study—on the eastern flank of the Mor Range which is the southernmost part of the Axial Belt (Fig. 1a, b). The Duddar deposits, all lying close to each other, include Duddar North, Duddar South, Kharrari North and Kharrari South ore bodies (Fig, 1c). The Duddar deposits, having grid reference Latitude 26° 50′ and Longitude 66° 55′ on Survey of Pakistan Topographic Quadrangle 35J/16, and located at about 200 Kilometers north of Karachi, can be reached from Karachi by turning eastwards at Khurkhera 85 Kilometers along the Quetta Highway, and travelling a further 110 Kilometes on a weather

dependent unpaved road. The entire trip takes about three and a half hours.

Since no detailed geological work existed on the sulfide mineralization in the Duddar area, the objective of this report is to describe in detail the host rocks, the ore mineralization the associated alterations, the pattern of mineralization and a comparative study of the different ore bodies. The large scale geological map of the Duddar area shows the Duddar and Kharrari ore bodies, their enclosing host rocks, the mineralized zones and the structural features (Plates 1, 2).

The mineralization occurs within a sequence of shallow marine, carbonates and clastic sediments of the Shirinab Formation These sediments are a part of the continental shalf deposits exposed on the western edge of the Indo-Pakistan Plate (Fig. 1a). These Mesozoic miogeosynclinal platform type sediments are predominantly composed of reefoid, colitic, pisolitic limestone with quartzose sandstone and shales.

The major tectonic evolution which occurred from late Cretaceous to early Tertiary and its close proximity to tha major fault systems such as Chaman and Ornach—Nal Transform Fault Zones are responsible for the complex physiography of the region. Significant thrust faulting folding and structural deformation occur.

REGIONAL STRATIGRAPHY

The Jurassic sequence with a brief account of the Cretaceous rocks and the Bela Ophiolites is described below :

Jurassic Sequence

The Jurassic sequence comprises the following formations :

1. Sember Formation
   (Late Jurassic to Early Cretaceous)
2. Shirinab Formation
   (Early to Middle Jurassic)

It consists of three distinct units :

1. Anjira Member
   Early to Middle Jurassic
   (Toarcian to Bajocian)
2. Loralai Member
   Early Jurassic
3. Spingwar Member
   Early Jurassic

Spingwar Member (Js)

The Spingwar Member (Js) is exposed on the west side of the area (Kharrari Ore body) and pinches out southwards (Fig. 1c). It is dominantly composed of sandstone intercalated with shales and sandy limestone which forms steep dips sharp protruding and elevated ridges. The sandstone is thin bedded, well laminated, occasionally thick bedded, orthoquartzitic, farruginous, calcareous, white to light grey, brown ; weathers rusty brown to yellowish and light grey, medium to coarse grained, medium hard and friable. It is internally laminated and locally cross bedded. Rare conglomeratic beds are quite compact. The intercalated shale is thin bedded, light grey to dark grey, soft and calcareous. The standstone grades into medium to thin bedded, laminated, fine grained, and grey to light grey, light brown calcareous standstone. The sandy limestone occurs in the upper of the sandstone beds. Quartz veinlets occur along fractures and joints. The member is mostly unfossiliferous, except some poorly preserved mollusc shells in the calcareous sandy limestone.

The Spingwar member of coarse to fine cross-bedded and cross-laminated detrital beds and sandy limestone indicates varied, unstable and shallow depositional environment.

Loralai Member (J1)

The Loralai Member (J1) exposed extensively is distinguished by its dark grey to black, intensely folded and almost uniform limestone lithology (Fig. 1c). It forms the highest cliff-making and sub-rounded ridges. It is medium to thick bedded, argillaceous, micritic, finely crystalline, resistant, colitic, pisolitic, highly fossiliferous, with bioturbated beds. Rusty weathering and orange to yellow mottling in the limestone beds are characteristic. Sub-lithographic, nodular limestone is interbedded occasionally. Ferruginous silty limestone beds, few in number, weather reddish brown or yellow. Dark grey interbedded sandy limestone and frruginoussilly limestone beds are present in the lower part. The content of the grey to blackish grey, soft, calcareous and intercalated shale increases in the upper horizons. The member contains abundant gastropods, lamellibranches, (*Pecten weqla, Girilla*), crinoids (*Isocrinus*), brachiopods (*Spiriferina* sp.), corals at different levels (Fatmi, 1986).

The Loralai Member was formed when the sea was shallow, warm and rich in carbonates. The presence of bioturbated and shelly limestone beds, the orange—yellow mottling with colitic, pisolitic textures suggest a shallow and stable condition with active current motions. The member (268 meters thick) grades conformably into the overlying Anjira Member.

Anjira Member (Ja)

The Anjira Member (Ja), a regularly alternating sequence of limestone and shale, presents a conspicuous greyish black and brown to khaki weathering outcrop, a step—like morphological pattern (Fig. 1c). The limestone is argillaceous, sub-lithographic, thin-bedded, fine-grained, olive groy to dark grey. The silty and non-calcareous upwards. The presence of ammonites in the basal part is a characteristic feature. The common fossils include brachiopods (*Spiriferina, Terebratula*), corals (*Montlivaltia* sp.), a lower and upper Toarcian, lower and middle Bajocian mollusca fauna includes ammonoids and nautiloids as *Bonieiceras, protogrammoceras, dactylioceratids, Cenoceras* (Zidi Formation, Khuzdar regioh, Fatmi, 1986). On the basis of fossils, a Toarcian to early Bajocian age is assigned to the Anjira Member.

The occurrence of alternating beds of limestone and shale suggests fluctuating conditions due to rejuvenation of the source area. The tectonic contacts have obscured the true thickness of the Anjira Member. However, it is 100 meter thick in the type locality near Anjira, 400 meters near Khuzdar (Fatmi, 1986) and more than 80 meters in the area.

Sembar Formation (Ksb)

(Late Jurassic to Early Cretaceous)

Comprising calcareous shale with widely spaced interbeds of siltstone, the Sember Formation (Ksb) crops out along the eastern flank of the Mor Range and occupies the Kanrach Valley. The shale is medium to thin-bedded, laminated and grey to dark greenish grey. It is flanky splintery, and characterized by a prominent pencil-like cleavage fabric and thin laminae. The siltstone is calcareous, medium to thin bedded, dark maroon, greenish grey to grey and hard. The greenish tinge is due to glauconite commonly present in the rocks. Calcite veins are common. The formation contains foraminifers, but the common fossils are belemnites, *Hibolithes pistilliformis, Hibolithes subfusiformis* and *Duvalia* sp. (Shah, 1977). Most of the invertebrate fauna is of Neocomian (early Cretaceous) age (Williams, 1959). The species range from late Jurassic (Tithonian) to Aptian. The basal beds have yielded late Jurassic (Kimmeridgian) cephalopods (Fatmi, 1986).

The formation is 126 meters thick near Khuzdar and 500-900 meters thick in the Windar Nai (Williams, 1959) where it is mostly covered by alluvium. The lower contact is marked by the post-Bajocian unconformity; there is a depositional gap extending from the upper Bajocian to Oxfordian. In places, the formation is in faulted contact with the underlying Anjira Member.

Cretaceous Sequence

The Sember Formation passes upwards into the overlying Upper Cretaceous Goru Formation, the Parh Limestone, the Mughal Kot Formation and the Pab Sandstone exposed along the eastern Mor Range in the KanrachValley and extends to the western Pab Range.

Bela Ophiolites

The Bela Ophiolitic Complex, extends from Khuzdar to the Arabian Sea Coast. It is exposed along the western flank of the Mor Range marked by a tectonic sheared contact (Fig. ib). It is part of a discontinuous zone of the ultramafic complexes and associated melanges emplaced during Paleocene-lower Eocene (Allemann, 1979).

The cumulative units of dunite, pyroxenite followed by gabbros, commonly resulting from the differentiation of the olivine, pyroxene and plagioclase, are frequently present. A variety of rock fragments of diabase, gabbros with reddish to white silicified, calcareous slates, isolated plagiogranites, serpentinite, harzburgite, and unoriented blocks of the Jurassic and Cretaceous rocks are repeatedly encountered. A major component of the ophiolitic suite consists of the ultramafic sheeted dykes, plagiogranites followed by pillow lavas.

REGIONAL TECTONICS

The sinuous, oroclinal fold and thrust belt originating due to the collision of progressively converging Indo - Pakistan Plate and the Eurasian Plate had a significant structural impact in the region.

The resulting present structural configuration of the Indo-Pakistan Plate is composed of the following significantly defined tectonic boundaries :

1. Convergent Boundaries : Characterized by the intracontinental collision, obduction and thrusting of the Indo-Pakistan Plate in the northern region with the Himalayas (Sarwar and Dejong, 1979) and by the subduction of the oceanic crust with a wide accretionary wedge in the southern margin of Makran and Chagai (Fig. ib ; (Farah et al., 1984).
2. Transform Boundary : Developed by a large north south strike-slip zone with minor thrusting (Wilson, 1965).

The massive continent-continent collision initiated in the late Eocene (Powell, 1979) caused counterclockwise rotation of the Indo-Pakistan Plate. This rotation developed early thrusting and folding of the miogeosynclinal sequence. The sinuous oroclinal bends (Carey, 1955) developed in the colliding boundaries. Important tectonic features formed on the northwestern margin of the sub-continent include the Khuzdar Knot, the Axial Belt, the Sulaiman Range and the Karachi Arc.

The Chaman and the Ornach-Nal Faults developed along the western margin of the Indo-Pakistan Plate when the convergence became more oblique and intensified. The north trending major Chaman Fault and its en echelon extension, the Ornach-Nal Fault

(Lawrence and yeats, 1979; Auden, 1974 are surface expressions of the currently active transform plate boundary between Indo-Pakistan and Afghan blocks. The Chaman Fault is closely analogous to the San Andreas Fault of California (Lawrence and Yeats, 1979) and possessing other similarities, such as, spatial and temporal distribution of seismicity and surface morphology of the fault trace (Armbuster et al., 1979).

The Khuzdar-Karachi region, comprising the area under study, is considered to have acted as an independent tectonic unit, which rotated counterclock wise during the northward drift of the subcontinent in Eocene time. The drag reoriented the pre-existing structures, changed strikes, dip directions and the fold axes, which are prominently displayed in the complexly folded Khuzdar Knot (Sarwar and DeJong, 1979). The southern part where the Karachi Arc was formed, dragged eastward as a coherent mass with the widening up of the area, the Bela Trough. The Bela Ophiolites exposed on the western flank of the Mor Range, were tectonically emplaced eastward onto the continental shelf during Paleocene (Allemann, 1979).

The Mor Range, (Fig. ib), extends for 160 kilometers, trending N W with an average width of 8 kilometers. It constitutes shallow marine carbonate and clastic sediments of the Shirinab Formation. These sediments have undergone a complex tectonic history involving early folding and thrusting during the early plate convergence. Later tectonic pulses caused thrusting and refolding of pre-existings tructures. The NW-trending thrust faults, strike slip faults, vertical faults all nearly parallel to the general bedding strikes, the numerous subsidiary faults, and the tectonic truncations of the stratigraphic units define clearly the structural complexity of the tectonized Mor Range. The tectonic influences experienced by the area are reflected by the northwest strike slip faults, intense foldings and fracture zones.

DUDDAR ORE BODIES

The Duddar North is the most promising of all the four are bodies exposed in the Duddar area. Having a northwest trending shape the North Body is about 285 meters long and 35 meters wide. It is enclosed within the steeply eastward dipping rocks of the Anjira member. The Duddar South, separated from the Duddar North by almost of 370 meters stretch of alluvium, is about 265 meters long and 30 meters wide following the same northwest trend. The development of a dark black to orange color silisified gossan over the Duddar South is a distinguishing feature. The Kharrari South is located at 0.65 km. north of the Duddar North. The Kharrari North is separated by 185 meters wide Kharrari Nai from the Kharrari South. Both the Kharrari ore bodies are occupied by rough terrain of the moderate to steep north trending linear ridges, separated by narrow valleys.

HOST ROCKS

The shallow marine shelf carbonate and clastic sediments of the Shirinab Formation are the host for the zinc lead-barite mineralization. They are monotonously exposed in the rugged elevated terrain of the Mor Range and extend northwards until they terminate in the Khuzdar Knot. The Sember Formation constitutes the eastern flank of the Mor Range. The sequence has a north—south trend with dips ranging from 45-75 degrees following the grain of the Mor Range.

Host Rocks of Dudder North Ore Body.

The Duddar North Ore body trends northwest and is about 285 meters along and upto 35 meters wide (Plate 1). It is enclosed within the eastward dipping Anjira Member (65-75 degrees). The Anjira Member comprises an alternating sequence of limestone and shales with minor intercalations of siltstone and mudstone. The limestone is typically fine grained and mudstone. The limestone is typically fine grained and weathers to a yellowish brown to golden color. The frame work constituents of the limestone includes the microcrytalline lime mud and subordinate sparry calcite ; the matrix is micritic. Sparry calcite occurs as coarse, fibrous, recrystallized, sublithographic spar. Replacement type, vein-filled, and pore-filled spar is also present. The lime mud suggests weak currents not strong enough to winnow away the lime ooze which remains as matrix. Fossiliferous limestone contains pelecypod fragments whose organic content has been replaced by sparry calcite. Ammonite fossils are present near the basal contact with the Loralai Member.

The siltstone and mudstone occur in thin laminations and intermixed with the unaltered limestone and with the lenticular bodies of barite. The siltstone is fine to medium grained, of dark grey to black in color with fine to coarse silica grains mostly of angular shape. They show variegated oxidation halos and alternating leached zone. Silicification is common with the multicolor mudstone.

Carbonaceous shales, exposed mostly along the fault zone on the southwest footwall in the main barite pit are sheared, fiscarbonaceous shales, as thin coatings, tabular and wavy scales, and veinlets is common.

Host Rocks of Duddar South Ore Body

The Duddar South Ore body, separated from the Duddar North body by almost a 370 meters alluvium stretch is about 265 meters long and upto 30 meters wide is oriented in a northwest trend (Plate 1). Like the Duddar ore body, the mineralization is hosted by the Anjira Member. The conspicuous silicified gossan developed over the sulfide zone is hosted by siltstone, clays and limestone which are silicified. The framework of the allochem limestone does not vary much from that of the Duddar North body.

The limestone is composed of the microcrystalline lime mud. Recrystallized spar calcite occurs as vein fillings with brecciated rock fragments. Metastable aragonite-filled veins are occasionally observed. A thin section taken from the sediments associated with the gossan shows the presence of intraclasts, which are the penecontemporaneous reworked carbonate sediments from within the area of deposition. This indicates the same depositional cycle as the sparite.

The siltstone is fine to medium grained associated with the shales and mud stone. Dissolved molds of pelecypod shell fragments are at times replaced by spar calcite. Presence of algal stromatolite of blue green algae showing replacement by calcite and lime mud suggests a tidal flat environment. Fossil fragment mostly of molluscs also suggest shallow water conditions.

Host Rocks of Kharrari South Ore Body

The Kharrari South body, 0.65 km. north of the Duddar North body, is hosted by rocks of

the Loralai and Spingwar members (Plate 2). The contact between the members is marked by a high angle thrust fault. The limestones of the Loralai Member are typically dark grey to black, medium to thick bedded and massive at places, biomicrite and oomicrite having microcrystalline matrix. Orange to yellow mottling is characteristic of the limestone on weathering. Intermixed zones of nodular limestone are present. Reddish brown to yellow, ferruginous marly and calcareous beds are prominent and usually follow the general bedding and are occasionally mineralized with galena and barite. The limestone is fossiliferous commonly consisting gastropods, brachiopods, bivalves and corals. Sandy limestone and grey calcareous shales are interbedded. The bioturbated shelly limestone beds with comicritic texture indicate shallow and stable conditions with low energy currents.

The Spingwar Member in the Kharrari South is predominantly composed of thin to medium bedded, orthoquartzitic, ferruginous, calcareous. medium to coarse grained sandstone. It is well laminated, cross bedded and ripple marked in the area. Grey, soft and calcreous shale is intercalated with sandstone. Minor silstone and shale is non-calcareous at places. The framework constituents of the sandstone are predominantly monocrystalline and polycrystalline quartz which are medium to coarse grained.

The sandstone sequence characterized by cross-bedding and cross-lamination, detrital beds; sandy limestone indicates varied, unstable, shallow marginal conditions.

Host Rocks of Kharrari North Body

The Kharrari North body, separated from the Kharrari South by the 185 meters wide Kharrari Nai (stream) is hosted by the Spingwar and Loralai Members which are the northward extension of the same lithologies from the Kharrari South (Plate 2). The ferruginous beds are more prominently exposed and are mineralized with rare sporadically distributed galena and barite.

Structure in the Duddar Area

Regional tectonics have subjected the area to strctural complexities reflected by the numerous faults, fractures and folds both in the ore bodies and the adjoining host rocks (Plate 1).

Rocks exposed just to the west of Duddar North form a straight westwards tapering ridge show prominent anticlinal and synclinal folds plunging steeply northwest. The axial plane attitude, of these conical folds, ranges from N30W to N45W with 50 SW to vertical inclinations. Thrust and vertical faults are also present in these rocks, and at some places mark tectonic contacts within the Jurassic sequence. Slickensides, mostly horizontal have been observed along the fault surfaces. On the ridge to the northeast, the Loralai Member overlies the Anjira Member indicating a thrust fault. In the vicinity just north of ore body, intraformational thrust and vertical west dipping faults, were observed in the Sember formation.

A vertical strike slip fault (a-a, : Plate 1), running northwest the footwall of the ore body has sheared the carbonaceous shales and the contact rocks. Alkaline springs are presant along the fault trace. Barite, exposed in the open-pit, shows asymmetrical foldings. These

minor folds, about 20 to 50 cm broad and closely spaced, are developed near the northeast pit wall. The folds commonly trend N45W and plunge 45-65 degrees northwest. The cleavage and cross-joints have 40 NE to 60 NE inclinations. Minor faults and fractures are present along the contacts.

Structure in the Kharrari Area

There are significant differences in structures mapped in the Kharrari areas to thos seen in the Duddar region. The main structural components observed in the Kharrari area are the system of thrust, strike slip, and numerous subsidiary faults, fractures and shear zones, and narrow folds (Plate 2).

A major high angle thrust fault (a-a' : Plate 2), traversing the middle part of the Kharrari South with a wavy north-south, trend is traceable for about 300 meters. It is truncated by a northwest trending fault (b-b' : Plate 2) at its northern extremity, whereas its southern extension is covered by alluvium. This thrust fault (a-a' : Plate 2) also marks the contact between the Spingwar and Loralai Members. Both middle and the northern parts of Kharrari North are highly faulted and folded. There a pattern of northwest-trending faults (c-c'), minor faults (d-d', e-e', f-f') and fractures (g-g', h-h' : Plate 2) has been observed. The faults (c-c' : Plate 2) and most of the fractures terminate southeastward at 35 - 40 degree angles against the major thrust fault (a-a' : Plate 2). The narrow and linear, northnorthwest and northwest trending, anticlines are approximately 15-50 meters broad. Those developed in the Spingwar sandstone, are common in the middle Part. Usually, the eastern flanks of the anticlinal folds are truncated by intraformational faults. A few sinistral shear fractures showing enechelon structures (like i-i' : Plate 2) are developed in the sandstone. The low lying ridges, in the SE part are highly folded and faulted. The microscopic structures showing intense floding and faulting appear analogous to the major structures.

The two north trending main faults, (j-j', k-k' : Plate 2) cross the entire length of the Kharrari North and extend beyond the northern limits of the area (Plate 2). The thrust fault (j-j' : Plate 2), traceable for about 200 meters, has produced a sheared zone in the central part of the area. The other thrust fault (k-k' : Plate 2), passing over the steep hill-top on the eastern side, marks the contact between the Spingwar and Loralai Members. The Loralai Member wedges against the faults (k-k', l-l' : Plate 2).

MINERALIZATION

Duddar North Ore Body

The Duddar North ore body is the most promising so far found in the area, with sphalerite and galena as the principal ore and marcasite and pyrite as the abundant sulfide gangue minerals. Barite is widely exposed and occupies the central part of the Duddar North body, and is nearly concordant with the general bedding trends (Plate 1). The exposed mineralized zones vary in thickness from 2-5 meters. They are oxidised and altered particularly adjacent to both the upper and lower contacts of the barite. The barite has been mined intermittently on a small scale by excavating long, narrow (averages 6 meters in width), parallel-sided deep pits (about 30 meters deep), in the northwest part of the

Duddar North Ore Body.

The footwall oxide zone, on the southwestern side, overlies the fissile carbonaceous shales marking a thin contact zone with the non-calcareous siltstone and intercalated with an oxide zone (0-5 meter thick), is followed by a fractured limestons (1 meter) and a siliceous gossan (1.5 meters). this mineralized zone cannot be extensively traced downward in the pit. Near the middle of the footwall a small patch of siliceous limestone nodules (20 cm diameter) mixed with light brown calcareous shale is observed. Black fissile thinly layered gypsiferous shales and a network of criss-crossing veinlets of calcite and yellow oxides are noted along the southwest wall. Shales from the contact zone with the overlying barite. The barite, varying form 3.5 to 16 meters in thickness is medium to thinly bedded. It is hard, compact fine-grained, dark grey and intercalated with thin black shales. Marcasite and pyrite, occur as finely disseminated, micro-veinlets, thin laminations and clusters. Cerussitic white alterations, probably after galena, are observed as surface coatings or fracture fillings. The steeply dipping wall-rocks (2-3.5 meters thick) on the east side are intercalated with the barite and in the southeast part are partly altered, oxidized and contain unaltered limestone and barite, silicified yellowish brown clays and mudstone. A thin zone of barite crops out separately and parallel to the main barite body along the northeast side, and extends to the north-west part of the ore body. The hanging wall oxide zones, on the northeast side, are moderately to intensely oxidized and contain unaltered limestone and in some places thinly layered barite. The oxide zones comprise limonite, hematite, goethite and altered sulfides in stringers, veinlets, fracture-filled veins and fine disseminations. Sphalerite and galena are mostly leached out and consequently are rarely seen at the surface. Box works, vug and solution cavities can be seen in these zones. The variegated alteration and oxidation halos of orange-brown and reddish to maroon color capping the mineralized zones are conspicuous.

Duddar South Ore Body

The characteristic feature in the Duddar South body is the development of a prominet siliceous gossan of dark maroon to black desert varnish. The principal gossan exposure is in the southeast part, but extends to the northwest where it overlies the barite zone (Plate 1). The gossan is highly silicified, rarely calcareous, limonitic, ferrugenous, cellular and porous. Ift is associated with siltstone and siliceous clays. The barite, unlike the barite in Duddar North, is not extensively exposed. It is light grey to white, and has ill-defined banded structucre. Marcasite and pyrite are rarely associated with barite at the surface. Minor oxidation along fractures and surfaces is observed. Lens-shaped oxide zone, extending 70 meters in northwest direction in the northwest part of the ore body, is up to 8 meters thick. It is bordered by barite, in a small, abandoned pit. A slumped zone of lens shaped unaltered limestone (15x 35 cms) embedded in non-calcareous shales occurs at the contact between the oxide zone and the barite. The northeast contact zone between gossan and unaltered limestone is marked by a 3—6 cm thick, silicified siltstone. Along the northeast wall small patches of silica sinter crop out.

Kharrari Ore Bodies

The Kharrari ore bodies occur on north-trending linear ridges, separated by narrow valleys. The moderate to steep slopes of the linear ridges are commonly covered by slumped boulders, a characteistic weathering feature of the Jurassic rocks in the region.

Field observations favour a strong structural control for the mineralization in the Kharrari ore

bodies. The mineralization observed is mainly localized along faults, fractures, shear zones and relate structural features. The shear zones developed along the thrust fault are mineralized with barite and specks of minor galena. The mineralized pattern of northwest tending veins of barite, quartz and sulfide zones lie in the faults and fractures. The barite (g-g' : Plate 2) and quartz veins (h-h' : Plate 2) are lenticular and follow an enechelon fracture-pattern. They thicken in the middle and thin out along their northwest and southeast linear extensions, following an enechelon fracture-pattern (Plate-2). The thin linear veins, extending discontinuously over the distances of 50-100 meters, in north-northwest directions, are aligned with the fracture or fault zones. In the southeast part, where the folded and faulted Loralai limestone crops out, a gossan has developed with barite and rare galena.

A zone of siliceous gossan, containing barite, galena and altered sulfides, forming lens-shaped bodies, is traceable for a distance of about 200 meters along the fault in the middle part of the Kharrari North (Plate 2). The fractures and subsequent minor faults are also mineralized.

The mineralization, distributed in an irregular pattern, is qualitatively similar to, but differs in the form of occurrence, from the Duddar ore bodies. The mineralization in the Duddar area is restricted to the upper stratigraphic unit of alternating limestone and shales. The mineralization occurs predominantly in nearly parallel zones and disseminations, which follow the general strike of the units. These tabular deposits show no sign of being crossed by later solutions or sulfide veins. In case of the Kharrari ore bodies, which occur in the lower unit of sandstone and the middle unit of thickly bedded limestone, the mineralization is distributed in an irregular pattern and is associated with various structural features.

Recent Siliceous Sinter

A number of modern siliceous sinters can be observed occuring along several of the faults in the area. A conspicuous siliceous sinter crops out along the intersection of a main fualt (a-a' : Plate 2) and a northwest trending fault (c-c' : Plate 2) in the Kharrari South ore body. Sinters of smaller size are also present in the other ore bodies. These sinters are compact, hard and brines and salty solutions are oozing from them even today. Minor fractured filled oxidation is seen in association with the sinters.

CONTRASTS AND SIMILARITIES

The contrasts and similarities between the Duddar and Kharrari ore bodies, from the field observation are summarized in Table 2.

ACKNOWLEDGEMENTS

The authors are indebted to Mr. Waheeduddin Ahmad, the then Director General Geological Survey of Pakistan, for his guidance to execute the project and to Mr. Nayyar Ahsan, Assistant Director. for his participation in the field.

REFERENCES

Allemann, F. 1979. Time of emplacement of the Zhob Valley Ophiolites and Bela Ophilites : *in* Farah, A., and DeJong, K.A., eds., Geodynamics of Pakistan. Geol. Surv. Pakistan, 215-242.

Azam, S., Tariq, M.A., and Subhani, A.M., 1988. Geology of Duddar, Quadrangle 35 J/16 Lasbella District, Baluchistan : Geol. Surv. Pakistan, Inf. Rel. 300.

Armbruster, J., Seeber, L., Quittmeyer, R., and Farah, A., 1979. Seismic network data from Quetta, Pakistan : The Chaman Fault and the fault related to the 30 May 1935 Earthquake : Geol. Bull. Peshawar Univ. **13**, 129-142.

Auden, J.B., 1974. Afghanistan-West Pakistan in Mesozoic Cenozoic Orogenic Belts. Data for Orogenic Studies : Geol. Soc. London, Spec. Publ. **4**, 235-253.

Carey, S.W., 1955. The Orocline concept in Geotectonics : Papers and Proc. Royal Soc. Tasmania, **89**, 1407-1422.

Farah, A., Lawrence, R.D., and DeJony, K.A., 1984. An overview of the tectonics of Pakistan : *in* Haq, B. U., and Milliman, J.D., eds., Marine Geology and Oceanography of Arabian Sea and Coastal Pakistan, Van Nostrand Reinhold Company, 161-176.

Fatmi, A.N., 1977. Mesozoic of Pakistan : *in* Shah, S.M.I., ed., Stratigraphy of Pakistan, Mem. Geol. Surv. Pakistan, **12**, 29-56.

Fatmi, A.N., Hyderi, I.H., Anwar, M., and Mengal, J.M., 1986. Stratigraphy of "Zidi Formation" (Ferozabad Group) and "Parh Group" (Mona Jhal Group), Khuzdar District, Balochistan, Pakistan : Rec. Geol. Surv. Pakistan, **75**, 32 p.

Jankovic, S., 1983. Exploration and preliminary evaluation of the lead-zinc-barite, deposits Lasbela-Khuzdar District, Balochistan, Final Report, (Unpublished) Pak/79/016, UNDTCD/ UNDP, 158 p.

Hunting Survey Corporation Limited, 1960. Reconnaissance Geology of part of West Pakistan, A Columbo Plan Co-operative Project Report, Government of Canada, Toronto: 550 p.

Lawrence, R.D. and Yeats, R.S., 1979 Geological Reconnaissance of the Chaman Fault in Pakistan : *in* Farah, A. and DeJong, K.A., eds., Geodynamics of Pakistan, Geol. Surv. Pakistan, 351-357.

Powell, C. McA., 1979. A speculative tectonic history of Pakistan and surroundings : Some constraints from the Indian Ocean : *in* Farah, A., and DeJong, K.A., eds., Geodynamics of Pakistan, Geol. Surv. Pakistan, 5-24.

Sarwar, G. and DeJong, K.A., 1979. Arcs, Oroclines, Syntaxes, the curvatures of mountain belts in Pakistan : *in* Farah, A. and DeJong, K.A., eds., Geodynamics of Pakistan, Geol. Surv. Pakistan, 341-349.

Shah, S.M.I., 1977. Stratigraphy of Pakistan : Mem. Geol. Surv. Pakistan, **12**, 138p.

Shcheglov, A.D., 1969. Main features of endogenous metallogeny of the southern part of West Pakistan : Mem. Geol. Surv. Pakistan, 7. 3—14.

Williams, M.D., 1959. Stratigraphy of the lower Indus Basin, West Pakistan : Proc. 5th World Petroleum Cong., New York, Sec. 1, Paper 19, 377-390.

Wilson, J.T., 1965. A new class of faults and their bearing Continental Drift : Nature' **207**, 343-347.

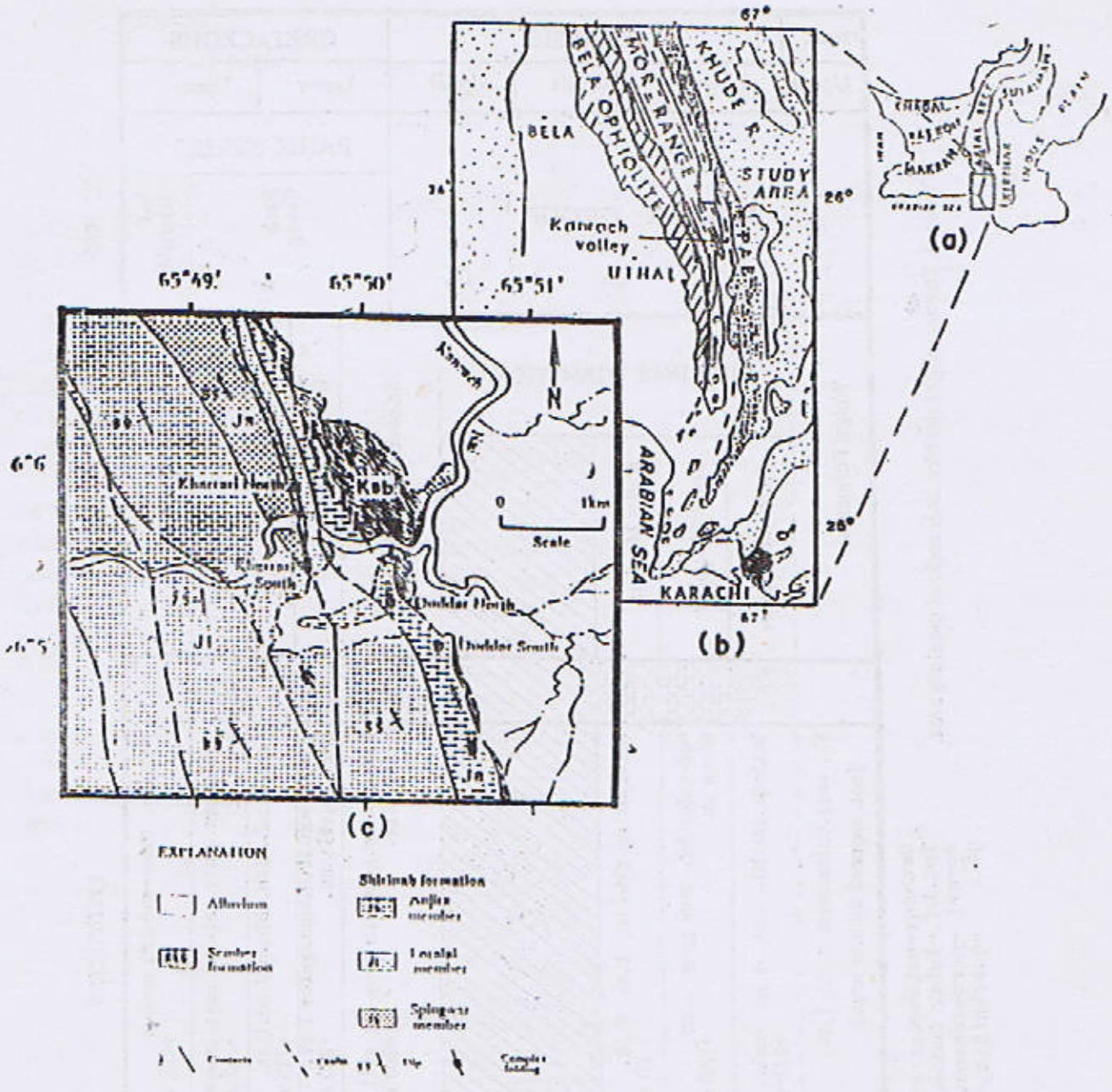

Fig. 1 Index map showing the location of the study area
a) In the southern part of Axial Belt, south-eastern Balochistan and
b) On the eastern flank of Mor Range (small rectangle)
c) Regional geological map showing the relative positions of Duddar North, South, Kharrari North and South ore bodies.

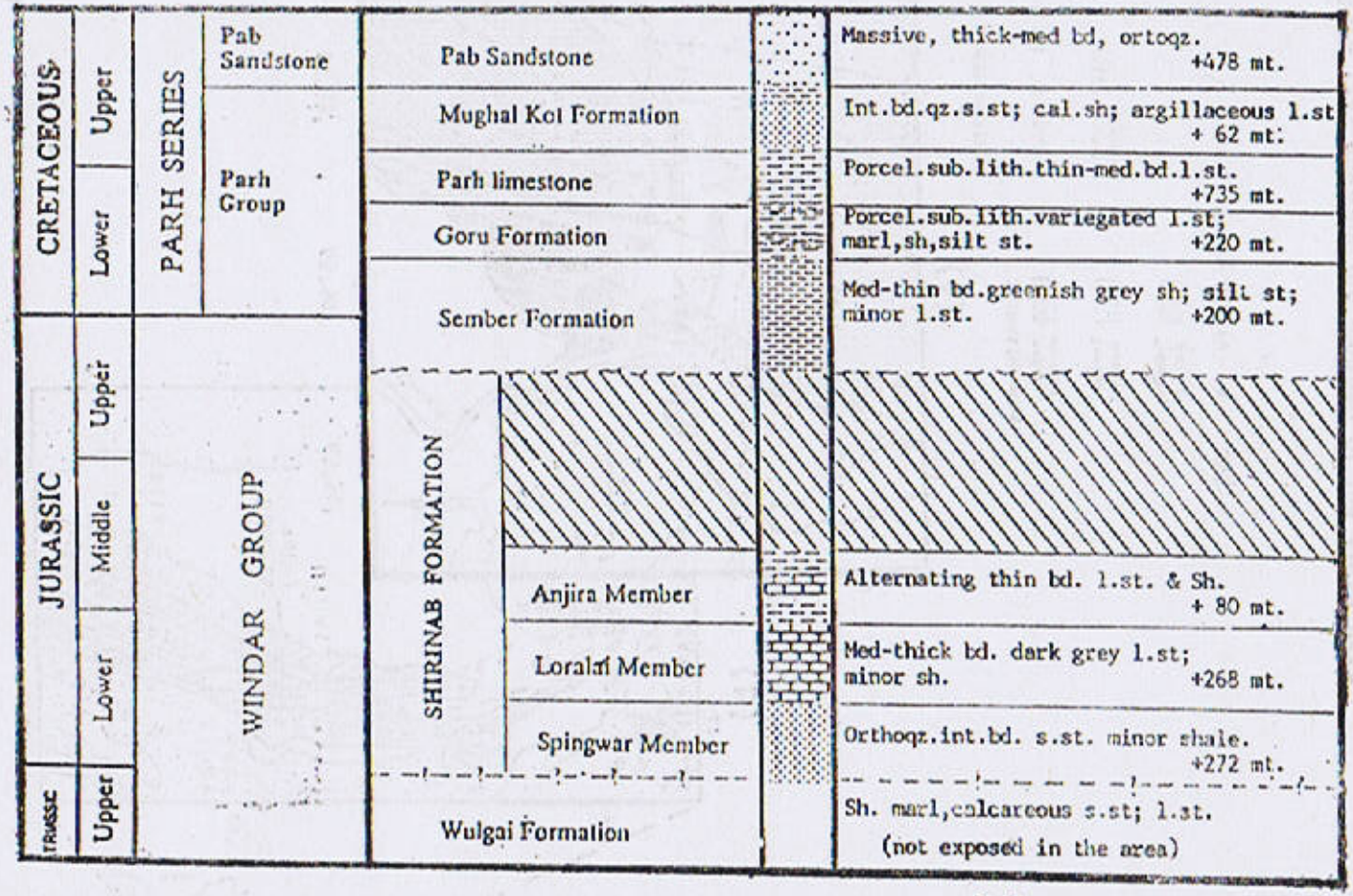

Table 1. Stratigraphy of the Mesozoic rocks of the study area.

Orthoqz=orthoquartzitic
Int.bd.=Inter bedded
Porcel =porcelaneous
qz =quartzitic

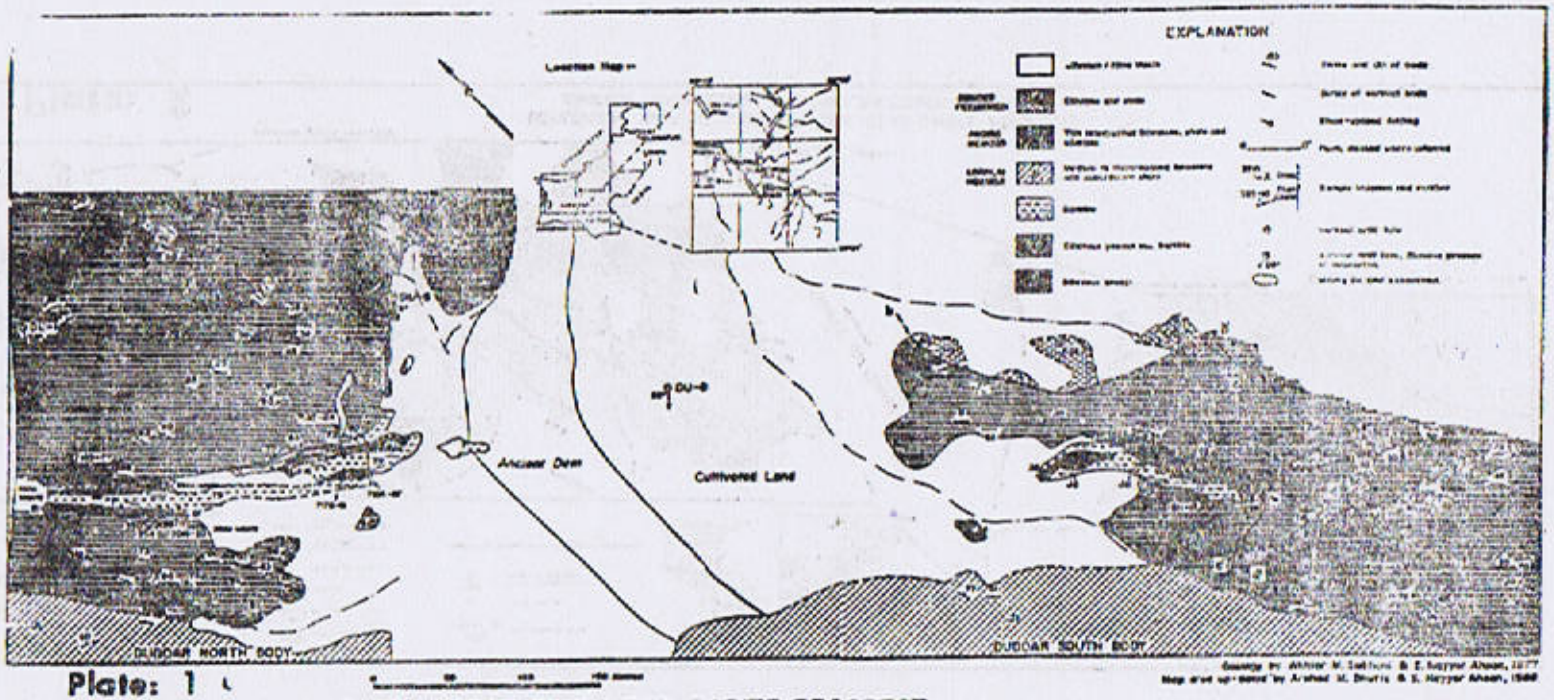

Plate: 1

GEOLOGICAL MAP OF DUDDAR ZINC-LEAD-BARITE PROSPECT

KANRACH TEHSIL, LASBELA DISTRICT, BALOCHISTAN, PAKISTAN

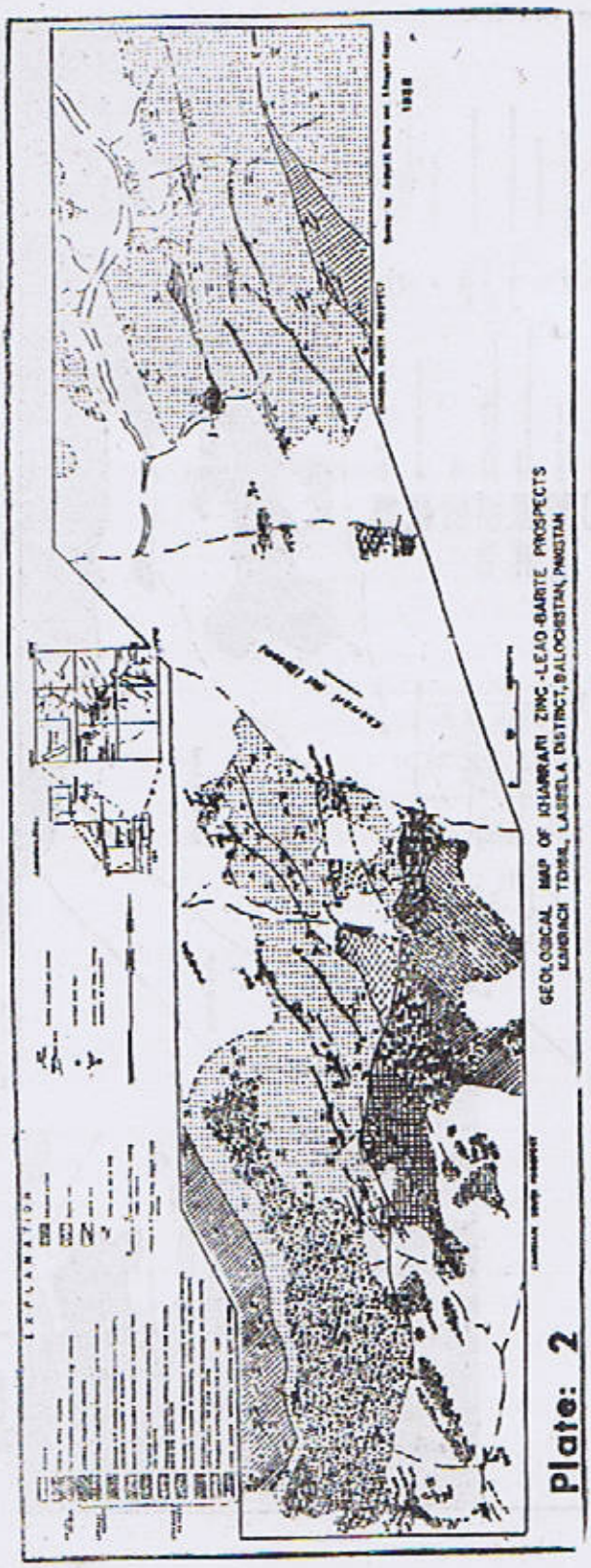
EXPLANATION
GEOLOGICAL MAP OF KHARRARI ZINC-LEAD-BARITE PROSPECTS
KANRACH TEHSIL, LASBELA DISTRICT, BALOCHISTAN, PAKISTAN
Plate: 2

TABLE - 2

Summary of contrasts and similarities between the Duddar and Kharrari ore bodies.

	Duddar ore bodies	Kharrari ore bodies
Host rocks	The mineralization occurs within the upper stratigrephic horizon of the Shirinab Formation-the Anjira Member composed of alternating limestone and shale, with minor siltstone.	The mineralization is associted with the lower and middle horizons-the Spingwar and Loralai Members composed of the sandstone and limestone respectively.
Structure	The structural deformation is not intense.	The intensity of structural influence and the deformation is more pronounced.
	The mineralization is similar qualitatively, consisting of zinc, lead and barite, to the Kharrari ore body.	The mineralization is similar qualitaitvely to the Duddar ore bodies, and consists of zinc, lead and barite.
Mineralization	The mineralization appears in a regular pattern, nearly in parallel zones.	The mineralization is distributed in an irregular fashion.
	The mineralization almost follows the general northwest bedding trend and appears concordant.	The mineralization is commonly localized to the faults, fractures, shear zones and the related structural zones.
	Galena is rarely present on the surface of the ore zones.	Galena is present at the surface of the ore zones, as unoxidized or incompletely leached, in the form of scattered specks, crystalline form or in veins.
	Marcasite and pyrite are commonly present at the surface, both as altered and fresh, usually associated with barite.	Marcasite and pyrite are rarely seen at the surface of the mineralized zones.
	Ferruginous zones are rarely observed.	Ferruginous zones, 1 to 2, 5 meters thick, orange to yellowish brown, are frequently present, usually parallel to bedding.

TABLE 2 (Continued)

Gossan	The silicified gossans of maroon to dark black desert varnish are prominently developed - in the Duddar South ore body.	The silicified gossans are poorly developed.
	The gossans are intensely silicified and are associated with barite and altered sulfides, but rarely galena.	The intensely altered and oxidized isolated gossans, less silicified than those in the Duddar area, contain barite and galena.
Barite	Barite abundantly exposed and mined, is dark grey to black, bedded (Duddar North); and light color, soft and poorly bedded (Duddar South).	Barite, not exposed extensively like the Duddar ore bodies, is light grey to white, present as irregular clusters, columnar banding radiating aggregates, fractured filled cavaties and veins.
	Linear and thin veins of quartz and barite are not prominently developed.	Quartz and barite, light to dense white, occassionaly contaminated with oxides are present in northwest trending thin veins (Kharrari South).

Geol. Bull. Punjab Univ. 1992, 27, 47-62

MICROFACIES, DIAGENESIS AND ENVIRONMENT OF DEPOSITION OF DATTA FORMATION FROM JASTER GALI, DISTRICT ABBOTTABAD, HAZARA, PAKISTAN

BY
FAWAD AHMAD CHUHAN, MOHAMMAD NAWAZ CHAUDHRY
AND
MUNIR GHAZANFAR
Institute of Geology, Punjab University, Lahore-54590, Pakistan

Abstract : *Datta Formation shows marked vertical variation in the environment of deposition from continental, subtidal, intertidal to supratidal. However, in the Galiat area this formation is predominantly marine as opposed to dominantly continental facies of Salt Range. The petrographical/sedimentological study of this formation shows the following lithologic units. Fine grained quartz and clay cemented ferruginous sublithic arenite with streaks and layers of grit ; alternating bands of medium grained intraclast bearing oolitic-pelletoidal limestone intercalated with nodular marl ; fine grained quartz cemented quartz arenite intercalated with shale ; fine to medium grained quartz cemented quartz arenite ; nodular marl ; limestone (sparse biomicrite, wackestone) ; coarse to medium grained oolitic, carbonate cemented quartz arenite with streaks and layers of grit. Recycled clastic component is dominant. Tourmaline, zircon, epidote and sphene indicate an ultimate derivation from an igneous, metamorphic sialic basement with subordinate basic/metabasic component. The granitic component was predominantly S-type. The diagenetic events show that kaolinite cement is early as well as formed at final stage. The early diagenetic kaolinite cement was partially transformed to illite at a depth of at least 3500-4000m whereas quartz and non-ferroan carbonate cements were formed after the early diagenetic kaolinite. The non-ferroan carbonate cement was transformed to ferroan carbonate cement. A part of ferroan dolomite, so formed, was probably dedolomitized at the final stage.*

INTRODUCTION :

Gee (1945) and earlier workers named this unit as variegated stage. However, Danilchik (1961) and Danilchik and Shah (1967) renamed it as Datta Formation, which has now been approved by the Stratigraphic Committee of Pakistan. The name Datta Formation is also applied to the lower part of the Samana beds of Davies (1930) in parts of Kohat, Kala Chitta and Hazara, Red beds and part of Kioto Limestone of Middlemiss (1896) and lower part of Maira Formation of Davies and Gardezi (1965).

The Datta Formation underlies the Shinawari Formation, lower part of which has yielded lower Toarcian ammonites. The age is

therefore inferred as Early Jurassic, mainly pre-Toarcian. It is an important unit of Kohat Potwar and Hazara basin. It shows marked lateral as well as vertical lithological variation. The formation was deposited in sub-tidal, inter-tidal, supratidal and continental environments. Useful minerals such as silica sand, fire clays and bauxite are also present in it. The formation is also an important hydrocarbon reservoir.

In Hazara the Datta Formation is composed of sandstone, siltstone, marl, shale and limestone. In Kala Chitta and Salt Range it is composed of variegated sandstone, siltstone, shale and mudstone with fire clay, silica sand, laterite, calcareous, dolomitic and carbonaceous horizons. (Shah 1977, Hussain et al. 1967, Cheema 1974, Ashraf et al. 1973 and Baloch 1986). The type section is located in Datta Nala (Lat. 33°-N : Long 71° 19'E) in the Surghar Range. The thickness at type locality is 212 metres. Its maximum reported thickness is 400m in Shaikh Budin Hill in Surghar Range. In Hazara area its thickness at Jaster Gali is 18.4 metres. Datta Formation has a disconformable lower contact throughout its extent. In Hazara area it overlies the Hazara Formation unconformably (Precambrian) besides Palaeozoic formations.

Geology of Jaster Gali Area

In the area studied (Fig. 1) Datta Formation directly overlies the Hazara Formation of late Precambrian age. The Cambrian Abbottabad, Hazira and Galdanian Formations are missing. The regional stratigraphy of Hazara area is summarized in Table 1. The studied section is on the right bank of Harno River near Jaster Gali. Here Datta Formation is composed of quartz arenites with beds of arenaceous, dolomitised, oolitic and pelletoidal limestone with intercalations of marl and shale. Towards the bottom is a thin layer whereas at the top is a very thick band of gritty quartz arenite. The measured section along with microfacies and lithological details is given as Table 2.

TABLE 1

Stratigraphic Table of Hazara area.

Age	Formation	Lithology
Miocene	Murree	Grey and reddish sandstone and shale
Middle Eocene	Kuldana	Maroon to varicoloured shales and marls
Early to Middle Eocene	Chorgali	Thinly bedded limestone and marls
Early Eocene	Margala Hill Limestone	Nodular foraminiferal limestone
Late Paleocene	Patala	Greenish grey/khaki shales with limestone beds
Middle Paleocene	Lockhart Limestone	Nodular foraminiferal limestone
Early Paleocene	Hangu	Sandstone, claystone, laterite

Age	Formation	Litholog
———	Disconformity———	———
Late Cretaceous	Kawagarh	Fine grained light grey limestone
Early Cretaceous	Lumshiwal	Grey to brownish coarse sandstone
Late Jurassic to Early Cretaceous	Chichali	Dark grey shales with sandstone beds medium grained
———	Disconformity———	———
Middle Jurassic	Samana Suk	Limestone with dolomitic patches
Early Jurassic	Datta	Sandstone, quartzite, microconglomerate
———	Disconformity———	———
Early Cambrian	Hazira/Galdanian	Calcareous siltstones and shales
Precambrian	Abbottabad	Dolomites with sandstone, shale and boulder bed at base
———	Unconformity———	———
Late Precambrian	Hazara Slate	Slates, sandstone and quartzites

TABLE 2

Measured section of Datta Formation at Jaster Gali, District Abbottabad.

Cummulative thickness of Zones (m)	Sample No.	Sample Position (m)	Description of zones
			Samana Suk Formation begins.
DJ–VII 18.4m	DJ–26	18.00	**Coarse to medium grained, oolitic carbonate cemented quartz arenite with streaks and layers of grit.**
	DJ–25	17.9	
	DJ–24	17.0	
	DJ–23	16.8	Thickly bedded to massive looking, very hard micro-conglomeratic, carbonate cemented sandstone. Concentration of granules varies from place to place. Grain size is usually 2-4mm and goes upto 6mm. Fresh colour
	DJ–22	15.2	

Cummulative thickness of Zones (m)	Sample No.	Sample Position (m)	Description of zones
			is dark grey to brownish grey. Weathering colour is rusty brown to rusty grey.
DJ–VI 15.1 m	DJ–21	15.0	**Limestone (Sparse biomicrite, Wackestone)** Oyster bearing limestone with pyrite nodules and worm borings. Fresh colour is dark grey whereas weathering colour is light grey.
DJ–V 14 m	DJ–20	14.0	**Nodular marl.** Nodular marl with nodule thickness of 4cm-1.5cm and lenght of 4-9cm. Fresh colour is medium grey and weathering colour is rusty grey.
DJ–IV 13.2 m	DJ–19 DJ–18 DJ–17	13.0 12.6 11.8	**Fine to medium grained, quartz cemented quartz arenite.**
	DJ–16 DJ–15 DJ–14 DJ–13 DJ–12 DJ–11 DJ–10 DJ–9 DJ–8	11.1 10.8 10.2 9.6 9.0 8.2 7.4 5.7 5.1	It is medium to fine grained, quartz cemented sandstone. Bedding thickness is 15-50 cm whereas at some places it is just 3-6cm. Fresh colour is off white to light grey and weathering colour is reddish brown. This zone is heavily jointed with joint space of 6-40cm.
DJ–III 5 m	DJ–7 DJ–6	4.5 4.2	**Fine grained quartz cemented quartz arenite intercalated with shale.** It is quartz and clay cemented sandstone having bedding thickness of 5-6cm. It is having rapid alternations with shale whose thickness varies from 0.2—2cm. Fresh colour is medium to light rusty grey, and weathering colour is light rusty brown.

Cummulative thickness of Zones (m)	Sample No.	Sample Position (m)	Description of zones
DJ–II 4 m	DJ–5	3.5	**Alternating bands of medium grained intraclast bearing oolitic-pelletoidal limestone intercalated with nodular marl.**
	DJ–4	3.0	
	DJ–3	1.7	
	DJ–2	0.8	
			Nodular marl having thickness of 1.5-4cm whose fresh colour is light grey and weathering colour is light rusty brown to light grey embedded in arenaceous oolitic/-pelletoidal dedolomitized limestone with belemnites. Fresh colour of limestone is light to medium grey and weathering colour is light rusty brown to light grey.
DJ–I 0.5 m	DJ–1	0.25	**Fine grained quartz cemented ferruginous gritty sublithic arenite.**
			Massive, gritty ferruginous sandstone. Rusty brown to dark grey on fresh and weathering surfaces. It also contains a few fine granule sized rock fragments of Hazara Formation.
			Unconformity
			Hazara Formation

PETROGRAPHY

Mineral composition of Datta Formation from Jaster Gali section is given in Table. 2. Textural parameters and porosity descriptions are based on detailed measurements and evaluation. The relevant tables are available on request.

The unit in contact with Hazara Formation (DJ-I) is sublithic arenite whereas rest of the units are compositionally mature. The clastic parts are texturally sub-mature to mature.

The measured section is compositionally mature and texturally sub-mature to mature. Textural parameters are discussed after Tucker (1988). Heavy minerals are tourmaline, sphene, zircon and epidote indicating a very restricted suite. Pyrite, limonite, hematite and magnetite occur as ore minerals. Pyrite and ferroan carbonate occur side by side indicating positive correlation thus suggesting reducing conditions of their formation. This formation can be divided into the following units.

DJ-VII Coarse to medium grained oolitic, carbonate cemented quartz arenite with streaks and layers of grit.

DJ-VI Limestone (Sparse biomicrite, Wacke stone).

DJ-V Nodular marl.

DJ-IV Fine to medium grained quartz cemented quartz arenite.

DJ-III Fine grained quartz cemented quartz arenite intercalated with shale.

D-II Alternating bands of medium grained Intraclast bearing oolitic/pelletoidal limestone intercalated with nodular marl.

DJ-I Fine grained quartz and clay cemented ferruginous sublithic arenite with streaks and layers of grit.

DJ-I. Fine grained quartz and clay cemented ferruginous sublithic arenite with streaks and layers of grit.

This unit is iron oxide and quartz cemented quartz arenite. Quartz is fine grained, submature, poorly sorted, sub-rounded to sub-angular. Quartz is being replaced by kaolinite and illite at places. Rock fragments of Hazara Formation are present occasionally in this unit.

DJ-II. Alternating bands of meduim grained intraclast bearing oolitic/pelletoidal limestone intercalated with nodular marl.

The limestone bands in this unit include arenaceous (with rounded quartz grains) oopel-intra biosparite P-II/1 (packstone) and biosparite (mudstone). The microsparite is neomorphosed to coarse sparite. It is non ferroan, being transformed generally to ferroan calcite. Patches of ferroan dolomite are present occasionally.

DJ-III. Fine grained quartz cemented arenite intercalated with shale.

The sandstone intercalations in this zone show fine grained, texturally mature, well sorted sub-rounded to sub-angular quartz grains with long to concavo-convex contacts with limonitic staining at places and few microstylolites. Besides quartz cementation, iron oxides (limonite and hematite) also serve as a cement (P-II/2).

DJ-IV. Fine to medium grained quartz cemented quartz arenite.

This unit is medium to fine grained, texturally mature and moderate to well sorted. Quartz grains are sub-angular to angular. Quartz grains show concavo convex contacts to complete suturing (P-II/3, P-II/6). Microstylolites are abundant (P-II/4. P-II/5). Kaolinite and illite are present from trace amount upto 7% (P-II/4, P-II/5, P-II/6). Some quartz grain contacts show limonitic staining.

DJ-V. Nodular Marl.

It is a thin nodular marly unit.

DJ-VI. Limestone (Sparse biomicrite, Wackestone).

This sparse biomicrite (wackestone) unit contains non-ferroan calcite being replaced by ferroan calcite cement (P-I/1). Some bioclasts are partially and some wholly transformed to ferroan calcite with some showing micritized boundaries. Worm burrows are common with low amplitude undulating seams (low amplitude stylolites). Neomorphic spar is rare.

DJ-VII. Coarse to medium grained oolitic, carbonate cemented quartz arenite with streaks and layers of grit.

It is a coarse to medium grained carbonate cemented quartz arenite (P-I/2) with dedolomitized rhombs at places. Carbonate cement (P-I/2) is usually non-ferroan being replaced by ferroan one. One distinguishing feature of this unit is dahllite/collophane oolites forming concentric rims around quartz

and opaque minerals nuclei besides an occasional micritized pellet (P-I/3, P-I/4). The quartz grains are rounded to subrounded, poorly sorted unequigranular to bimodal showing point to long contacts with one another, with some of the fractures filled with ferroan carbonate cement (P-I/5, P-I/6). Quartz overgrowths over quartz and polycrystalline quartz grains are rare. In some portions carbonate replaces quartz extensively turning them into arenaceous dedolomitized limestone (P-I/6). This unit, therefore, is interpreted to have been deposited as a sandstone but was later on attacked by carbonate cements and parts turned into a floatstone (Chaudhry et al, 1992).

DIAGENESIS

Clay minerals.

Kaolinite is the first as well as the last cement formed at shallow depth due to the influx of meteoric waters which are slightly acidic due to the presence of slight amount of CO_2. The evidence of its being an early diagenetic mineral is shown by the fact that it fills the pore spaces between the quartz grains (P-II/6), and this kaolinite was later on subjected to high pressures leading to the transformation into illite by the following reactions.

(1) $A12Si\,205(OH)4 + KAlSi\,308 = KAlSi3010$ (Kaolinite) (K—feldspar) (Illite) $(OH)2 + 2Si02 + H20$ (Quartz)

This transformation takes place at a depth of at least 3-5-4 km (Bjrlykke and Aagaard, 1992).

But here kaolinite/illite cement does not exceed 7% whereas it is present upto 39% in the quartz and kaolinite/illite cemented quartz arenites of Datta Formation from Bara Oter section described by Chaudhry et al (1992). This leads to the conclusion, that Bara Oter section contains more chemically unstable grains like feldspars which were transformed to illite (Reaction 1).

Quartz

The second cement to form appears to be quartz which occurs as overgrowths. Its origin seems to be pressure solutioning of grains at depth greater than 2.5 km. We rule out the possibility of early quartz cementation due to the fact that at low temperatures and hence depth rate of quartz precipitation is too low for enormous amount of quartz precipitation for kinetic reasons. And also due to the fact that no amorphous silica (Radiolaria, diatom) is present which could have precipitated at 1500m resulting in a chert like texture. So the only possible source of quartz seems to be pressure solutioning.

Carbonate Cement

For quartz cement to precipitate we need slightly acidic pore water which dissolves also carbonate shells present. The rate of quartz precipitation is much slower as compared to rate of carbonate dissolution. As we have oolitic/pelletoidal/fossiliferous limestone bands, therefore build up of carbonate in pore water resulted in precipitation as ferroan calcite (DJ-VI, VII and II).

The final episode is marked by the deposition of late diagenetic kaolinite which is not transformed to illite. Either it is late diagenetic or source of K+was not present for its transformation into illite. At this stage probably some of the ferroan dolomite was dedolomitised as is shown by dedolomitised rims in DJ VII.

ENVIRONMENT OF DEPOSITION

Unit No. DJ-VII containing rock fragments of Hazara Slates which were reworked during marine transgression, overlies the Hazara Formation and was probably deposited in continental to shallow marine conditions. Afterwards there was a general marine transgression followed by shallowing upward marine sequence ending up in a tidal mud flat when deposition of Lower Jurassic Samanasuk Limestone commenced. The outlines of depositional environments are given below.

ZONE	NAME	ENVIRONMENT OF DEPOSITION
DJ-VII	Coarse to medium grained oolitic, carbonate cemented quartz arenite with streaks and layers of grit.	High energy, marine, Upper subtidal to intertidal lag deposit. Probably a break in deposition or extremely low rate of sedimentation.
DJ-VI	Limestone (Sparse biomicrite, Wackestone).	Low energy marine subtidal to intertidal.
DJ-V	Nodular marl.	Low energy, marine, intertidal.
DJ-IV	Fine to medium grained quartz cemented quartz arenite.	Low energy, marine.
DJ-III	Fine grained quartz cemented quartz arenite intercalated with shale.	Very low energy, marine.
DJ-II	Alternating bands of medium grained intraclast bearing oolitic/-pelletoidal limestone intercalated with nodular marl.	High energy, Lower intertidal to subtidal, marine.
DJ-I	Fine grained quartz and clay cemented ferruginous sublithic arenite with streaks and layers of grit.	High energy. Continental but reworked lag deposit (Onset of marine transgression).

ACKNOWLEDGEMENT

The authors are highly obliged to Dr. Ahmed Raza Yasin of Oil and Gas Development Corporation, Islamabad for critical evaluation of materials and manuscript.

Table 3 : Mineral composition of Datta Formation Jaster Gali, Distt. Abbottabad.

Zone	I	II			III		
Sample No.	DJ-1	DJ-2	DJ-3	DJ-4	DJ-5	DJ-6	DJ-7
Quartz	72	8	2	1	17	70	82
Carbonate	—	89	93	96	80	3	5
Kaolinite	5	—	—	—	—	3	5
Illite	3	—	—	—	—	5	2
Collophane/Dahllite	—	—	—	—	—	—	—
Ore	20	3	3	3	3	16	5
Tourmaline	—	—	—	—	—	Tr	Tr
Sphene	—	—	—	—	—	—	—
Zircon	—	—	—	—	Tr	Tr	—
Epidote	—	—	—	—	—	—	—
Mica	—	—	—	—	—	—	—
Chert	—	—	—	—	—	—	—
Carbonaceous matter	—	—	2	—	—	3	1
Porosity	5	4	5	7	6	6	4

Zone	IV						
Sample No.	DJ-8	DJ-9	DJ-10	DJ-11	DJ-12	DJ-13	DJ-14
Quartz	94	93	91	93	95	93	90
Carbonate	—	—	—	—	—	—	—
Kaolinite	1	2	2	1	1.5	1.5	2
Illite	2	0.8	2	1.5	1	2	2
Collophane/Dahllite	—	—	—	—	—	—	—
Ore	2.5	4	4	3	2	3	4.5
Tourmaline	0.1	0.1	0.5	0.6	0.4	0.4	1
Sphene	0.2	0.1	0.3	0.3	0.1	0.1	0.2
Zircon	0.1	Tr	0.1	0.1	Tr	—	Tr
Epidote	—	—	0.1	0.2	Tr	—	0.1
Mica	0.1	—	Tr	0.3	—	—	0.2
Chert	—	—	—	—	—	—	—
Carbonaceous matter	—	—	—	—	—	—	—
Porosity	7	3	3	4	4	3	3

Table 3 : (continued)

Zone	IV					V	VI
Sample No.	DJ-15	DJ-16	DJ-17	DJ-18	DJ-19	DJ-20	DJ-21
Quartz	89	89	91	93	97	9	2
Carbonate	—	Tr	Tr	Tr	Tr	90	96
Kaolinite	3	3	3	2	Tr	—	—
Illite	2.5	3	2	1	Tr	—	—
Collophane/ Dahllite	—	—	—	—	—	—	—
Ore	4	4	3	3	2.5	1	2
Tourmaline	0.7	0.4	0.3	0.3	0.2	—	—
Sphene	0.3	0.3	0.5	0.4	Tr	—	—
Zircon	Tr	Tr	Tr	—	—	—	—
Epidote	Tr	0.2	0.2	0.2	—	—	—
Mica	0.5	0.1	Tr	0.1	0.2	—	—
Chert	—	—	—	—	—	—	—
Carbonaceous matter	—	—	—	—	0.1	—	—
Porosity	4	4	4	1	1	2	6

Zone	VII				
Sample No	DJ-22	DJ-23	DJ-24	DJ-25	DJ-26
Quartz	77	54	58	53	47
Carbonate	20	40	35	40	45
Kaolinite	—	—	—	—	—
Illite	—	—	—	—	—
Collophane/ Dahllite	—	5	—	—	6
Ore	2	1	6	6	1
Tourmaline	0.2	Tr	0.6	0.6	0.3
Sphene	0.1	Tr	Tr	0.1	—
Zircon	Tr	—	—	—	0.1
Epidote	0.5	Tr	0.3	0.3	—
Mica	0.2	—	0.1	—	0.1
Chert	—	—	—	—	0.5
Carbonaceous matter	—	—	—	—	—
Porosity	3	4	3	3	5

REFERENCES

Ashraf. M., Ahmad, M., & Faruqi, F.A., 1973. Jurassic bauxite and kaolinite deposits of Chhoi area, Kala Chitta Range, Punjab, Pakistan. *Geol. Bull. Punjab Univ.* **12**, 41-54.

Baloch, I.H., 1986. A mineralogical study and the industrial utilization of bauxitic clays of Nawa area, Kala Chitta Range. Attock District, Pakistan. *Acta Mineralogica Pakistanica*, **2**, 144-152.

B^{T}Jørlykke, K., and Aagaard, P., 1992. Clay minerals in North Sea sandstones. In : Houseknecht, D. W. and Pittman, E. D. (eds.), Origin, diagenesis and petrophysics of clay minerals in sandstones. *Soc. Econ. Pal. Min. Spec. Publ.* **47, 65—80.**

Chaudhry, M.N., Chuhan, F.A., and Ghazanfar, M., 1992. Diagenesis, environment of deposition and burial history of Datta Formation from Bara Oter, Distt. Abbottabad *Kashmir Jour., Geol.*, **10.**

Cheema, M.R., 1974. Geology of Chhoi-Jabbiwala Kas area with emphasis on early Jurassic high alumina clay and bauxite deposits, northern Kala Chitta, Cambelpur District, Punjab Province, Pakistan. *Geol., Surv., Pakistan Technical Report*, **129**, 19-43.

Danilchik, W., 1961. The Iron formation of the Surghar and western Salt Range, Mianwali District, West Pakistan *U.S. Geol., Surv.*, Prof., Paper **424-D**, 228-231.

Danilchik, W., and Shah, S.M.I., 1967. Stratigraphic nomenclature of formations in Trans-Indus mountains, Mianwali District, West Pakistan. *U.S. Geol, Surv.*, Proj., Report (IR) PK-**33**, 445.

Davies, R.G., 1930. The fossil fauna of Samana Range and some neighbouring areas ; Part I, An Introductory note : *Mem., Geol., Surv., India. Pal., Indica*, New Series, **15**, 15.

Davies, R.G., and Gardezi, A. H., 1965. The presence of Bouleiceras in Hazara and its geological implication : *Geol. Bull. Punjab Univ.*, **5**, 23-30

Gee, E.R., 1945. The age of the Saline Series of the Punjab and of Kohat : *Proc., Nat., Acad., Sci., India Sec., B.* **14**, Pt. 6, 269-310.

Hussain, T., and Khan, A.L., 1967. Fire clay deposits of Kala Chitta Range, District Campbellpur, West Pakistan. *Geol., Surv., Pakistan Report*, 1-89.

Middlemiss, C.S., 1896. The geology of Hazara and the Black Mountains.*Mem., Geol., Surv., India*, **26**, 302.

Pettijohn, F.J., Potter, P.E., Siever, R., 1986. Sand and Sandstone. Second Edition. Springer-Verlag New York, 552.

Selley, R.C., 1985. Elements of Petroleum Geology. W.H. Freeman and Company New York. 449.

Schmidt, V., and Mcdonald. D.A., 1979. The role of secondary porosity in the course of sandstone diagenesis. *Soc. Econ. Pal. Min. Spec. Publ.*, **26**, 175-207.

Shah, S.M.I., 1977. Stratigraphy of Pakistan. *Mem., Geol., Surv., Pakistan* **12**, 138.

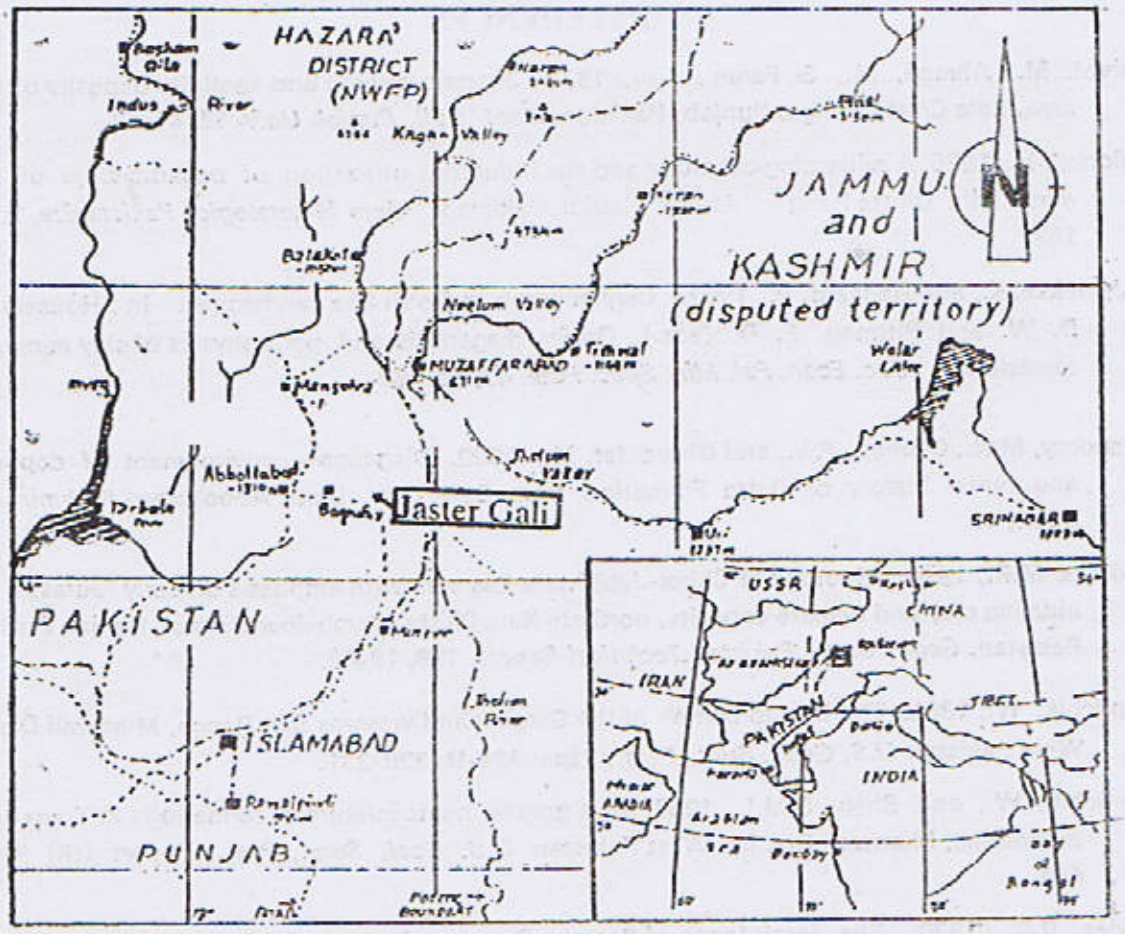

Fig.1: Geographic location of investigated area.

PLATE - I

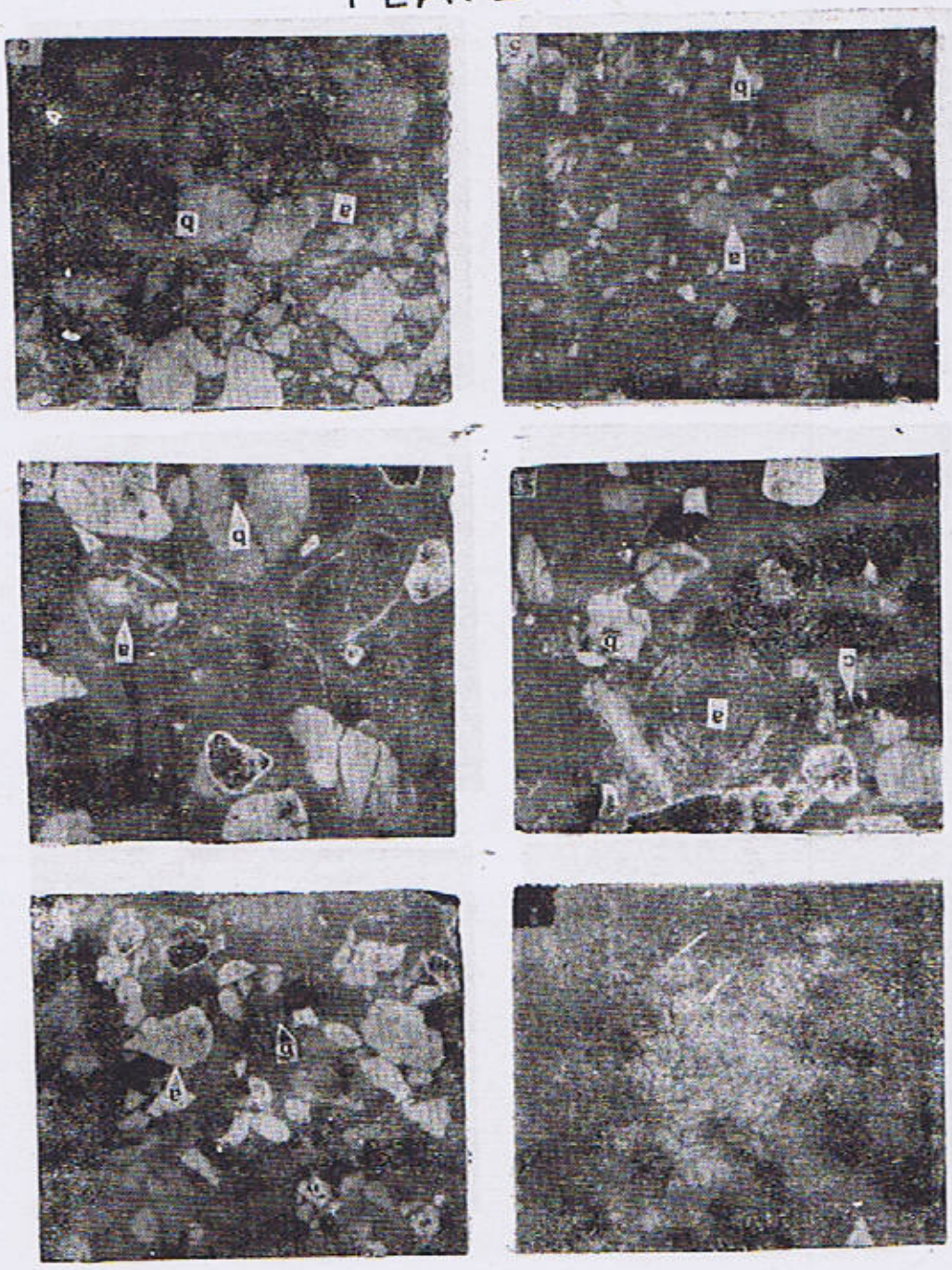

PLATE - II

Geol. Bull. Punjab Univ., 1992, 27, 63-68

COMPUTER PROGRAMME FOR METAMORPHIC PARAGENESIS OF CARBONATE ROCKS

By

MUHAMMAD ANWAR, JAVED AKHTER AND CHAUDHRY ASGHAR ALI

Geological Survey of Pakistan, 16 - G, Model Town, Lahore, Pakistan.

Abstract: *A BASIC Computer Programme has been prepared for the computer plotting and the component's resolution in triangular variation diagrams for the metamorphic paragenesis of carbonate rocks i.e. SiO_2 CaO, and MgO system. Molecular proportions are used in this method, which are obtained from chemical analysis, dividing weight percentages by molecular weights of the constituent components. The programme can help in the quick calculations of the parameters for plotting/resolution of the constituent minerals directly on the triangular diagram according to the molecular proportions of SiO_2 : of CaO : MgO.*

INTRODUCTION :

Minerals composed of three components may be represented within the plane of a triangle. As an example, Forsterite Mg_2SiO_4, Wollastonite $CaSiO_3$, Dolomite $CaMg(CO_3)_2$, Magnesite $MgCO_3$, Quartz SiO_2 and Calcite $CaCO_3$ consist of three components, CaO, MgO and SiO_2 in different proportions (Winkler, 1975). Limestones composed of Calcite, Dolomite and Quartz and their metamorphic derivatives may be regarded as belonging to five components system CaO-Mgo-SiO_2-CO_2-H_2O. Disregarding CO_2 and H_2O, the relevant rocks can be represented in a triangular diagram CaO-MgO-SiO_2 (Miyashiro, 1973).

Molecular proportion of a component is obtained by dividing the weignt percentage with its molecular weight. The molecular weights of SiO_2, CaO and MgO are taken as 60.09, 56.08 and 40.32 respectively. The molecular proportions of the three components are recalculated to 100.

Because of the geometric advantages, compositions are most conveniently represented in an equilateral triangle. Each corner of the triangle represents a pure component i.e. 100% CaO, 100% MgO and 100% SiO_2. Each side allows the representation of a mixture and a mineral consisting of two components, while the interior of the triangle allows the representation of mixtures and minerals consisting of

*BASIC means Beginners All-Purpose Symbolic Instruction Code.

all the three components (Winkler, 1975).

The Computer Programmes included in this papar are based on the original work. However, Hutchison (1973) gave an idea of the molecular proportion's method.

Casio Programmable Calculator, model No. F X 702 P having calculation range of $\pm 1 \times 10^{-99}$ to 9.99×10^{99} has been used for these programs. It has 1630 steps and 26 memories and the memories can be expanded upto 226 by the reduction in the number of steps. Its portability can be easily judged by its weight of 176 grams (Akhter, 1986).

DISCUSSION

(a) *Composition Plotting :*

A rock of known chemical analysis may be plotted in the triangular variation diagram with the help of Programmable Calculator. Fig. 1 shows the position of majority of the common minerals which occur in metamorphic calcareous rocks. Their molecular percentage ratios are shown in Table-1.

TABLE—1

Molecular Percentage Ratio of common minerals occurring in metamorphic calcareous rocks.

Mineral	Formula	Molecular percentage ratio		
		SiO_2	CaO	MgO
Quartz	SiO_2	100	0	0
Calcite	$CaO.CO_2$	0	100	0
Magnesite	$MgO.CO_2$	0	0	100
Dolomite	$CaO.MgO(CO_2)_2$	0	50	50
Diopside	$CaO.MgO.2SiO_2$	50	25	25
Wollastonite	$CaO.SiO_2$	50	50	0
Forsterite	$2MgO.SiO_2$	33	0	67
Grossularite	$3CaO.3SiO_2.Al_2O_3$	50	50	0
Andradite	$Ca_3Fe_2Si_3O_{12}$	50	50	0
Talc	$Mg_6(Si_8O_{20})(OH)_4$	57	0	43
Vesuvianite	$Ca_{10}(Mg, Fe)_2Al_4(Si_2O_7)_2$ $(SiO_4)_5$ $(OH, F)_4$	43	47·5	9·5
Tremolite	$Ca_2(Mg, Fe)_5(Si_8O_{22})(OH, F)_2$	53·4	13·3	33·3

The following entries are made in the Progiammable Calulator for determining the factor of plotting the composition :

```
10 VAC : INP "Wt% — SiO2=" ,A, "Wt%
   — CaO=" ,B, "Wt% — MgO=" .C
20 E=60. 09 : D=56.08 : F=40.32
30 Q=(A/E+B/D+C/F) : R=100/Q : SET F 2
40 PRT "M, PP% — SiO2 =" A/E * R
50 PRT "M.PP% — CaO=" : B/D * R
60 PRT "M. PP% — MgO=" ; C/F * R
70 PRT "SUM M. PP %AGES=" A/E * R +
   B/D * R + C/F * R
80 INP "TRI<SIDE LEN=",W
90 PRT "SPCTO SiO2=" ; W-(A/E*R)/100*W
100 PRT "SPC TO CaO=" ; W- (B/D * R)/100
   * W
110 PRT "SPC TO MgO=" ; W-(C/F * R)/100
   * W
120 GOTO 10
```

After inputting the data, the Computer prints the percentages of each component in terms of the distances markable on the two adjacent sides from the respective corners. These distances are marked on the relevant sides with the help of a Compass and joined by straight lines, parallel to opposite sides. In this way one line is drawn for each component The point of intersection of these three lines represents the Composition of the individual sample.

The plotted composition can be correlated with facies diagram (Fig. 2). Metamorphism in Albite-epidote hornfels facies of contact metamorphism or in the greenshist facies of dynamo-thermal metamorphism gives rise to the common mineral assemblages Calcite + Tremolite+Quartz, or Calcite+Tremolite+ Dolomite. These common assemblages are shown in the facies diagram and are indicated by solid tie lines between important mineral combinations. An assemblage of three outtines a triangle (Hutchison, 1973).

A limestone sample has the three constituents as :

1. Wt % of CaO=39.22
2. Wt % of MgO=9.70
3. Wt % of SiO_2=10.20

The data is required to be plotted on 10 cm equilateral triangular diagram. After inputting the data and the distances from the respective corners as under :

Molecular	Propertion %age	Distance form the respective corner (cm)
CaO	63.02	3.70
MgO	21.68	7.83
SiO_2	15.30	8.47

The distances, as discussed earlier, determine the position of the point which represents the composition of the sample (Fig. 3).

(*b*) *Compostion Reading* :

These composition of the point P in equilateral triangle ABC can be read on the triangular diagram by drawing the lines from the vertices A, B and C through the point P. These lines join the opposite sides BC, CA and AB at MN and O, respectively. The distance between point O and vertex A is termed as X, between N and C as Y and that between M and B as Z, as shown in the Fig. 4. The distances X, Y and Z are measured. The side length of the triangle is also measured.

The following entries are to be made in the Programmable Calculator for composition reading :

```
05 VAC : INP "TRI<SIDE LEN=", W
```

```
10  INP "X=", X, "Y", Y, "Z=",Z
12  X = X/W * 100 : Y = Y/W * 100 : Z =
    Z/W * 100
20  J (X/(100-X) ) : K = (Y/100-Y) )
30  L = ( (100-X)/Z) : M = (Z/(100-Z) )
40  N = ( (100-Z)/Z) : O = ( (100-Y)/Y)
50  A = (100/(1+J+O) )
60  B = (100/(1+M+L)
70  C = (100/(1+K+N) )
80  PRT "A % = " ; A
90  PRT "B % = " ; B
100 PRT "C % = " ; C
110 GOTO 05
```

Test Example :

Input data

Tri>Side Len = 127 mm

X = 105 : Y=53 : Z = 28

Print out Results

A % (SiO_2) = 13.95

B % (SaO) = 67.01

C % (MgO) = 19.04

CONCLUSIONS

A Computer method convenient for composition plotting/reading of triangular variation diagram for metamorphic paragenesis of carbonate rocks has been described. It provides a time saving alternative to the lengthy caculations involving series of steps with several branches. In this programme, molecular weights, molecular ratios and amounts of different oxide components have been used. Parameters for plotting the composition are obtained by simply feeding the amounts of different oxide components i.e. SiO_2, CaO and MgO. The percentage composition reading of a point from triangular variation diagram can easily be made by insetring point co-ordinates. Any units of length can be used. Mineral explpration geologists, petrographers and geochemists, especially working with metamorphic paragenesis of carbonate rocks will find these programs very useful.

AKCNOWLEGEMENTS

This work owes to the enlightement provided by Drs. Farhat Hussain and Nasir Ali Bhatti. The authors would like to thank M/S Muhammad Hafeez Butt, Iftikhar Mustafa Khadim and Zaki Ahmed Ashraf for their useful and clarifying comments.

REFERENCES

Akhter, J., 1987. Basic Programming for Magnetic Calculations from vertically polarized bodies of simple geometrical shapes. *Kashmir Jour. Geol.* 5. 133-140.

Hutchison, C.S., 1973, Laboratory Handbook of Petrographic Techniques. John Wiley, New York. 527p.

Miyashiro, A., 1973. Metamorphism and Metamorphic Belts. George Allen & Unwin, London. 334p.

Winkler, H.G.F., 1975, Petrogenesis of Metamorphic Rocks. Springer Verlag, New York 433. p.

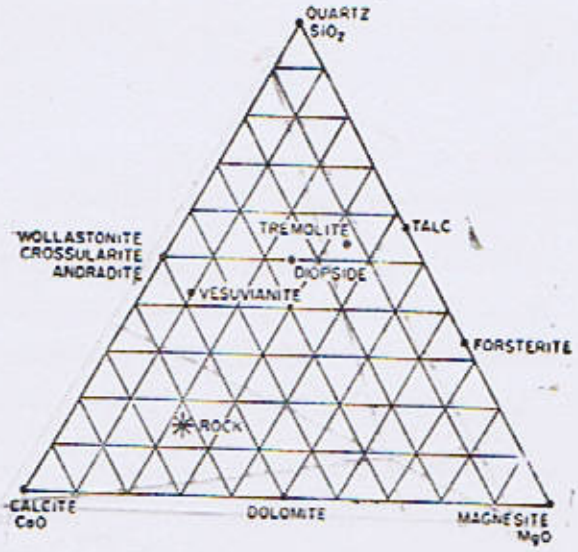

FIG. 1 POSITION OF THE COMMON MATAMORPHIC MINERALS IN SiO_2-CaO-MgO SYSTEM

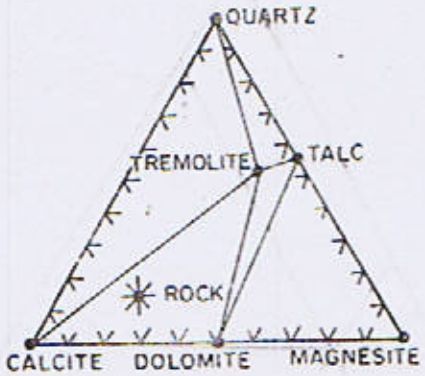

FIG. 2. FACIES DIAGRAM FOR MINERAL PARAGENESIS IN THE ALBITE-EPIDOTE HORNFELS OR GREENSCHIST FACIES.

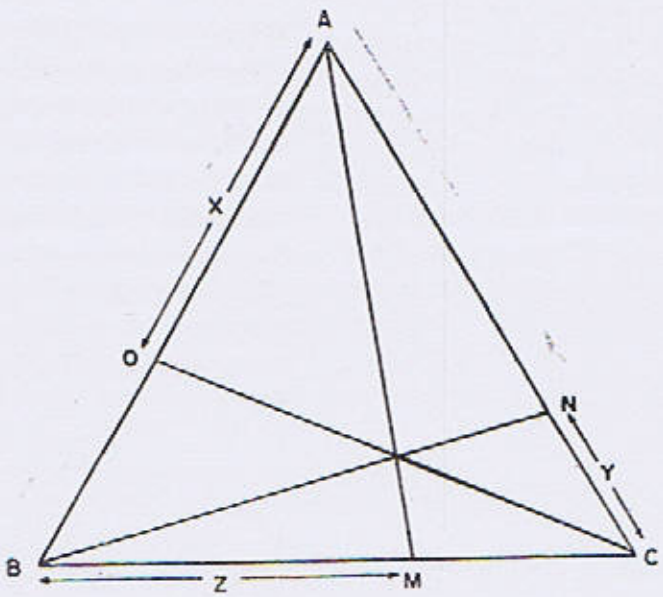

FIG. 4. TRIANGULAR VARIATION DIAGRAM SHOWING THE POSITION OF A POINT OF COPOSITION A_{20} B_{30} C_{50}.

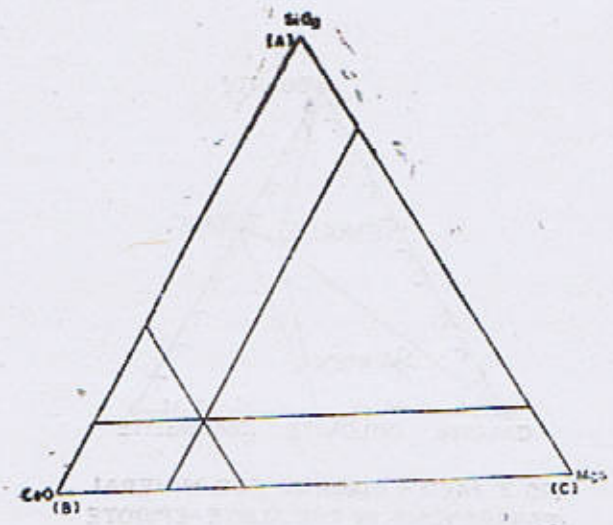

FIG. 3. COMPOSITION PLOTTING

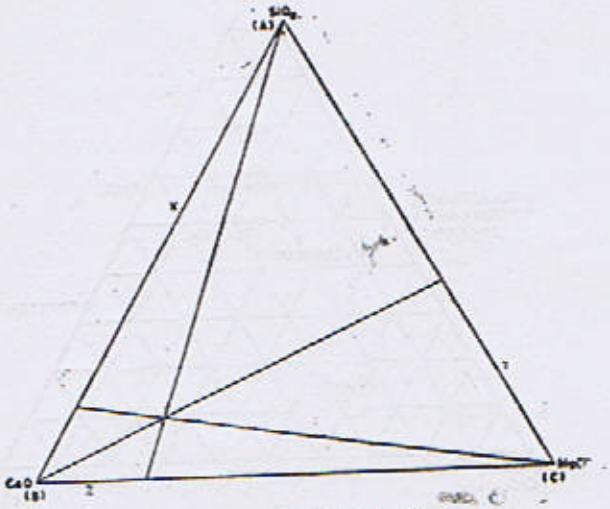

FIG. 5. COMPOSITION READING.

Geo. Bull. Punjab Univ. 1992, 27, 69-96

MUTUAL INFLUENCE OF CHEMICAL ACTIVITY IN INJECTION MIGMATITE AND PEGMATITES IN EVJE-IVELAND AREA OF SOUTHERN NORWAY

BY

SHERJIL AHMAD KHAN LODHI

PCSIR Laboratories Complex, Lahore-54600, (Pakistan)

Abstract. *Field observations, mineralogical and geochemical investigations show that the conacts of Injection Migmatite (country rock) has been influenced by Pegmatites at least in centimeter area. Rb and pb is very openly moved from pegmatitic soltuions towards Injection Migmatite, whereas Sr in Injection Migmatite was mobilized due to Pegmatites and migrated towards the contact. Garnet, biotite and monazite are new mineral at contacts. The influenced area at the contacts is not depending on the length and thickness of the pegmatitic bodies.*

INTRODUCTION

It is observed in the field that the contacts of Injection Migmatite (countary rock) are influenced by the Pegmatites, at least in centimeter area. Therefore, different profiles are measured across different Pegmatites and the samples of Injection Migmatite are collected with narrow to far away distance from the contact, to know upto which distance the influence has taken place. As the Migmatite is strongly banded into leuco, mela-and Intermediate bands (Lodhi, 1983), it is important to take the samples from the same band and with approximately the same hornblende composition.

FIELD OBSERATIONS

The studied area lies between the cities of Evje and Iveland of Southern Norway, Longitude 7° 52' to 7° 54', Latitude 50° 31' to 58°. 33' The area is famous for pegmatitic veins, dykes and bodies, which are counted to be more than 500. The country rock of Pegmatite in Evje-Iveland is Migmatite (Lodhi, 1983), which is surrounded by granitic gneisses and augen-ganisses and are supposed to be of pre-cambrian age, forming the base of Baltic Shield (Barth, 1947, 1960). Kahama. (1982) described the investigated area as a part of Dalsandian fo'ded region, which has an age of 800-1200 M. Y. The southern tip of Norway, most likely b long to Telemark Basement (Oftedahl, 1980).

Migmatite of Evje-Iveland is strongly banded and is differentiated into leuco, mela and intermediate bands, according to their hornblende composition. The leuco bands show very sharp contacts with mela and intermediate bands, whereas the intermediate and mela bands show gradual contacts.

Different profiles are measured and the oriented samples are taken along the bands, perpendicular to the contacts. Figures 1—4, show the sample location in contact with different Pegmatites with varying length and thickness. The samples were taken in very narrow margin from both the hanging and foot contacts of Pegmatite 2A with Migmatite (Fig. 4) to understand the phenomenon of influence on both sides.

The lengths of the profiles are measured intentionally so long, to study the country rock away from the contacts, which is not influenced by pegmatitic solution.

PREVIOUS WORK :

Rose (1978) was the first author, who studied the influence of pegmatitic solution on the country rock of Granite at Brabat, south-west Africa (Namibia). He noted a change in mineral composition at the contacts upto 5cm, whereas the change in trace elements components was observed maximum upto 1m in the country rock (Granite) of magmatic origin. The element Rb has migrated into Granite, whereas the pegmatitic solutions are not influenced by the country rock.

In the investigated area of Evje-Iveland, the country rock (Injection Migmatite) is of metamorphic origin. Therefore, it was thought, that here the mutual influence of Pegmatite and Migmatite can show another trend. For this purpose, four Pegmatites-Migmatite contacts are selected in the area (Figs. 1-4).

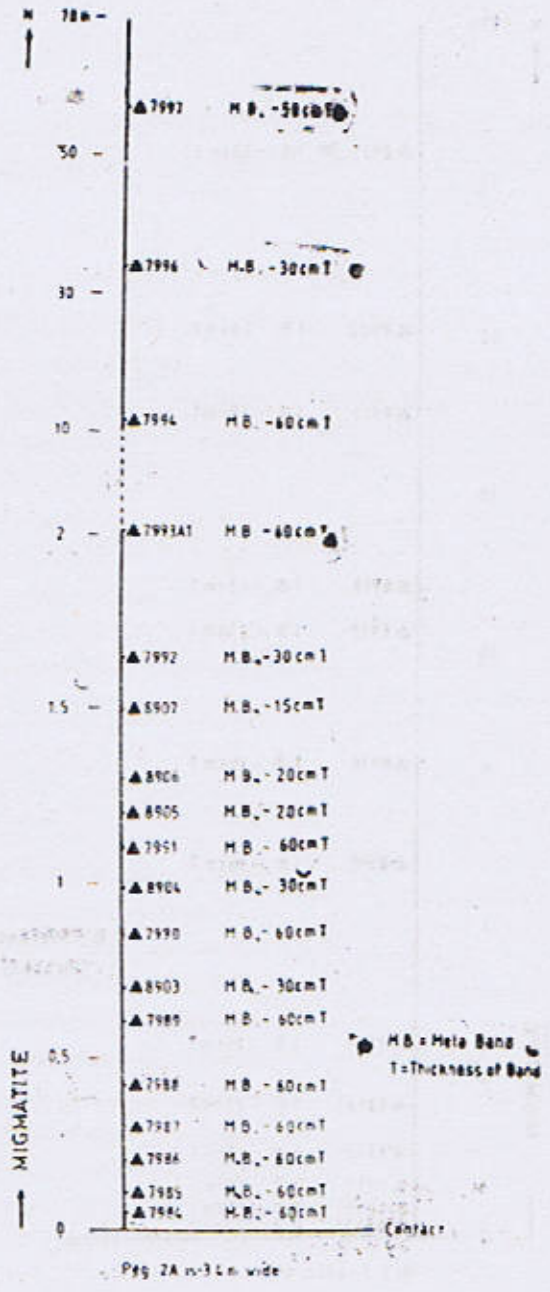

Samples loction of the profile perpendicular to the contact with Pegmatite 2A along the Mela-Band of Migmatite.

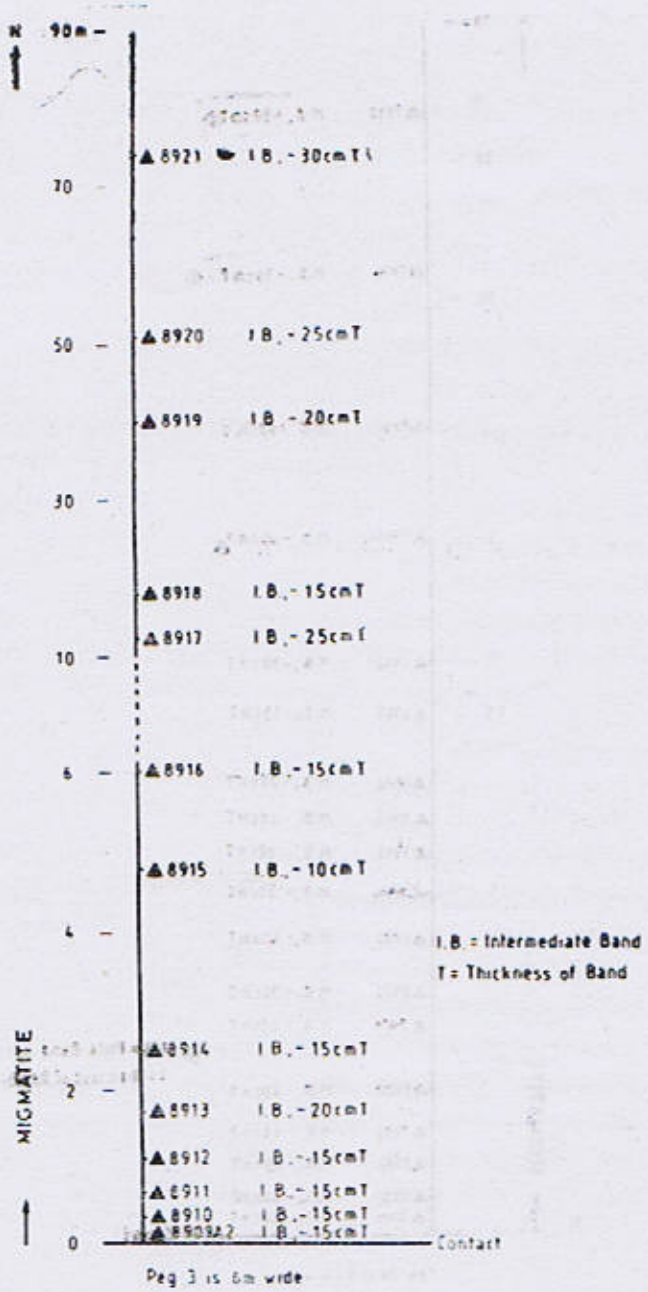

Fig.2 Samples location of the profile perpendicular to the contact with Pegmatite 3 along the Intermediate-Band of Migmatite.

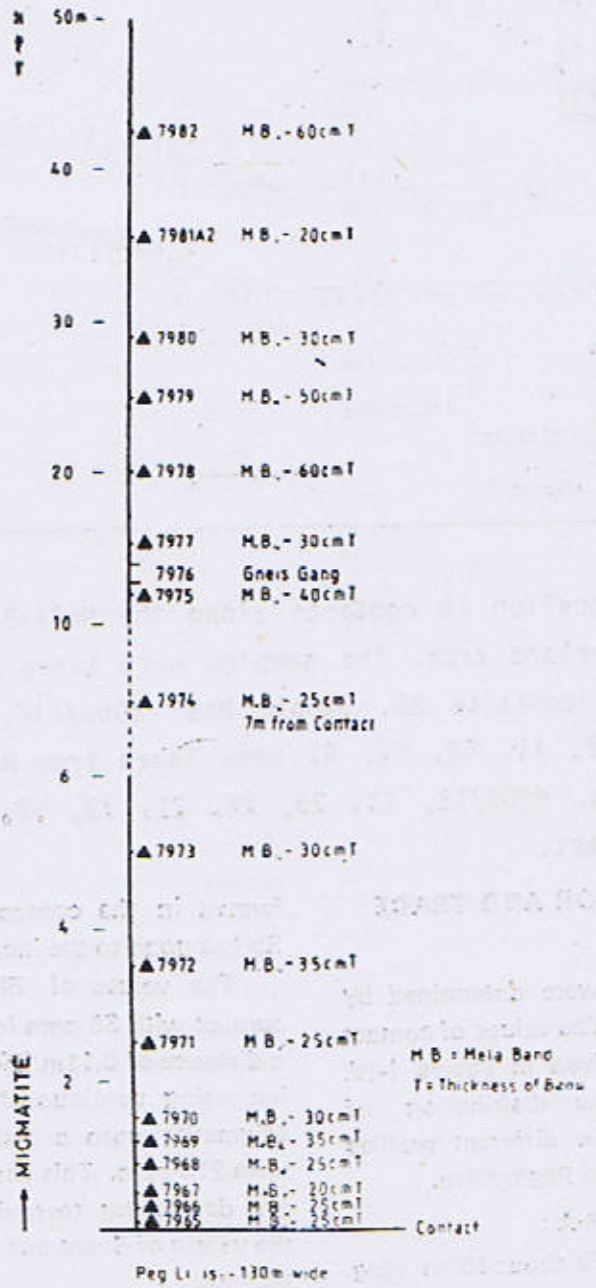

Fig.3 Samples location of the profile perpendicular to the contact with Pegmatite Li along the Mela-Band of Migmatite.

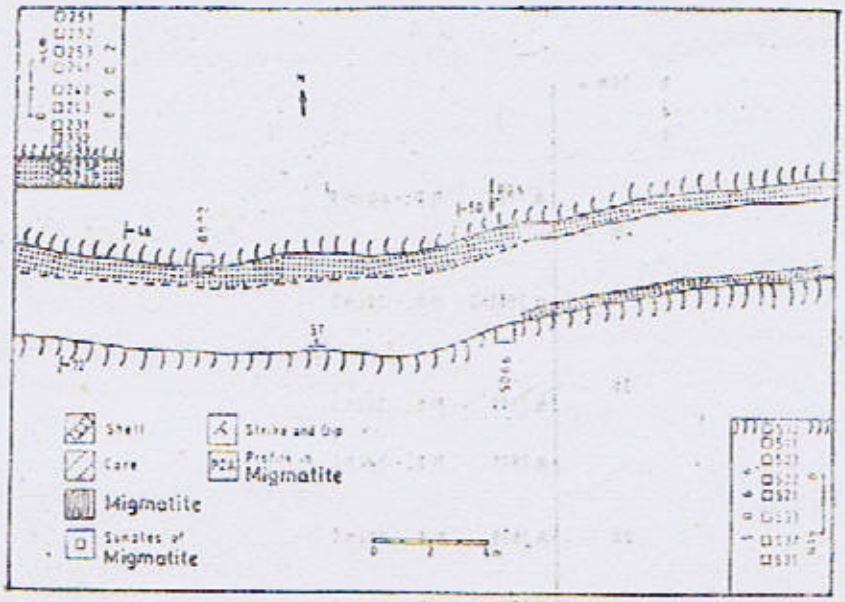

Fig.4 Samples location at contacts along the Mela-Band of Migmatite of Evje-Iveland area. The samples were taken at both the contacts of Pegmatite 2A. Sample Nos. 8902/21P, 33P, 33A, 32A, 31, 43, 42, 41, 53, 52, 51 were taken from North contact and sample Nos. 9905/12, 11, 23, 22, 21, 33, 32, 31 belonged to south contact.

DISTRIBUTION OF MAJOR AND TRACE ELEMENTS

The trace elements were determined by X-ray Fluoresence (XRF). The values of contact Migmatite samples are given in Tables I-IV. Figures 5 to 12 show the distribution of elements in Migmatite in different profiles with contact to four selected Pegmatites.

Contact with pegmatite 2-A :

Pegmatite 2-A (Fig. 1) is about 100m long and show a width of 3,4m. Here, when we follow the trend of Rb from contact to away from it in Migmatite samples (Fig. 5), this element rises from 37 to 710 ppm upto a distance of 0,05m, the values decreasing to zero upto a distance of 1,10m from contact. As biotite is a new mineral formed in the contact, it is very possible that Rb has gone to the increasing biotite.

The values of Rb are decreasing from contact with 39 ppm in Migmatite to zero upto a distance of 0,11m (Fig. 5). The Sr values are increasing continuously away from contact in Migmatite upto a distance of 0,30m (Abb. 5) upto 213 ppm. This shows that the values of Sr are decreasing towards contact. Afterwards, the values of Sr are not showing any remarkable change.

The values of Zn are decreasing away from the contact to a distance of 0,42m to 25ppm. Afterwards the values remain constant upto 110 ppm (Fig. 5). The values of Ni and Cr remain constant upto a distance of 0,60m from contact in Migmatite. Afterwards they show no change in their values (Fig. 5).

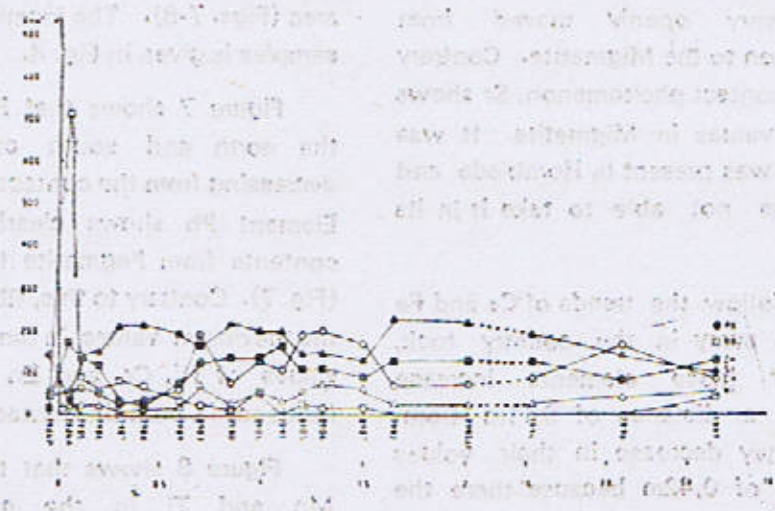

Fig.5 Pb, Rb, Zn, Sr, Cr and Ni in Mela-Band of Evje-Iveland Migmatite. The influence of Pegmatite is upto 1,10m. Profile is perpendicular to the contact with Pegmatite 2A, see Fig.1 for the location of samples. The values of samples are given in Table-I.

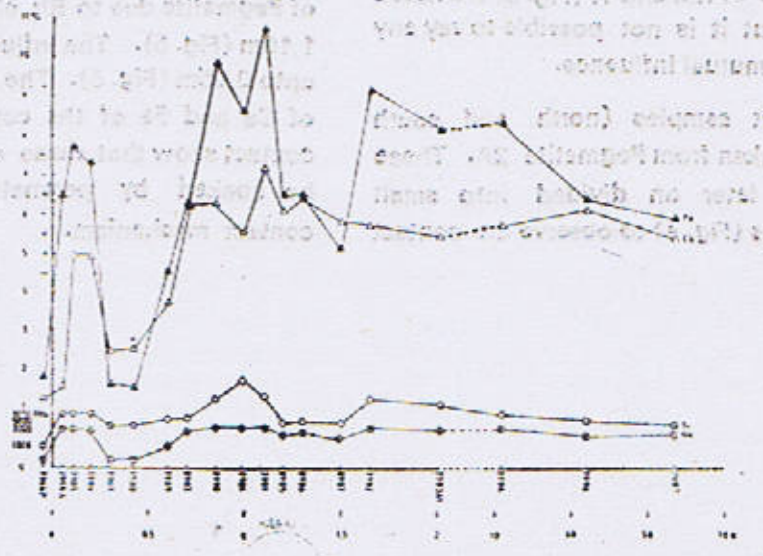

Fig.6 Fe, Ca, Ti and Mn in Migmatite. The samples are same as in Fig.5.

From Figure 5, it is noted that Rb and Pb elements are very openly moved from pegmatitic solution to the Migmatite. Contrary to this, due to contact phenomenon, Sr shows decrease in its values in Migmatite. It was thought that Sr was present in Hornblede and the biotite was not able to take it in its structure.

When we follow the trends of Ca and Fe from contact to away in the country rock, the values of these elements increase maximum upto a distance of 0,11m from contact, then they decrease in their volues upto a diftance of 0,42m because there the samples contain more quartz and less plagioclase. Afterwards, the values of Ca and Fe are increasing continuously away from contact upto 0,70m, when they reach to the maximum values in other samples. Afterwards change in values is depending entirely on mineral composition of the Migmatite. Here the influence is noted only upto a distance of 0,70m.

The minimum values of Fe and Ca together with the values of Mn and Ti (Fig. 6) are noted with interest, but it is not possible to say any thing about the mutual influence.

The contact samples (north and south contact) were taken from Pegmatite 2A. These samples were later on divided into small oriented samples (Fig. 4) to observe the contact phenomenon at a very close distance in contact area (Figs. 7-8). The location of these divided samples is given in Fig. 4.

Figure 7 shows that Rb, Pb and Sr in both the north and south contact samples are decreasing from the contact towards Migmatite. Element Pb shows clearly the decrease in contents from Pegmatite to the country rock (Fig. 7). Contrary to this, Rb and Sr show clearly the maximum values in the contact zone. The values of Ni, Cr and Zn do not show any influence in both the contact zones.

Figure 8 shows that the values of Ca, Fe, Mn and Ti in the exo-contact-zone of Migmatite are higher than in Pegmatite. The elements Ti and Mn do not show any type of mutual influence among Migmatite and Pegmatite. In contrast to this, Ca and Fe show decrease in their values in both the contact zones, because the samples show more quartz than plagioclase.

Rb, Pb and Sr are the elements, which have migrated from pegmatitic salution towards Migmatite (Fig. 5, 7). The maximum influence of Pegmatite due to Rb element is noted upto 1,10m (Fig. 5). The influence of Pb is observed upto 0,05m (Fig. 5). The decrease in the values of Ca and Fe of the country rock just in the contact show that these elements can possibly be soaked by pegmatitic solutions during contact mechanism.

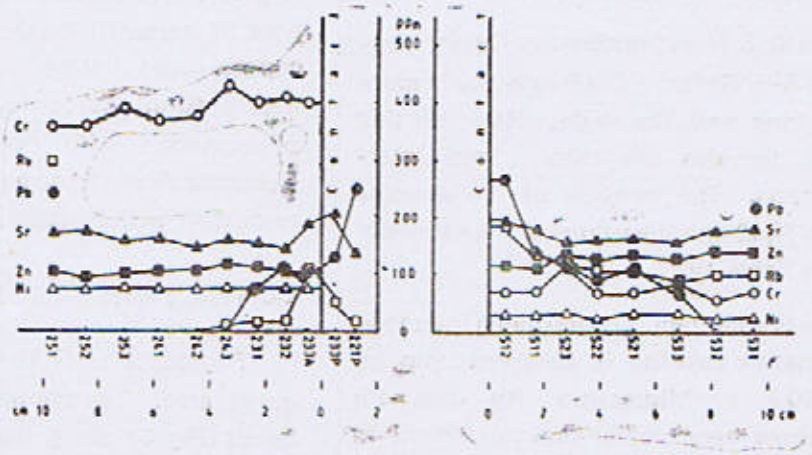

Fig.7 Trace elements of Pb, Sr, Zn, Rb, Cr and Ni in Mela-Band in close contact-zone of North and South contact with Peg. 2A. See Fig.4 for the location of samples and Table-II & III for the values of sample 8902/21P, 33P, 33A, 32, 31, 43, 42, 41, 52, 51 and sample 9905/12. 11, 23, 22, 21, 33, 32, 31.

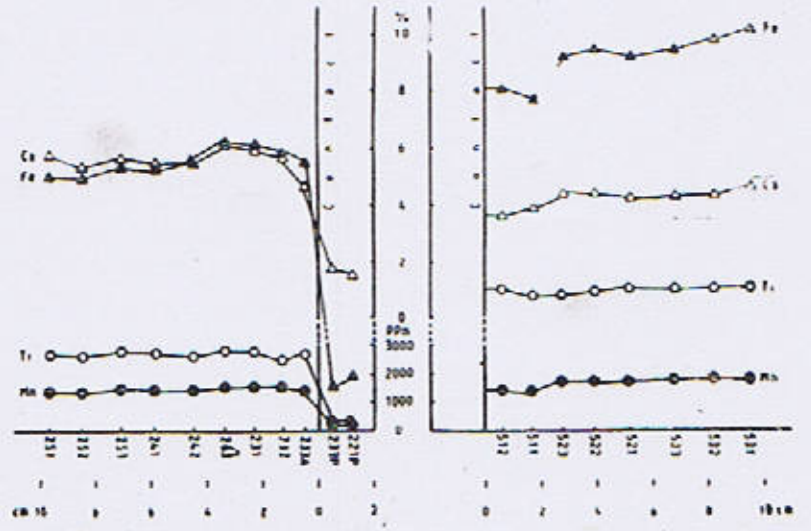

Fig.8 Fe, Ca, Ti and Mn in close contact-zone of North and South contact with Peg. 2A. The samples are same as in Fig.7.

CONTACT WITH PEGMATITE 3

Pegmatite 3 is a horizontally lying pegmatite with E-W Strike, The Pegmatite is more than 25m long and 6m wide. Here in this profile the samples are taken from Intermediate bands. The location of the samples is given in Fig.2 and the values of the elements are given in Table-IV.

Here in this contact, the maximum influence of the pegmatitic solution is observed upto 1m (Figs. 9-10) in Migmatitie. Rb and Pb elements show very clearly the enrichment in their values in exo-contact (Fig. 9), whereas Ca and Fe have become poor in their contents (Fig.10). All other elements do not show any type of mutual influence of Pegmatite and the country rock. Here the values of Sr have decreased in exo-contact, just contrary to the phenomenon with Pegmatite 2A. All other elements show the same behaviour, as is noted in contact with Pegmatite 2A.

CONTACT WITH PEGMATITE LI

Pegmatite Li is the largest in the investigated area. The samples are taken from melabands (Fig. 3) along the profile, perpendicular to the contact with Hanging Shell. The values of the elements are given in Table-V.

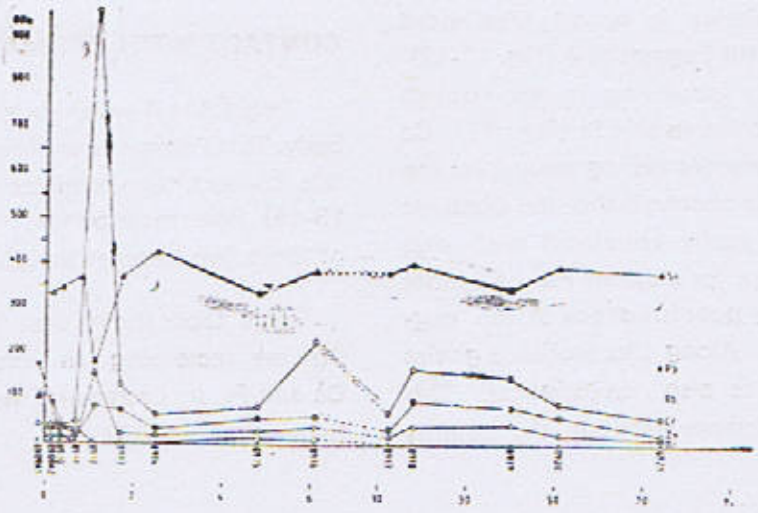

Fig.9 Sr, Pb, Rb, Cr, Zn and Ni in Intermediate Band of Evje-Iveland Migmatite. The influence of Pegmatite is upto 1m. Profile is perpendicular to the contact with Pegmatite 3. See Fig.2 for the location of samples. The values of samples are given in Table-IV.

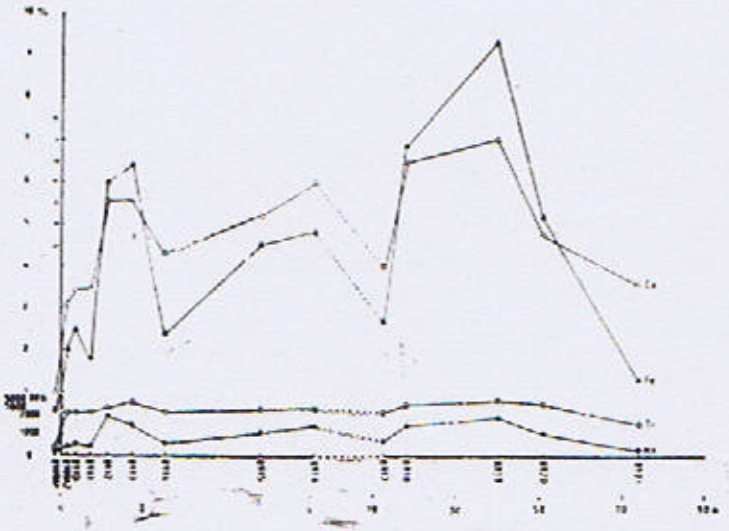

Fig.10 Ca, Fe, Ti and Mn in Migmatite. The samples are same as in Fig.9.

The maximum influence on Migmatite by the pegmatitic solution is upto 1, 50m noted in this contact with Pegmatite 4 (Fig. 11-12). The element Rb is increasing in exo-contact (Fig. 11). In opposite to this Sr (Fig. 11), Ca and Fe (Fig. 12) are decreasing away from the contact. Here, it is observed that the elements behaviour can be easily correlated with that Pegmatite 3, except for element Pb. All other elements show very poor influence of the pegmatitic solutions. Along this profile, a gneiss dyke (Im thick) is also investigated. This dyke shows the influence of Rb on the country rock (Fig. 11).

CONTACT WITH PEGMATITE 4

Pegmatite 4 is a horizontally lying lensic body. This Pegmatite is about 100m wide. From this contact, two samples were collected (Fig. 13-14) from mela-bands. The element values of these two samples are given in Table-IV.

This table shows that the elements Rb and Pb are increasing in exo-contact, whereas Ca and Fe are decreasing like the contacts with Pegmatites 3 and Li.

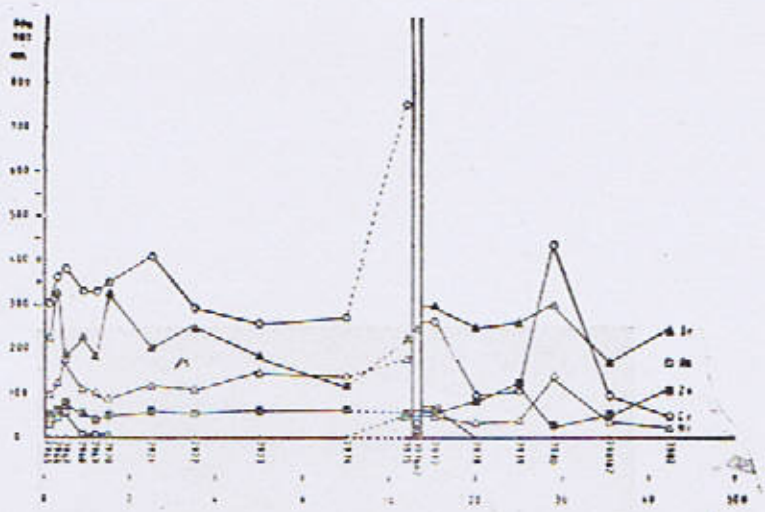

Fig.11 Sr, Rb, Zn, Cr and Ni in Mela-Band of Evje-Iveland Migmatite. The influence of Pegmatite is upto 1,50m. Profile is perpendicular to the contact with Pegmatite Li. See Fig.3 for the location of samples. The values of samples are given in Table.V.

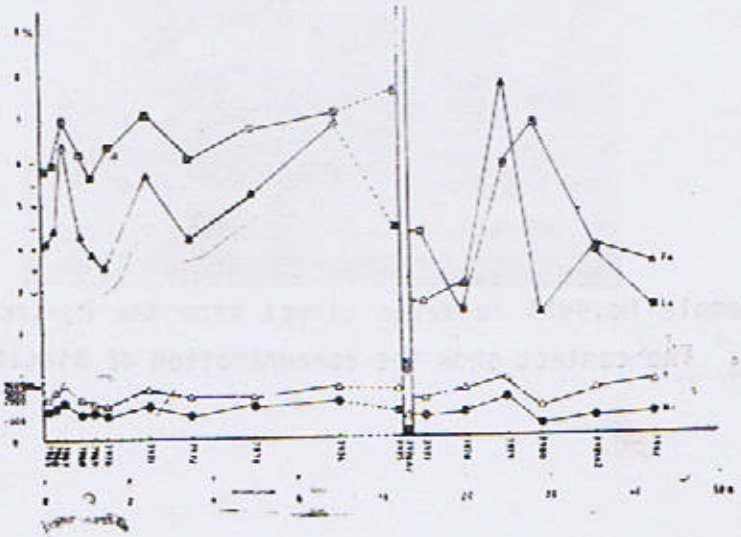

Fig.12 Fe, Ca, Ti and Mn in Migmatite. The samples are same as in Fig.11.

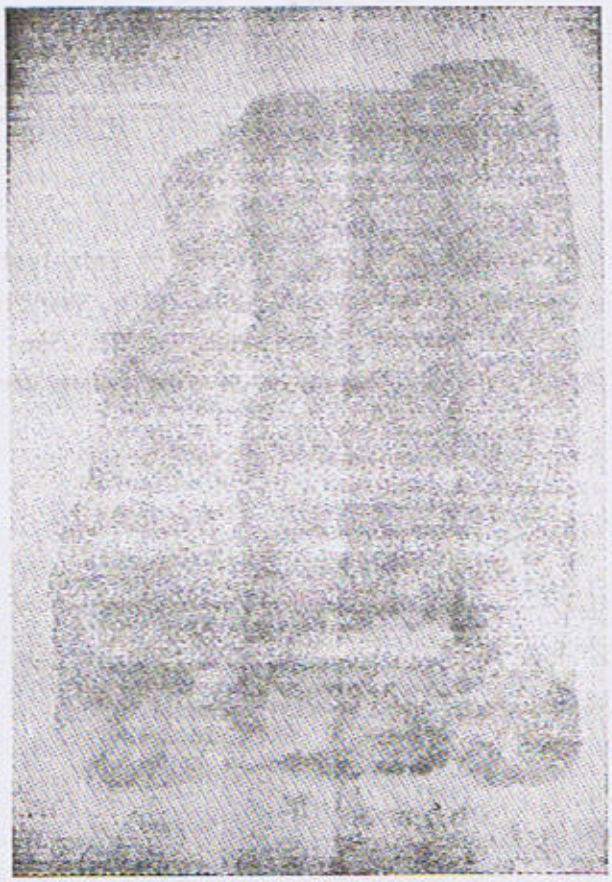

Fig.13 , Sample No.9915 is taken direct from the contact with Pegmatite, 4. The contact show the concentration of Biotite.

*Fig.14 Sample No. 9916 is taken direct from the contact with Pegmatite 4. The contact show the concentration of Garnet and Biotite.

CHANGE IN MINERAL COMPOSITION

Thin section studies reveal that the country rock in Evje-Iveland area has been influenced by pegmatitic solutions, at least, to an area of centimeter.

MINERAL COMPOSITION AT CONTACT WITH PEGMATITE 4

Two large contact samples were taken direct from the contact with Pegmatite 4 numbered as 9915 (Fig. 13) and 9916 (Fig. 14) and are studied in detail. Sample 9915 shows the concentration of biotite at the contact. Thin section study of this sample shows, that upto 5cm distance from contact, whole of the horbiende has been changed into biotite hornblend can be seen after a distance of 5cm form contact (Fig. 16). This shows, that the influence of pegmatitic solutions has charged the mineral composition upto 5cm. Biotite in the contact area is dark reddish brown. Therefore, they are named as Titania-Biotite. These biotite are formed by the influence of Pegmatite : Green Hornblend+ Iron ($Ti+Fe^{+2}$) = Titania Biotite with the help of water component of the pegmatitic solutions.

Zircon is concenterating in the contact zone, specially as inclusions in biotite. These Zircon are present in Intermediate-Bands of Migmatite, it is possible that during contact meta-morphism, these zircon have found their way in biotite.

Fig.15 T.S. 9915A1. Concentration of Biotite (Bt) at contact with Pegmatite 4. The upper right corner of the photo show the pegmatite border. 1Ni.

Fig.16 T.S. 9915A2. Hornblende is present at a distance of 5 cm from contact and show that the influence of pegmatitic solution is upto this distance.

Apatite is also concenterating in the contact zone. It is assumed that at the contact, water and phosphor, as volatile components pegmatitic solutions have played a role in the formation of biotite and apatite. The small idiomorph Monazite are also present in the contact zones. They may be formed by phosphor and rare earth elements of the pegmatitic solutions.

Thin section study of sample 3916 (Fig 14) shows that garnet is developing together with biotite at the contact with pegmatite 4 (Fig. 17). These garnets are almandin garnet with the composition Alm_{75} $spess_{21}$ And_4 (Lodhi, 1983) and are formed by contact metamorphism. It was supposed, that iron and flourides of pegmatitic solutions together with Si, Mg, Mn and Ca from the country rock might have played a role in the formation of these garnets.

The low values of Ca in both the contact-samples of pegmatite 4 (Table-VI) are due to less percentage of plagioclase. Quartz is relatively increasing at the contacts. The composition of plagioclase is An_{43} at both the contacts. Sericite and sassurite are the hydrothermal alteration of plagioclase, formed due to the water of pegmatitic solutions.

MINERAL COMPOSITION AT CONTACT WITH PEGMATITE 2A :

Thin section studies in the contact zone of Peg. 2A show that the influence of

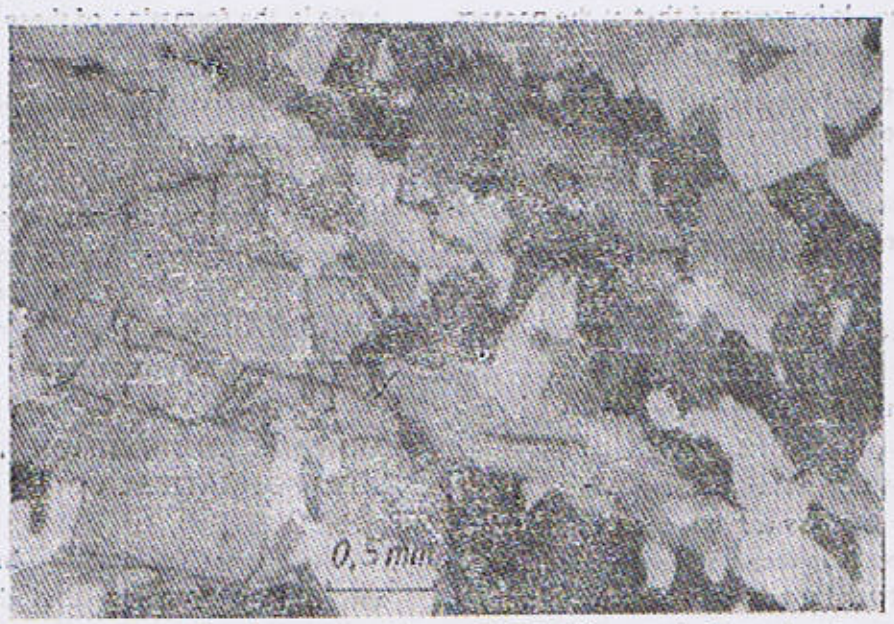

Fig.17 T.S. 9916A2. Concentration of Biotite and Garnet at contac with Pegmatite 4.

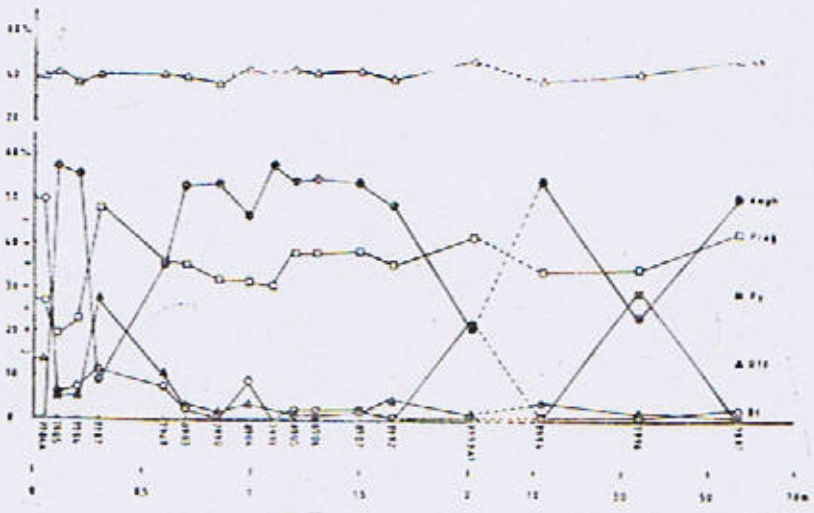

Fig.18 Presentation of Modal analysis of Mela-Bands of Migmatite in Evje-Iveland area along the profile, perpendicular to the contact with Peg. 2A. The samples are same as in Fig.5&6.

pegmatitic solution on the country rock is seen upto 5cm from the contact. This pegmatite is 3,5m wide. Here, in this contact all the hornblende have changed into biotite. Plagioclase is less in amount whereas Quartz is in abundant. The composition of plagioclase at contact is An_{40}. Figure 18 shows the modalic composition of different minerals of the country rock at contact with Pegmatite 2A.

Apatite is increasing in the contact zone. Zircon and monazite are also present in the contact.

MINERAL COMPOSITION AT CONTACT WITH PEGMATITE 3

The petrographic stuies at contact with Pegmatite 3 show that the maximum influence of pegmatitic solutions on the mineral composition of Migmatite, in contrast to geochemical investigation of trace elements, is observed only in centimeter area. Here, all the hornblende are converted into biotite. All the changes in mineral composition at this exo-contact-zone coincide with the contoct of Pegmatite 2A, except that of plagioclase. Here at this contact with Pegmatite 3, some plagioclase show zoning. Figure 19 shows the distribution of modal analysis in the country rock at contact with Pegmatite 3.

MINERAL COMPOSITION AT CONTACT WITH PEGMATITE Li

Thin section studies at this exo-contact-zone show the influence of pegmatitic solution on the mineral composition of the country rock upto a distance of 10 cm from contact. Here, except the garnet, all other changes in mineral composition are coinciding with that of Pegmatites 2, 3 and 4. Figure 20 shows the modalic representation of different minerals in Migmatite. The country rock at this profile is rich in clino-pyroxene. At contact, plagioclase has been altered into sericite due to the pegmatitic solutions.

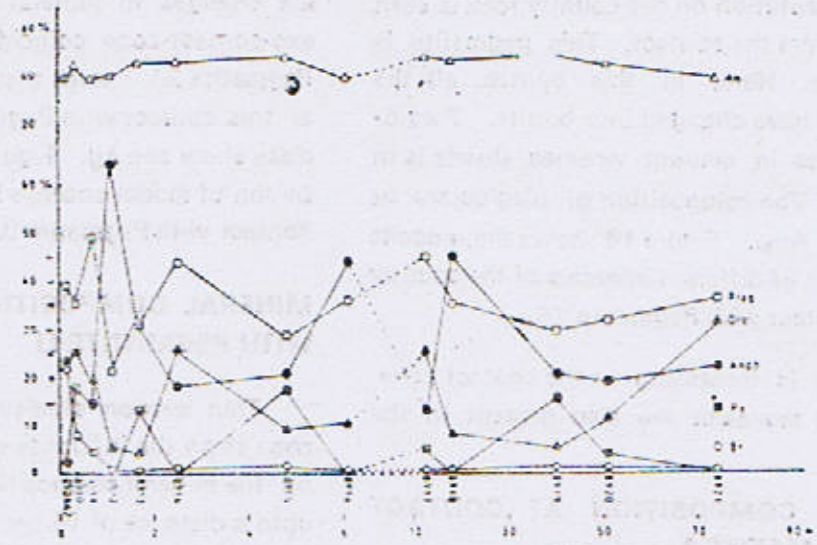

Fig.19 Presentation of Modal analysis of Intermediate Bands of Migmatite in Evje-Iveland area along the profile, perpendicular to the contact with Peg. 3. The samples are same as in Fig.9&10.

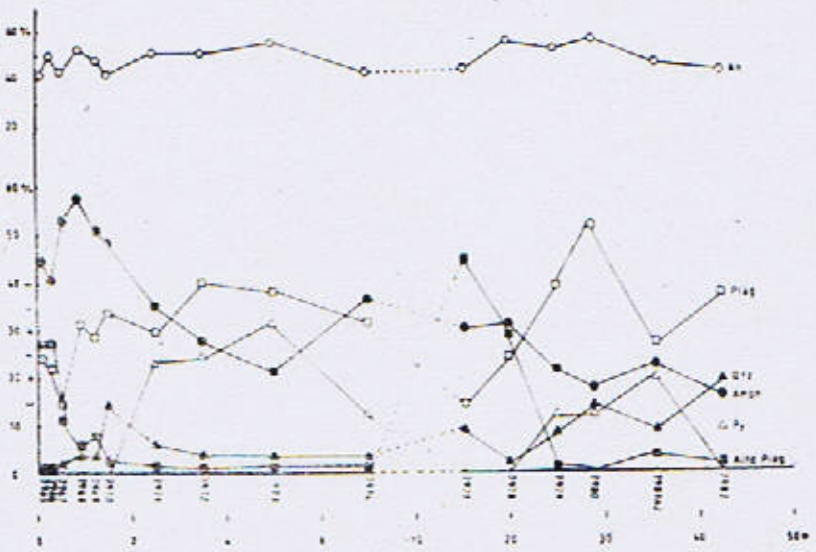

Fig.20. Presentation of Modal analysis of Mela-Bands of Migmatite in Evje-Iveland area alont the profile, perpendicualar to the contact with Peg.Li. The samples are same as in Fig.11&12.

CONCLUSIONS

The mineral and geochemical studies show that the influence of pegmatitic solution on the country rock (Migmatite) bring changes in mineral composition upot 5cm for the contacts with Pegmatites 2A, 3 and 4, whereas the contact with Pegmatite Li show the changes in mineralogy upto 10cm in exo-contact-zone. All the hornblende have changed into biotite. For the concenteration of biotie, apatite and Monazite, the volatile components (rich in water and phosphor) of pegmatitic solutions are responsible. almanedine-garnet at contact with Pegmatite 4 has formed due to the contact-metamorphism. Zircons are the parts of leuco-bands of Migmatite, which have migrated to the exo-contact-zone during contact phenomenon. At the contact zones, the plaglioclase is less than quartz, therefore, the contacts are poor in Ca and Fe. The composition of plagioclase at the contacts is An_{40}. Sericite and Sassurite are the alteration products of plagioclase, caused by the pegmatitic solutions.

The changes in trace elements occur in an area of 1, 10m (Fig. 5, contact with Pegmatite 2A) ; 1,0m (Fig. 9, contact with Pegmatite 3) and 1,5m (Fig. 11, contact with Pegmatite 4). The elements Rb and Pb are mostly migrating towards the country rock (Fig. 5.7, 9 and 11). The element Sr, except contact with Pegmatite 2A (Fig. 5 and 7) show decrease in their contents, therefore, it is thought that Sr has gone to the pegmatitic solutions (Fig. 9 and 11). Ca and Fe (Fig. 6, 8, 10 and 12) show decrease in theirs vlaues, this is due to the presence of more quartz than plagioclase at the investigated contacts with country rock.

In this investigated area, the country rock has been influenced by pegmatitic solutions differently. The intermediate - (contact with Pegmatite 3) and mela-bands (contact with Pegmatite 2A and Li) show the same trend of influence. The influence on leuco-bands was not under taken, as the sampling was very difficult.

It can be summerized, that the influence of pegmatitic solutions is not dependent on the length and thickness of the pegmatitic bodies, it may be due to the multiple-emplacements inside the pegmatites (Uebel, 1980 and Lodhi, 1988). It is also possible that the lateral tectonic activities or due to the effect of Gravity the older Pegmatites have subsided to give the space for emplacement of younger Pegmatites, which may not have effected the country rock due to the cold and passive contacts of older generation of Pegmatites with Migmatite.

ACKNOWLEDGEMENT

This work is a part of approved Ph. D. Thesis, submitted to the Faculty of Geosciences, Technical University, of Berlin, Germany. The authoris grateful to Professor Dr. P. J. Uebel, Professor Dr. J. Stiefel and Dr. D. Rose for their guidance, discussion and cooperation.

TABLE - 1

Distribution of major and trace elements in Migmatite samples of the profile perpendicular to the contact with Pegmatite 2-A, as determined by XRF. The values of Ca and Fe are given in percentage, whereas other elements show ppm values.

Sample	Distance from contact	Ca	Ti	Cr	Mn	Fe	Ni	Cu	Zn	Rb	Sr	Y	Zr	Pb
7984	—0,05	1,3	1050	50	320	1,8	—	Sp.	15	37	47	463	194	137
7984A	0,05	1,5	9010	46	2120	6,5	18	28	175	710	49	236	112	39
7985	0,11	4,9	9730	65	2220	7,7	21	21	132	87	136	48	111	—
7986	0,20	4,9	9150	50	1900	7,3	20	31	119	50	147	39	129	—
7987	0,30	2,4	2430	25	360	1,5	6	20	34	82	213	19	143	—
7988	0,42	2,5	2470	35	320	1,5	13	14	25	69	217	20	141	—
7989	0,60	3,7	6250	60	1020	4,5	17	31	73	35	199	33	195	—
8903	0,70	6,2	6400	190	1890	6,2	70	25	123	24	172	75	71	—
7990	0,85	6,3	12510	75	2380	9,8	25	71	137	10	220	38	98	—
8904	0,99	5,5	17400	130	2140	8,6	46	202	135	47	201	61	153	—
7991	1,10	7,1	13170	105	2670	10,7	28	57	163	—	200	42	109	—
8905	1,20	6,1	4670	190	1700	6,0	55	28	107	22	142	35	55	—
8906	1,30	6,5	5220	200	1800	6,0	67	39	108	15	144	29	51	—
8907	1,50	5,8	4550	170	1480	5,2	61	35	87	14	133	26	51	—
7992	1,65	5,7	12600	70	2050	9,2	23	42	128	—	227	36	127	—
7993A1	2,30	5,4	11230	70	1930	8,2	22	22	129	—	218	42	120	—
7994	11,70	5,8	9950	85	1920	8,3	22	68	121	—	193	33	116	—
7996	34,00	6,1	6300	165	1560	6,4	39	80	83	—	143	11	52	—
7997	57,00	5,4	3570	85	1710	6,0	49	40	129	40	103	81	70	—

TABLE - 2

Distribution of major and trace elements of contact sample 8902, with Pegmatite 2-A taken from Hanging-Shell. The sample is divided into further small parts. The values of Ca and Fe in percent and of other elements are given in ppm, as determined by XRF.

Sample	Distance from contact		Ti	Cr	Mn	Fe	Ni	Cu	Zn	Rb	Sr	Y	Zr	Pb
890221P	—0,012	1,5	240	Tr.	60	0,19	Tr.	24	Tr.	16	131		—	246
890233P	—0,005	1,7	270	Tr.	52	0,16	Tr.	22	Tr.	47	209	15	—	135
890233A	0,005	4,7	2720	400	1490	5,56	74	25	105	108	184	79	15	104
890232	0,013	5,6	2600	410	1530	5,80	74	26	107	17	146	61	22	107
890231	0,023	5,9	2800	400	1570	6,01	75	44	112	16	155	63	22	78
890243	0,034	6,0	2820	430	1590	6,05	75	44	120	13	162	64	19	—
890242	0,045	5,4	2630	380	1410	5,50	74	40	109	—	148	55	14	—
890241	0,059	5,5	2700	370	1400	5,32	74	40	104	—	162	60	10	—
890253	0,071	5,5	2800	390	1450	5,36	75	37	102	—	159	69	17	—
890252	0,085	5,2	2600	360	1280	4,95	72	35	95	—	176	61	19	—
890251	0,097	5,6	2760	360	1330	4,92	74	40	103	—	172	61	22	—

Tr = Traces

TABLE - 3

Distribution of major and trace elements of contact sample 9905, with Pegmatite 2-A taken from Foot-Shall. The sample is divided into further small parts. The values of Ca and Fe in percent and of other elements are given in ppm, as determined by XRF.

Sample	Distance from contact	Ca	Ti	Cr	Mn	Fe	Ni	Cu	Zn	Rb	Sr	Y	Zr	Pb
990512	0,006	3,7	10820	70	1410	8,1	30	64	116	183	193	49	139	262
990511	0,017	3,8	8730	70	1330	7,7	29	62	112	134	180	32	115	114
990523	0,028	4,3	8700	120	1700	9,2	32	56	135	120	155	38	112	114
990522	0,039	4,4	9400	70	1780	9,5	23	48	125	110	162	42	84	93
990521	0,052	4,2	10000	69	1700	9,2	30	52	136	105	164	41	109	105
990533	0,068	4,3	10500	87	1730	9,4	32	51	128	88	158	44	110	69
990532	0,082	4,3	10800	58	1810	9,8	24	56	143	101	179	62	105	—
990531	0,095	4,6	11300	70	1830	10,1	25	53	141	101	178	46	112	—

TABLE - 4

Distribution of major and trace elements in Migmatite samples of the profile perpendicular to the contact with Pegmatite 3, as determined by XRF. The values of Ca and Fe are given in percent, whereas other elements show ppm values

Sample	Distance from contact	Ca	Ti	Cr	Mn	Fe	Ni	Cu	Zn	Rb	Sr	Y	Zr	Pb
8909A1	—0,15	1,0	390	41	140	0,3	Tr.	Tr.	Tr.	107	101	50	31	174
8909A2	0,15	3,1	2500	39	410	2,1	15	22	32	94	331	31	138	89
8910	0,35	3,5	2700	37	590	2,5	10	21	31	34	345	16	121	—
8911	0,70	3,4	2300	46	440	1,8	12	21	21	18	362	16	152	—
8912	1,10	5,6	4400	956	1930	6,0	155	36	82	—	177	22	87	—
8913	1,70	5,5	7770	130	1450	6,4	20	50	74	—	373	Tr.	92	—
8914	2,50	4,3	2830	66	380	2,4	16	19	30	—	430	Tr.	143	—
8915	4,80	5,2	4240	80	1160	4,6	28	35	55	14	337	20	89	—
8916	6,10	5,6	4160	230	1450	4,8	38	34	62	15	381	18	97	—
8917	12,50	4,0	2540	70	730	2,7	19	39	30	—	380	15	119	—
8918	18,00	6,5	6360	170	1480	6,9	40	55	99	—	400	26	86	—
8919	40,00	7,0	8410	150	1850	9,3	45	72	82	—	346	27	73	—
8920	51,00	4,8	6970	70	1019	5,2	22	46	62	—	394	17	104	—
8921	74,00	3,6	1580	73	320	1,3	12	23	16	—	384	16	168	—

TABLE - 5

Distribution of major and trace elements in Migmatite and Gneiss samples of the profile perpendicular to the contact with Pegmatite 3, as determined by XRF. The values of Ca and Fe are given in percent, whereas, other elemenus show ppm values.

Sample	Distance from contact	Ca	Ti	Cr	Mn	Fe	Ni	Cu	Zn	Rb	Sr	T	Zr
7965	0,10	5,8	1900	300	1240	4,0	93	51	51	29	216	Tr.	36
7966	0,30	5,8	2800	360	1360	4,3	117	33	57	46	329	216	71
7967	0,50	7,0	7300	380	1700	6,4	172	141	73	57	180	30	42
7968	0,90	6,3	1960	330	1260	4,3	105	39	51	Tr.	220	Tr.	40
7969	1,20	5,6	1620	330	1220	3,8	100	42	42	Tr.	180	Tr.	37
7970	1,50	6,2	1530	350	1100	3,5	86	36	49	Tr.	448	Tr.	64
7971	2,50	7,0	4370	410	1580	5,7	116	52	57	—	200	Tr.	43
7972	3,50	6,1	2150	290	1170	4,1	107	36	54	—	246	Tr.	47
7973	5,00	6,7	2060	260	1500	5,2	146	36	61	—	184	Tr.	29
7974	7,00	7,1	5630	270	1790	6,9	136	120	64	—	120	Tr.	37
7975	12,00	7,5	3200	750	1250	4,5	175	120	53	52	224	22	49
7976A2	12,50	1,0	950	34	130	1,0	Tr.	22	15	55	238	15	86
7976A4	12.50	0,7	2300	23	190	1,5	Tr.	Tr.	33	87	200	Tr.	158
7977	15,30	4,2	1870	260	1010	2,6	48	45	54	62	295	36	83
7976A2 & 7976A2 are Gneiss samples.													
7978	20,00	2,4	3210	85	1120	3,1	32	51	81	—	245	12	168
7979	25,00	5,8	10170	104	1870	7,7	39	81	124	—	260	25	87
7980	29,00	6,8	1380	433	580	2,3	136	61	28	—	298	Tr.	69
7981A2	35,50	3,9	3190	93	880	3,8	35	71	46	—	166	16	97
7982	42,50	2,5	6770	46	1060	3,6	20	29	110	—	242	23	277

Tr = Traces

TABLE 6

Distribution of majar and trace elements in contact samples of Migmatite with Pegmatite 4. Biotite and Garnet are concentrated at the contact. The values of Ca and Fe are given in percent, whereas, other elements show ppm values, as determined by XRF.

Sample	Distance from contact.	Ca	Ti	Cr	Mn	Fe	Ni	Cu	Zn	Rb	Sr	Y	Zr	Pb
9915A1	0,013	1,0	5530	105	1950	4,7	33	25	128	373	34	222	73	101
9915A2	0,045	2,5	15540	67	3330	6,4	30	28	179	448	68	275	168	83
9916A3	—0,015	0,5	260	45	80	0,1	Tr.	—	—	300	36	88	Tr.	210
9916A2	0,015	1,3	10900	140	11500	9,7	39	67	250	850	55	1148	289	—
9916A1	0,050	1,0	8800	165	22100	10,4	29	36	200	690	27	1610	221	—

Tr = Traces

REFERENCES

Barth, T.F.W. 1947. The nickliferous Iveland-Evje amphibolite and its relation. N.G.U., **168a** 1-71.

Barth, T.F.W., and Dons, J.A. 1960. Precambrian of Southern Norway. N.G.U., **208**, 5-67.

Falkum, T. 1969. Geological investigation in the Precambrian of Southern Norway. N.G.U., **258**, **185-227**.

Johannes, W., and Gupta, L.N. 1982. Origin and evalution of a Migmatite. *Cont, Min. Pet.*, **79**, 114-123.

Lodhi, Sherjil A. K. 1983. Das Nebengestein in Pegmatit-Gebiet Evje-Iveland, Sued Norwegen, (Tektonik, Gefuege, Modalbastan und gegenseitige Beeinflussung von Nebengestein und pegmatitischen Loesungen). Dissertation, Technical University, Berlin. 1-180.

Lodhi, Sherjil A.K. 1988. Tectonic elements and emplacement of dykes and plug like bodies, as demonstrated by Pegmatites of Evje-Iveland area of Southern Norway. *Geol. Bull. Punjab Univ.*, **23**, 77-93.

Oftedahl, Chr. 1980. Geology of Norway. 26th Internat. Geol. Congr. Paris. Universitets for laget, Trondheim, Oslo, N.G.U., **356**, 1-167.

Rose, D. 1978 Geochemische und petrographiche Untersuchungen Zur Platznahme des zonar gebanten Pegmatits, Brabant, Suedwest-Afrika (Namibia). Dissertation, Technical University, Berlin. 1-200

Uebel, P.J. 1980. Emplacement of dykes and plug like bodies, as demonstrated by Pegmatites. *N. Jb. Miner. Abh.*, **138**, 207-227

———

Geol. Bull. Punjab Univ. 1992, 27, 97-106

DELINEATION OF FRESH WATER AQUIFER IN A SALINE AREA USING GEOELECTRICAL METHOD

By

UMAR FAROOQ

Institute of Geology, Punjab University, Lahore 54590, Pakistan.

AND

SHEHZAD A. QAZI

National Engineering Services Pakistan (Private) Limited, Lahore Pakistan.

Abstract : *The area near Matli town District Hyderabad is facing an acute problem of salinity and water logging where a sugar mill has been constructed. The non availability of the fresh water in this area is causing problem for the operation of sugar mill.*

An attempt has been made to locate fresh water aquifer in the saline area by employing electrical resistivity technique. A total number of 15 soundings using Schlumberger electrode configuration were carried out in and around the project area. Based upon the results of resistivity survey a fresh water aquifer zone has been identified in the vicinity of the project area. Considering various factors test hole drilling was recommended at a suitable location in this fresh water aquifer zone. During drilling operation water samples were collected at various depths which were analysed in the laboratory to check the water quality. The results of water samples and lithological log have confirmed the results of resistivity data. Based upon these studies 0.5 *cusec skimming type tubewell has been designed to meet the fresh water requirements of the sugar mill.*

INTRODUCTION

Matli Sugar Mill has been constructed about 45 km from Hyderabad city along Badin-Hyderabad Road (Fig. 1). The project area where mill is located faces an acute problem of salinity and water logging. Existing informations indicate that ground-water quality is brackish to saline. A tube well drilled near an irrigation canal south of the mill discharges water with 3000 ppm of dissolved solids. Another tubewell installed upto about 25 meters depth in the mill area discharges water with 7000 ppm of dissolved solids. In order to get the sugar mill in operation, sufficient quantity of fresh water was required which was making hard for the management to develop a dependable and permanent source.

As desired by the concerned authority, the problem was taken up by performing reconnaissance visit of the project area. During this visit a number of open wells were observed. Water quality tests showed that

some open wells have comparatively fresh water, which, therefore, formed the basis for the exploration of fresh water in the project area.

Keeping in view the usefulness of the electrical resistivity survey, it was planned to use it to delineate the lateral extension of fresh aquifer.

In the light of the results obtained, causes of salinity and water logging of the project area have been discussed and a fresh water aquifer zone in the saline area has been delineated.

FIELD PROCEDURE

The resistivity survey was conducted using an ABEM Terrameter SAS 300B. Schlumberger electrode configuration was used throughout the survey with a maximum current electrode separation of AB/2=100 meters. The subsurface resistivity is calculated from the electrode spacing, applied current, and measured voltage (Telford et al., 1985). Each sounding was conducted upto the depth confirming the low apparent resistivity values. A total of 15 resistivity soundings were performed at different locations in the area (Fig. 1).

DATA PROCESSING

Data processing has been completed in two steps. Partial curve matching using auxiliary point method was empolyed in first step to determine the approximate true resistivity earth models for each sounding curve. In auxiliary point method each branch of the apparent resistivity curve is approximated by a two layer apparent resistivity curve. The co ordinates of the cross of this two layer curve are considered to represent the thickness and the resistivity of a fictitious layer that replaces the sequence of shallow layers (Koefoed. 1979). For this purpose set of Ebert Auxiliary graphs were used. Final processing of the resistivity curves was made in second using computer programme which is capable of interpreting the resistivity curves using automatic iteration method. The computed true resistivity earh models were obtained and have been presented (Fig. 2).

RESULTS

Based upon the computed earth resistivity models, the project area can be classified into three different types of resistivity zonss having different true resistivity ranges. These ranges may be interpreted in terms of subsurface hydrogeological set up (Table-1).

TABLE-1

Resistivity Values and Corresponding Interpreted Lithology

Resistivity Zone	Resistivity Values Ohm-meter	Interpreted Lithology
Low	1-9	Silty clay saturated with saline water
Medium	10-20	Sandy, silty clay layer saturated with brackish water
High	21-45	Fine to medium sand saturated with fresh water

Based on the lithological log, chemical analysis of the water samples and the permeability of the aquifer, a skimming type tube well of 0.5 cusec has been designed to meet the requirement of the sugar mill.

HYDROGEOLOGICAL MODEL OF THE PROJECT AREA

On the basis of geoelectric section, the bore hole informations and other relevant geological observations, a hydrogeological model of the project area has been developed as described below.

Matli area was originally composed of thick clay/silty clay deposits. The tributaries of River Indus were flowing through the project area causing erosion of the pre-existing clay layers forming comparatively deeper channels and subsequently depositing sandy material in these channels. Later these Channels were abandoned with thin cover of sandy silty and clayey material. This picture corresponds with the geoelectric section along line AA (Fig 3.) The outcrop of the thick clay layers can also be observed at various locations in and around the project area. One of the prominent clay out crop is about 4 km from the test hole near Rabno Nothani Village.

The acute problem of water logging in this area may also be explained with the same interpreted hydrogeological model.

The project area is continuously being recharged with the system of irrigation canals. Fuleli is the major canal passing through the area of investigation which originates from Ghulam Muhammad Barrage. The seepage water from the canals as well as excess Irrigation water used for the cultivation of land, penetrates slowly in the subsurface sandy aquifer, underlying the semi impervious layer. The thick impervious clay layer below the aquifer offers obstruction to the water to be penetrated deeper into the subsurface. Since the permeable medium (sandy layer) is bounded in the channels large quantity of surface water therefore cannot be infiltrated in the aquifer zone and consequently, water level rises in the area, causing water logging. The water logging is interpreted to be severe in such locations where sandy layers are very thin. In such areas underlying thick clay layer have close contact with the overlying semi impervious material causing severe condition of water logging. This may be proved by observing geoelectric section, (Fig. 3) in which the surface is severely effected at location of VES 6 with water logging while at the locations of VES 13 and VES 14 the water table is comparatively deeper and the surface is being used for good agriculture.

CONCLUSION

Based on this study, it is concluded that electrical resistivity method is a reliable mean of delineating fresh water zone in the saline area. This method gives us valuable informations on the areal distribution of subsurface units and it also helps in formulating hydrogeological set up of the area where subsurface geological information is insufficient.

In the light of the aforesaid resistivity zoning, a geoelectric section along line AA has been constructed (Fig. 3). This section delineates three distinct subsurface lithologic untis. Many dry rocks are electrical insulators, and their resisititives are high. However, moisture filled porous media readily conduct the flow of electrical current and have much lower resistivites. Consequently, the resistivity of porous media is largely controlled by the amount of pore water, porosity and permeability of the porous media, and the dissoloved solids concentration of pore water (Benson, 1992). Along section AA, the upper unit is composed of sandy silty clay material which is present in the entire area and varies in thickness from 3 to 14 meters. It bears true resistivity values ranging from 10 to 20 Ohm-meters. This range of true resistivity values indicate the presence of brackish water in this zone. Geoelectrical investigations for salt water invaded zone was picked up by (Robert et al., 1980) near Venice and Homosassa on the west coast of Florida, USA. The salt water invaded zonewas clearly discernible as low resistivity layer of less than 10 ohm-meter and possibly as low as 2 to 3 ohm meter which offered an excellent contrast with the high resistivity values of 45 to 300 ohm-meter for fresh water. In the section along AA, a high resistivity zone is under lain by the medium resistivity zone. This zone bears true resistivity values ranging from 21 to 45 ohm-meters. The high resistivity values can be attributed to the presence of fine to medium sand saturated with fresh water. This zone is present in the entire area along section AA except at VES 6 where it is completely missing.

Below the high resisitivity zone, a low resistivity zone bearing true resistivity values ranging from 1 to 9 Ohm-meters is encountered. The low resisitivity values can be interpreted as clayey material saturated with saline water. This is present in the entire area up to the explored depth of 100 meters. On the basis of the interpretation of geoelectric section in terms of lithology, a test hole has been drilled near VES 8 location. During drilling operation, four water samples were collected from sandy aquifer at different depths. Chemical analysis of these samples was carried out in the laboratory and the results were compared with the international standards for various components of total dissolved solids (Table-2). The values indicate that the water is of good quality.

TABLE-2

Chemical Avalysis of Water Samples from Test Well Near Ves 8

Samples collected at various depths					International standard drinking water	
Parameter Tested	21 meter	31 meter	37 meter	43 meter	Permissible	Excessive
PH value	7.95	8.10	8.15	8.10	7.0-8.5	6.5-less than 9
*TDS (ppm)	580	568	524	608	500	1500
Chloride as Cl (ppm)	72	78	44	82	200	600
Total Hardness as $COCO_3$ (ppm)	387	380	405	370	—	—

*Total dissolved solids

A pumpout test was also carried out in the test hole in order to determine the aquifer yield.

REFERENCES

Benson, A. K., 1992. Integrating seismic, resistivity, and ground penetrating radar data to delineate the water table and groundwater contamination. Water-Rock Interaction, Kharaka and Maest (eds) Balkema, Rotterdam.

Bisdorf R. J. and Zohdy A. A. R. 1980. Geoelectrical investigations of salt-water encroachment of carbonate aquifers on the west coast of Florida. *Geophysics* 45, (4), 556.

Koefoed, O., 1979. Geosounding Principles, I Resistivity Sounding Measurements, Elsevier, Amsterdam.

Telford, W. M., Geldrat, L.P., Key, D. A., and Sheriff, R. E., 1985. Applied Geophysics. Cambridge University Press, London.

———

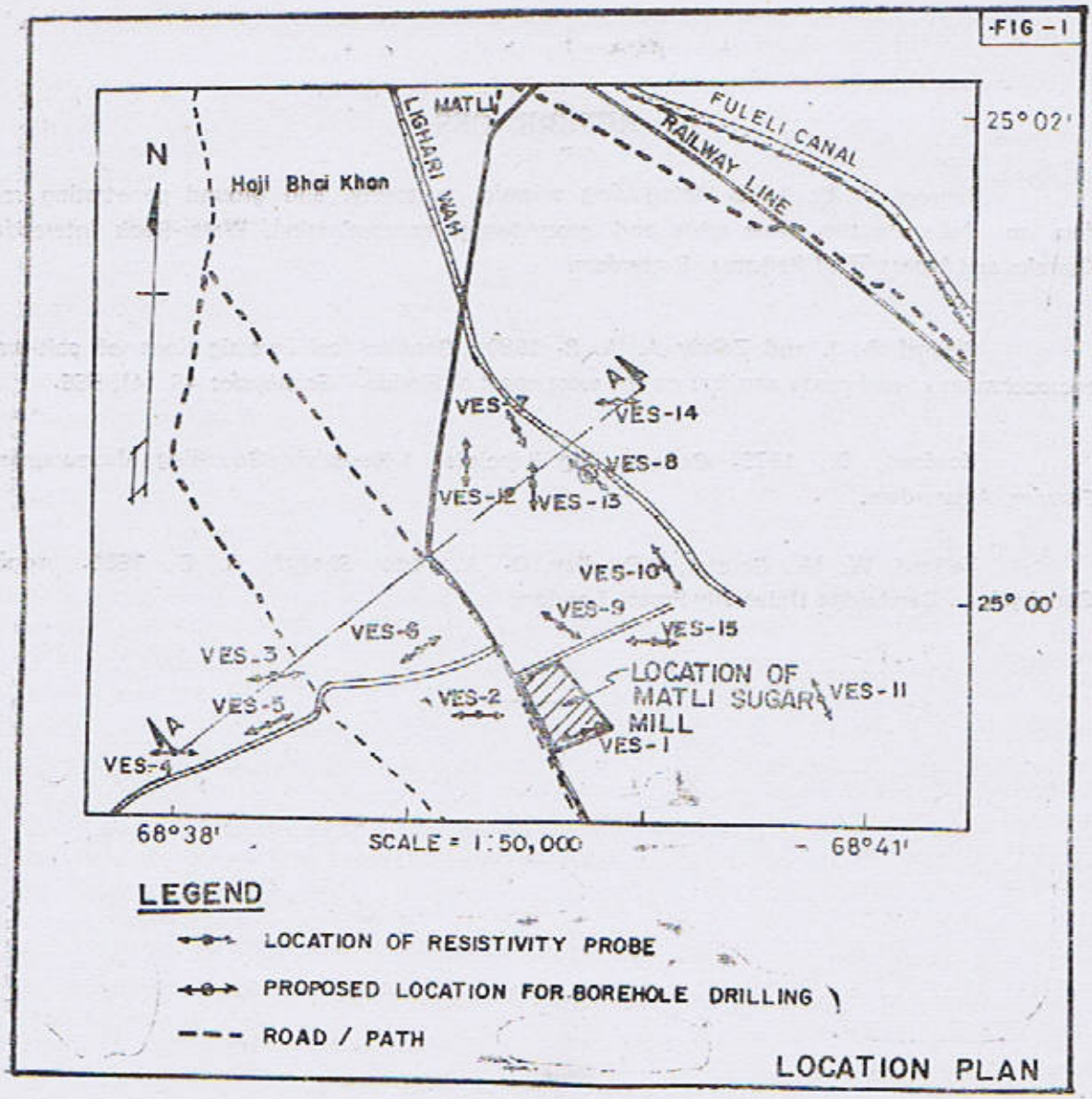
FIG - I
N
Haji Bhai Khan
MATLI
LIGHARI WAH
FULELI CANAL
RAILWAY LINE
25° 02'
25° 00'
VES-7
VES-14
VES-8
VES-12
VES-13
VES-10
VES-9
VES-15
VES-6
VES-3
VES-5
VES-4
VES-2
LOCATION OF MATLI SUGAR MILL
VES-11
VES-1
68°38'
SCALE = 1:50,000
68°41'
LEGEND
LOCATION OF RESISTIVITY PROBE
PROPOSED LOCATION FOR BOREHOLE DRILLING
ROAD / PATH
LOCATION PLAN

FIELD RESISTIVITY CURVES ALONGWITH TRUE RESISTIVITY EARTH MODEL

FIG 2 (a)

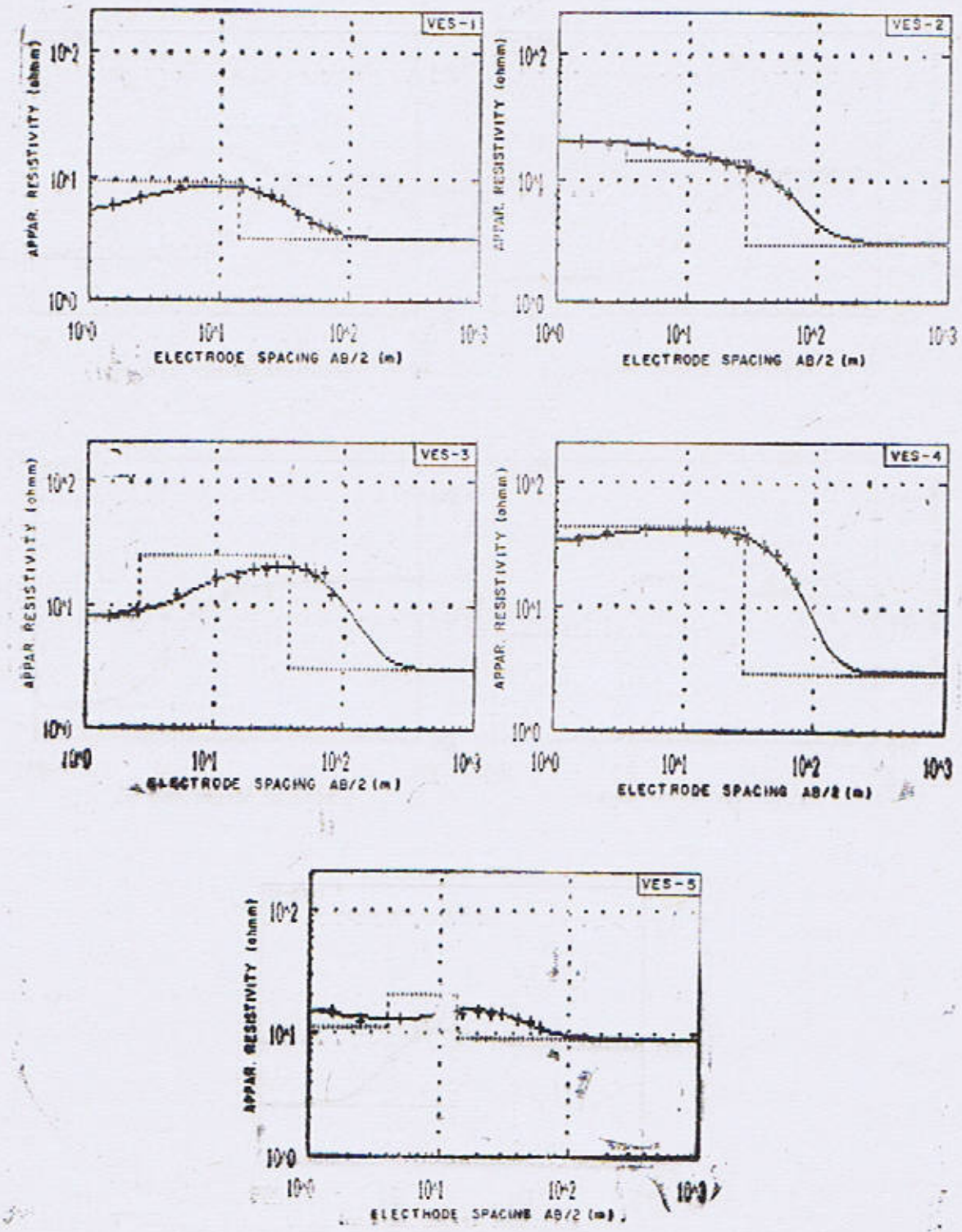

FIELD RESISTIVITY CURVES ALONGWITH TRUE RESISTIVITY EARTH MODEL

FIG. 2. (b)

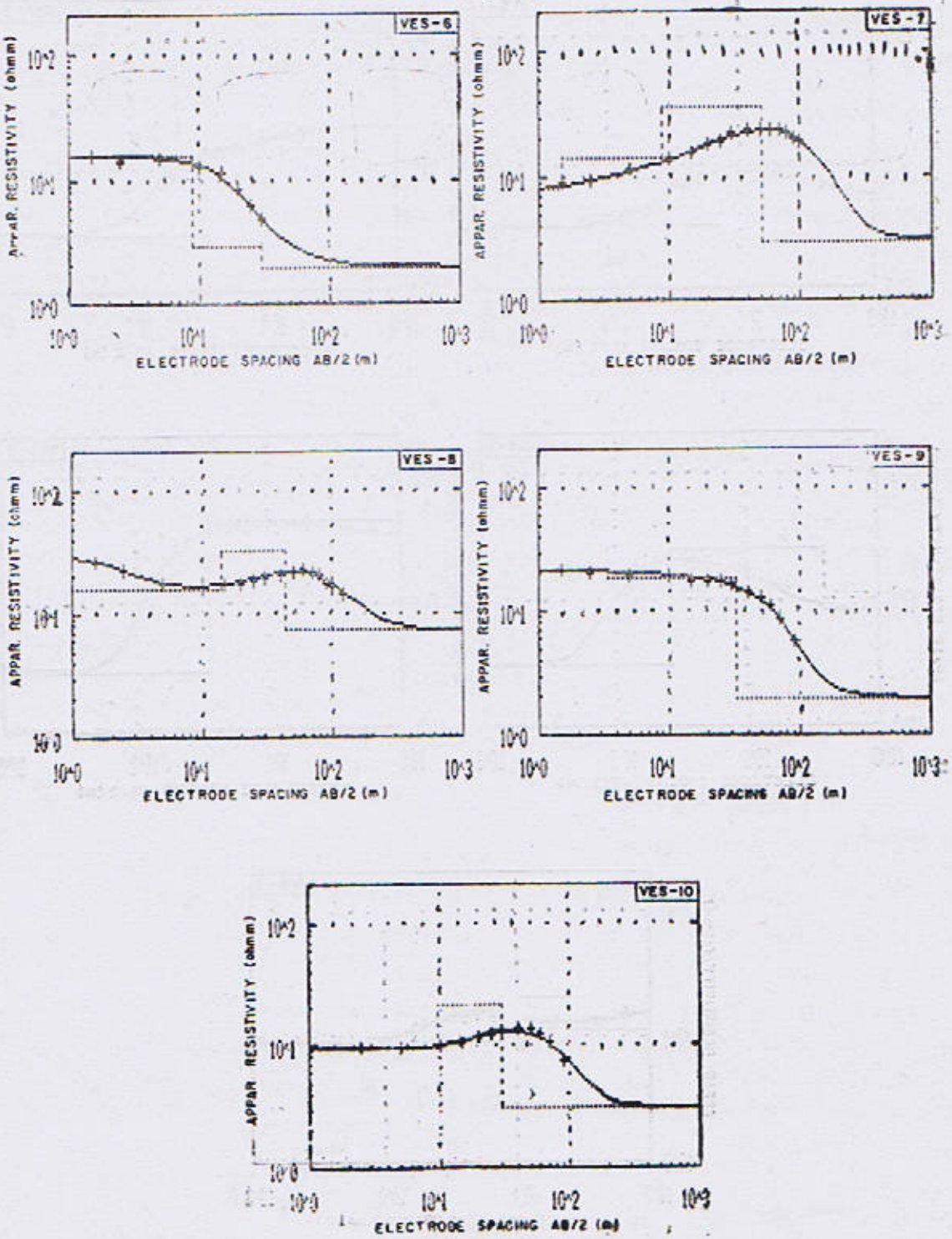

FIELD RESISTIVITY CURVES ALONGWITH TRUE RESISTIVITY EARTH MODEL

FIG. 2 (c)

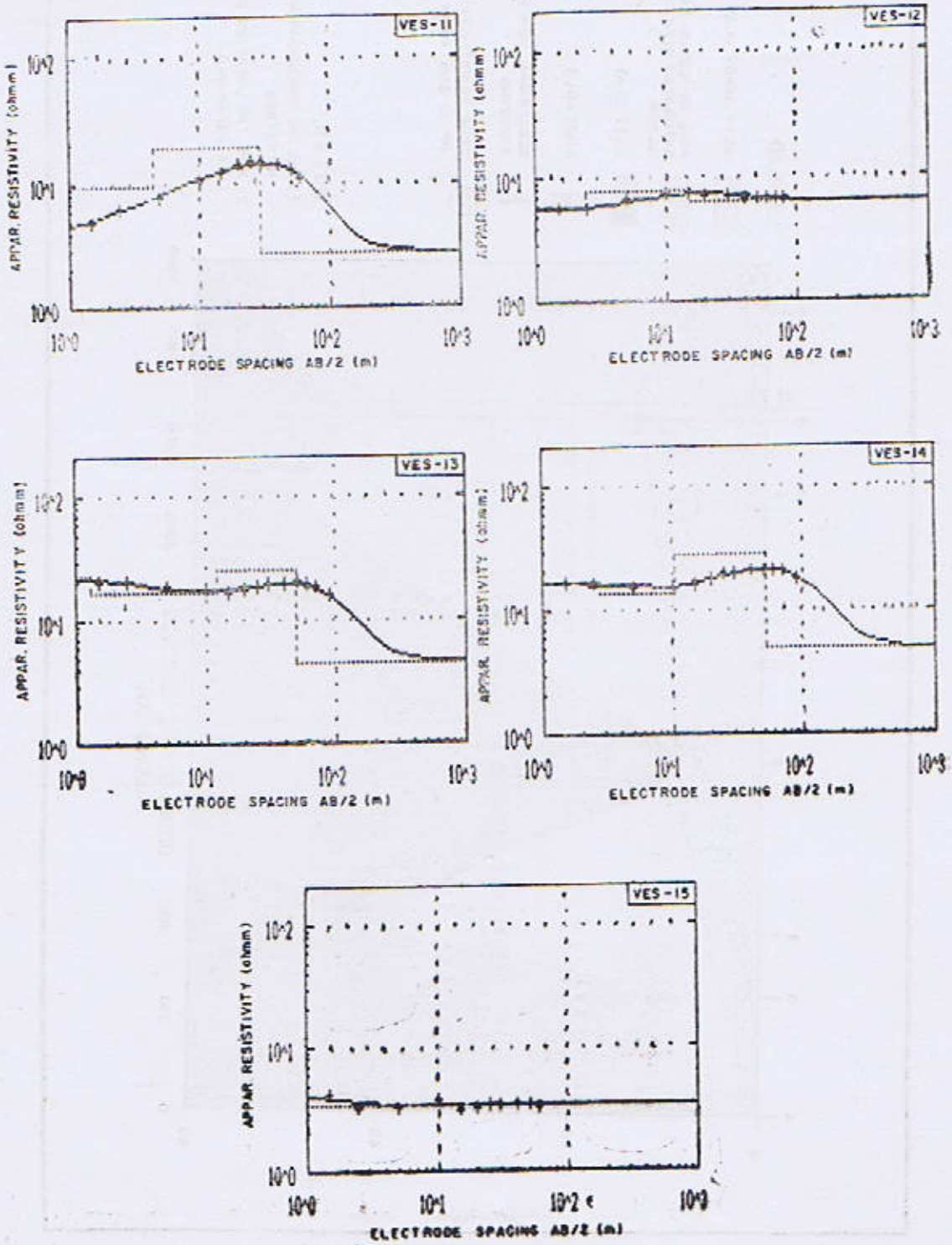

FIG. 3

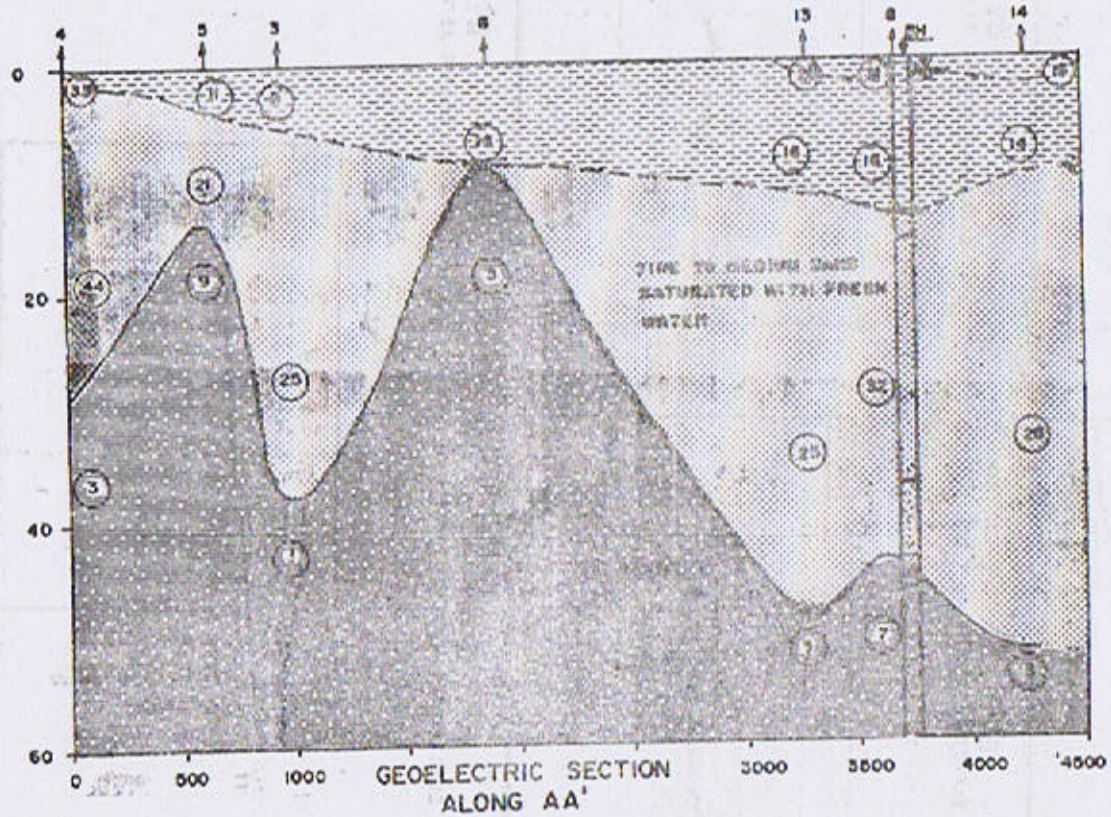

GEOELECTRIC SECTION ALONG AA'

Geol. Bull. Punjab Univ. 1992, 27, 107-110

RESISTIVITY SURVEYS FOR SUBSURFACE INVESTIGATIONS

BY
UMAR FAROOQ AND SHAFEEQ AHMAD
Institute of Geology, Punjab University, Lahore 54590, Pakistan

Abstract : *Certain case histories about the use of Resistivity Surveys for subsurface investigations are described in this paper. The relevant studies show its usefulness, particularly for hydrogeological studies, ground water contamination and acid mine drainage.*

INTRODUCTION

The usefulness of the Electrical Resistivity method in geological explorations depends to a considerable extent, on the resistivity contrast, which may be due to discontinuity of the rock formation or change in physical conditions. On these basis, resistivity method can be successfully employed for subsurface investigations, ground water investigations and water contaminations etc.

SUBSURFACE INVESTIGATIONS

King and Pesowski (1993), described the range of Electrical Resistivity for different lithological formations and specific conductance of some common groundwater ions. The porous for-mations, useful indicators for probable groundwater flow paths, are indicated by the presence of course of the subsurface layers. The chemical analysis of sulphate and conductivity measurements in groundwater showed a correlation between sulphates and electrical conductivity.

Young and Droege(1986), carried out Resistivity surveys using an ABEM. Terrameter SAS 300 to locate building sites at a nineteenth Fort in Michigan, built during the copper boom of the 1840 and located at the tip of Keweenaw Peninsula in the upper Peninsula of Michigan. The Resistivity surveys were made using a half-Schlumberger array with electrode spacings of 0.3, 0.6, 1.0, 1.5, and 2.0 m.

The Resistivity surveys indicated certain anomalies related to building foundation or excavations. A detailed study of Resistivity surveys over privies, Guard house, Carpenter shop and Blacksmith shop showed that probable locations of two walls of the Guard house and the locations of the privies could be determined by the use of Resistivity method. Young and Droege (1986), also concluded that Resistivity method was more useful than the Magnetic method for mapping building foundations.

GROUND WATER INVESTIGATION

Umar Farooq and Nasir Ahmad (1991), used Resisitivity technique for groundwater investigation in Mauli and Tutak areas, Balochistan. The southern part of Tutak Valley appears to be filled with coarser deposits probably gravel/boulder beds. These beds gradually disappear towards northern, north

eastern parts of valley at deeper depths. It has also been found that a prominent clay/shale layer, possibly the bed rock, appears at deeper depths throughout the Mauli Valley and may be identified in test holes. On the basis of the western and north resistivity studies, there is considerable scope of obtaining large quantities of water from the subsurface groundwater storage through shallow wells as tube wells.

White et al. (1988) described Resistivity surveys along with other geophysical techniqes in Victoria Province, Zimbabwe to locate borehole sites for water supply in basement granites and gneisses. The mean regolith resistivity for Victoria Province was found to be 60 ohm-meter with range of 20 to 200 ohm-meter. The lower resistivities represent a clay-rich lithology, while the higer resistivities represent partially saturated ordry regolith. The fractured bedrock resistivities ranged from 200 to 1000 ohm-meter with mean value of 370 ohm-meter, whereas the unfractured bedrock generally shows values higher than 3000 ohm-meter. Granite regolith zone a mean value of 236 ohm-meter as compared to 145 ohm-meter for gneiss regolith. White et al. (1988) also established optimum values of regolith thickness and formation resistivities for Victoria Province.

El. Abd and Awad (1991), using resisitivity survey data from bore holes identified five sabkha "Clusters" along the central axis of the coastal plain of west Red Sea Coast of Saudi Arabia. The electrical resistivity sounding identified such surface sediment layers and such surface channels through which sea water is drawn to the coastal plain.

WATER CONTAMINATION

Landfills pose a significant hazard to ground and surface water resources. Cartwright and McComas (1968), identified contaminant plumes generated by landfills using electrical resistivity techniques. Geophysical techniques have also been used to evaluate landfill containment system consisting of cover and liner. The cover of a landfill isolates decomposing refuse from the environment and minimises infiltration of precipitation and accumulation of contaminated ground water within the landfill. The landfill covers are often fractured or eroded. This may lead to escape to landfill gases and creation of leachate through infiltration of surface water.

Capenter et al. (1991), while assessing a fractured landfill cover in north eastern Illinois observed that resistivity soundings could not delineate cover thickness over areas of fractured or new cover where resistivity contrasts with the underlying refuse were minor. However, resistivity soundings zone cover estimates accurate to within 0.7m over unfractured mature cover where resistivities were 10 to 20 ohm-meter higher than in the refuse. The opening of cover fractures gave azimuthal resistivity variations as large as 16 ohm-meter, during dry weather.However, the same areas, under moist conditions showed little or no azimuthal resistivity variation.

Kearey and Brooks (1988), described surveys with respect to acid mine drainage of coal mine and showed a linear relationship between log resistivity and log ion concentration. With the increese of acid water contamination, the groundwater becomes more conductive and the resistivity values lower down from 60 to 200 ohm-meter to 6 to 12 ohm-meter. In a coal mine, coal can show variable resistivity values, depending upon its location and extent of the presence of contaminated water. Coal above the water table has high resistivity, and when associated with groundwater, it shows moderate resistivity and considerably low resistivity in presence of contaminated groundwater.

CONCLUSIONS

The geophysical techniques, particularly Electrical Resistivity, can provide valuable information about subsurface investigations. This can also be useful for the study of environmental problems and can also monitor the migration of contaminants.

REFERENCES

Carpenter P.J., Kaufmann, R.S. and Price, B. 1990. Use of resistivity soundings to determine landfill structure. *Ground Water*, 28, (4) 569-575.

Cartwright, K., and McComas, M.R., 1968, Geophysical surveys in the vicinity of sanitary landfills in nort-eastern Illinois: *Ground Water*, 6, 23-30.

Young C. T. and Droege D. R. 1986. Archaeological applications of resistivity and magnetic methods at Fort Wilkins State Park, Michigan. *Geophysics* 51, (3) 568-575.

El Abd Y.I. and Awad M. B. 1991. Evaporitic sediment distributions in Al-Kharrar Sabkha, west Red Sea Coast of Saudi Arabia, as revealed from electrical soundings. *Marine Geol.*, 137-143.

Kearey, P. and Brooks, M., 1988. An Introduction to Geophysical Exploration. ELBS Publications, UK.

King, A. and Pesowski, M., 1993. Environmental applications of surface and airborne geophysics in mining. *Canad. Min. and Metall. Bull.* 86, 58-67.

Umar Farooq and Nasir Ahmad 1991, Use of resistivity method in ground water studies of Mauli and Tutak Valleys, Balochistan, Pakistan, *Acta. Min. Pakistanica* 5, 62-69.

White C. C., Houston, J. F. T. and Barker., R.D. 1988. The Victoria Province Drought Relief Project, I. Geophysical siting of boreholes. *Ground Water*, 26, (3) 309-316.

Geol. Buil. Punjab Univ., 1994, 27, 111-115

GEOCHEMICAL DEGRADATION IN MOUNTANOUS REGIONS AND THEIR ENVIRONMENTAL EFFECTS

By

SHAFEEQ AHMED, UMAR FAROOQ AND RIAZ AHMED SHEIKH

Institute of Geology, Punjab University, Lahore-54590 Pakistan

Abstract : *Environmental changes are the net result of changes in the physical conditions such as air, water, gases, landforms and the social and cultural aspects ethics, economics and aesthetics etc. The changes in physical conditions are influenced not only by natural processes such as physical and chemical decomposition of rocks by processes like weathering, volcanic activity, landslides etc., but also as a result of man's activities to improve his living standards by mining activities and deforestation etc. These environmental changes cause a pollution within the affected area and its effects are migrated downstream as well.*

Eversince the creation of the earth the major role is being played by the chemical weathering processes within the earth's crust. Water acts as a conveyer of the dissolved constituents and of such weathering agents as CO_2 & O_2.

INTRODUCTION

The chemical weathering generally results from the followings :—

1. Solution of minerals in water without chemical breakdown e. g. common salt (NaCl) or gypsum ($CaSO_4 2H_2O$) which is readily accomplished by waters not already saturated with these compounds.

2. The chemical change of one mineral to another which is wholly soluble can be illustrated by the effect of water containing carbon dioxide upon calcium carbonate.

$$Ca\ CO_3 + HO_2 + H_2O = Ca\ (HCO_3)_2$$

3. Alteration of rock minerals by action of water to yield a soluble and an insoluble product.

Mineral	Principal Soluble Products
Olivine	SiO_2, Mg^{++}, HCO_3-
Calciumrich feldspar	Ca^{++}, HCO_3-
Augite	Ca^{++}, Mg, SiO_2, Fe^{++}, HOC_3-
Hornblende	Ca^{++}, Mg, SiO_2, Fe^{++}, HCO_3-
Sodium-rich feldspar	Na^+, CO_3, $^{--}SiO_2$, HCO_3-

Biotite	Mg^{++}, SiO_2, F^- and others
Potassium feldspar	K^+, SiO_2, HCO_3^-
Muscovite	K^+, SiO_2, HCO_3^-
Quartz	Essentially insoluble

4. Adsorption of material from a non-solid phase at the surface of a solid particle.

Under different weathering conditions, especially as relatad to climate, the relative importance of the above types of reactions will be different and the products of alteration of a single mineral may also be different.

The oxidative reactions of various rocks and minerals give rise to acidic solutions :

$$FeS_2(S) + 7.5\ O_2 + H_2O = F^{2+} + 2SO_4^{2-} + 2H^+$$

Pyrite

$$2\ FeCO_3(S) + 0.5\ O_2 + 2H_2O = Fe_2O_3 + 2H_2CO_3$$

Siderite

$$MnCO_3(S) + 0.5\ O_2 + H_2O = MnO_2(S) + H_2CO_3$$

The chemical weathering of silicates is the predominant reaction in nature and major source of many dissolved constituents e.g. :

$$Fe_2SiO_4(S) + 4H_2O = 2Mg^{2+} + OH^- + H_2SiO_4$$

$$Si_2O(S) + 2H_2O = H_4\ SiO_4$$

Quartz

$$4K.\ AlSi_3O_8(S) + 22H_2O = 4K^+(OH)^- + 8H_4\ SiO_4 + Al_4\ Si_4O_{10}(OH)_8(S)$$

These reactions are very slow processes and may require several years for their completion.

Frequently, silicates may undergo an acidic reaction :

$$Mg_2SiO_4(S) + 4H_2CO_3 = 2Mg + 4HCO_3 + H_4SiO_4$$

This reaction suggests the attack of carbonic acid on forsteritf and similar silicates may be a source of bicarbonate alkalinity.

$$Mg_2\ SiO_4\ (S) + 4H_2\ CO_3 = 2Mg + 4HCO_3 + H_4SiO_4$$

This reaction suggests the attack of carbonic acid on forsterite and similar silicates may be a source of bicarbonate alkalinity.

Minerals are essential for sustaining the economy of a country. The high growth rate of population and an urgent need to raise its standard of living demand an accelerated economic growth and progressively larger quantity of minerals. The exploitation of minerals not only provide employment opportunities but also help in the development of remote areas.

However, mining activities and the processing activities of minerals affect the environment as well.

The mining activities results in the disturbance of air, and its effects on water pollution are more alarming one, as these affect not only the inhabitants but also the population living downstream. This pollution takes many forms. The polluted water may be too acid, too alkaline or extensively loaded with dissolved substances such as iron, manganese and copper etc. water containing highly dissolved minerals make it unsuitable for certain purposes.

Caboi et al, (1992), described the results of stream waters from a former mining activity. They observed that the interaction of natural waters and the ore body consisting of Galena, sphalerite, siderite and iron-smithsonite veins in a quartz gangue with pyrite, chalcopyrite, barite,

anglesite, cerussite and greenokite as the more common associated minerals, brings large amounts of metal in solution.

Nordstrom et al., (1979), observed pyrite oxidation to be responsible for the acidity in many mine waters.

Ficklin et al., 1992, derived a classification scheme based on pH and metal concentrations, during study of mine drainages and material drainages in mineralized areas. According to the proposed classification of mine natural drainages, acid sulphate deposits and some quartz-pyrite-sulfide veins, produce high acid extreme-metal waters, Water from epithermal veins, sandstone-shale-hosted veins and high-pyrite carbonate-replacement deposits, are near neutral, high metal. Water from carbonate hosted deposits are near neutral, low metal. As a resultof this it is concluded that the most acidic drainage comes from mine rich in pyrite or pyrite-alunite and quartz pyrite veins. The mines located in host rocks that can behave as a buffer towards the acidic water, produces drainage water of near neutral pH value, but with high metal contents. The absence of pyrite in mines results a near neutral drainage water with low metal contents.

Sulfur bearing minerals, commonly associated with coal, when exposed to air and water, get oxidized and form sulfuric acid. This acid enters the streams in two ways :

(1) Soluble acid salts formed on the exposed spoil surfaces enter into solution during surface run-off.

(2) Ground water, while moving to nearly streams, may be altered chemically as it percolates through spoil or waste dumps.

As a result of acid drainage, minute concentrations of salts of metals such as Zinc, Lead, arsenic, copper and aluminium which are toxic to fish, wildlife, plants and aquatic insects enter streams. The acid drainage is also associated with undesirable slimy red or yellow, iron precipitates in streams draining through sulfide bearing coal or metal deposits,

Streams are also polluted by acid water from underground mines, preparation plants and natural seepage from unworked coal and other pyritic material,

Surface mining in certain cases has made so big excavations that look like craters on the moon. In cases this has destroyed the protective vegetative cover.

The underground mining of solid resources and the withdrawal of underground fluids-water, oil and gas can cause subsidence or sinking of the land.

The mining activities and mineral resources of mountainous regions provide means of earnings to the residents of those areas, At the same time it is necessary to be well aware of the short comings of these activities and proper remedies be taken to avoid any medical disturbances in those areas resulted from the disturbances in the balance of trace elements. This has caused a number of medical problems for the residents of those areas e.g. in Japan, as a result of the mining operatiens for Zinc, lead and cadmium. the mining wastes find their migration into rivers. The contaminated water downstream was used by farmers, for domestic and agricultural purposes. This caused a disease known as 'Itaiitai' in the people living in that area. This disease attacks bones, causing them to become so thin and brittle that they break easiiy.

The mining of clay, coal and other minerals may bring to the surface materials that contain

anomalous concentrations of elements harmful to plants and animals. The mining of clay for use in ceramic Industry in cases has resulted in severe disturbances in the metabolism of beef cattle ; these disturbances have interfered with growth, nutrition and reproduction of the cattle.

The more abundant elements in the average adult human body are O=65%, C=18%, H=10.0%, N=3.0%, Ca=1.5%, P=1.0%, S=0.25%, K=0.2%, Na=0.15%, Cl=0.15%, Mg=0.5%, Keller, 1981. The living tissue, animal or vegetable is composed of 11 elements. Five of these are H, Na, Mg, K & Ca while the remaining six are non metals and consists of C, N, P, S, Cl. The species having hemoglobin, contain Fe as well. In addition to these elements there are a number of other elements which are essential for the proper functioning of living tissues. These include F, Cr, Mn, Fe, Co, Cu, Zn, Se, Mo & I. There are a number of other elements such as Ni, As, Al, Ba, accummulates as tissues age and are called age elements.

The above mentioned elements have effects on a particular plant or animal. For example slelenium is toxic in seleniferous areas, but if present in a balanced state, is beneficial to animal production i.e. raising of cattle sheep etc.. The Se defficiency is rectified by supplementing food supply of animals with Se.

Similarly there are a number of other elements the presence or absence of which affect the environment. Flourine is fairly abundant in rocks and soils, derived from the parent rock and by volcanic activity. Flourine in the form of calcium flouride prevents tooth decay by increasing the crystalinity of calcium phosphate crystals and also assists in the development of more perfect bone structure that is less likely to fail with old age.

The iodine deficiency causes thyroid disease in which case the thyroid gland becomes enlarged and a child born to a mother suffering iodine defficiency may be born mentally retarded dwarf.

Similarly zinc has been found to be essential for all animals and people particularly during early stages of development and growth. Zinc deficiencies causes loss of fertility, delayed healing and disorders of bones, joints and skin.

The general impression that man is moving towards an age of diaster, appears to be true, due to increase in man made disasters although geo-hazards have always been with us.

Keeping in view of the above mentioned observations, necessary steps will have to be taken while carrying out mining activities particularly, the coal and sulphides bearing areas as mentioned by Ahmad, Z., 1969 ; Ahmad, S., (1978); (1980); (1981); and (1992), in Pakistan Extremere medial measures willbe required particularly in cases of mineral deposits, which easily undergo chemical weathering and produce soluble and suspended matters, that are easily carried away by streams and rain water and also where mining activities are near the urban and populated areas. The remedies to be adopted will vary from place to place depending upon the nature of mineral involved and the type of environment existing at the place of mining activities and downstream.

REFERENCES

Ahmad, S., 1978. Ore-Microscopic study of Galena Ores from The lichi Valley Gilgit, Pakistan. *Geol. Bull. Punjab Univ.*, **13**, 73-76.

Ahmad, S., 1980. A study of opaque minerals from Thak Valley igneous complex, N.W.F.P., *Pak. Jour. Sci.*, 199-200.

Ahmad, S. 1981. Preliminary account of the occurrence of Nickel Sulphides in Serpantinites of souch area, Kaghan Valley, Pakistan, *Geol. Bull. Punjab Univ.*, **16**, 78-85.

Ahmad, S. 1992. Lead-Zinc-Copper Mineralization in Treri Manjhotar area District Muzaffarabad (Azad Kashmir), Pakistan Acta Min. Pakistanica, **6**, 164-167.

Ahmad, Z. ; 1969. Directory of mineral Deposits of Pakistan. *Geol. Surv. Pakistan, Publ.*

Caboi, R. Cidu, R. Fanfani, L, Massoli Novelli, R ; and Xuddas, P, 1992. Metal contamination of stream waters from former mining activity. WATER ROCK INTERACTION A. A. Balkema/ Rotterdam/Brookfield, 367-370.

Ficklin, W. H ; Plumlee, G. S ; Smith, K. S. and McHugh, J. B., 1992. Geochemical classification of mine drainages and natural drainages in mineralized areas. WATER ROCK INTERACTION. A. A. Balkema/Rotterdam/Brookfield, 381-384.

Keller, E. A., 1986. ENVIRONMENTAL GEOLOGY Charles E. Merrill Publishing Company, London, 279-306.

Nordstrom, D. K ; Jenne, E. A. and Ball, J. W ; 1979, Redox equilibria of iron in acid mine waters, ACS Symposium Series 93 ; Washington, D. C ; American Chemical Society, 51-79.